



12-2014

# Autoimmune Susceptibility Imposed by Public TCR $\beta$ Chains

Yunqian Zhao

*University of Tennessee Health Science Center*

Follow this and additional works at: <https://dc.uthsc.edu/dissertations>



Part of the [Immune System Diseases Commons](#), [Medical Genetics Commons](#), and the [Medical Immunology Commons](#)

---

## Recommended Citation

Zhao, Yunqian, "Autoimmune Susceptibility Imposed by Public TCR $\beta$  Chains" (2014). *Theses and Dissertations (ETD)*. Paper 317.  
<http://dx.doi.org/10.21007/etd.cghs.2014.0381>.

This Dissertation is brought to you for free and open access by the College of Graduate Health Sciences at UTHSC Digital Commons. It has been accepted for inclusion in Theses and Dissertations (ETD) by an authorized administrator of UTHSC Digital Commons. For more information, please contact [jwelch30@uthsc.edu](mailto:jwelch30@uthsc.edu).

---

# Autoimmune Susceptibility Imposed by Public TCR $\beta$ Chains

**Document Type**

Dissertation

**Degree Name**

Doctor of Philosophy (PhD)

**Program**

Biomedical Sciences

**Track**

Microbiology, Immunology, and Biochemistry

**Research Advisor**

Terrence L. Geiger, Ph.D., M.D

**Committee**

Hongbo Chi, Ph.D. Elizabeth A. Fitzpatrick, Ph.D. Thirumala-Devi Kanneganti, Ph.D. Tony N. Mario, Ph.D.

**DOI**

10.21007/etd.cghs.2014.0381

**Comments**

Six month embargo expired June 2015

**Autoimmune Susceptibility Imposed by Public TCR $\beta$  Chains**

A Dissertation  
Presented for  
The Graduate Studies Council  
The University of Tennessee  
Health Science Center

In Partial Fulfillment  
Of the Requirements for the Degree  
Doctor of Philosophy  
From The University of Tennessee

By  
Yunqian Zhao  
December 2014

Copyright © 2014 by Yunqian Zhao.  
All rights reserved.

## **DEDICATION**

I still remember my enthusiasm evoked by Dr. Zhangliang Chen's statement "The 21<sup>st</sup> century is the golden century for life sciences", which inspired an entire generation of Chinese students with the dedication to biomedical research in the last ten years. Lots of them gave up, yet still persist the rest of them. No one can tell how much effect and failure paid behind, nevertheless, this persistence impels the development of science and benefits the human society indeed. Pay homage to those beautiful minds.

## ACKNOWLEDGEMENTS

I would like to express my deep gratitude to Dr. Terrence L. Geiger, my research supervisors, for his guidance and support through the whole study. His modest personality, solid knowledge, enthusiastic science passion, planning and organization capability, and meticulous scholarship influence everyone in the lab. This is the real treasure I can learn from him for my future career.

I would also like to thank my committee members: Dr. Hongbo Chi, Dr. Elizabeth A. Fitzpatrick, Dr. Thirumala-Devi Kanneganti and Dr. Tony N. Marion for their valuable advice and critiques in keeping my thoughts moving forward.

My grateful thanks are also extended to every lab colleague during the last five years. We work side by side; we discuss in group; we hang out together and laugh together. They are colleagues, but they also give me a second family overseas. They are Bofeng Li, Carol O'Hear, Heiber Joshua, Lindsay Jones, Phuong Nguyen, Rajshekhar Alli, Sharyn Tauro and Xin Liu.

Finally, I wish to give thanks for everyone helped in the last five years, no matter in science or in life and UTHSC and St Jude Children's Research Hospital for providing a great platform to achieve my goal.

## ABSTRACT

The major histocompatibility complex (MHC) is the strongest genetic risk factor for autoimmunity. It acts together with a corresponding TCR repertoire, yet, considering the extent of the repertoire's diversity, how this imposes disease susceptibility on a population is not well understood. We address the hypothesis that shared or public TCR, those present in most individuals, modulate autoimmune risk. High resolution analyses of autoimmune encephalomyelitis-associated T-cell receptor  $\beta$  chain (TCR $\beta$ ) showed preferential utilization of public TCR sequences, implicating them in pathogenesis. Disease-associated public TCR $\beta$ , when transgenically expressed in association with endogenously rearranged T-cell receptor  $\alpha$  chain (TCR $\alpha$ ), could further endow unprimed T cells with autoantigen reactivity. Enforced expression of two of six public but no private TCR $\beta$  further provoked spontaneous, early-onset autoimmunity in mice. These findings implicate public TCR in skewing repertoire response characteristics and autoimmune susceptibility, demonstrate how single TCR chains can bias autoantigen specificity, and suggest that subsets of public TCR sequences may serve as disease-specific biomarkers or therapeutic targets.

## TABLE OF CONTENTS

<b>CHAPTER 1. INTRODUCTION .....</b>	<b>1</b>
T-cell Receptor .....	1
T Lymphocytes .....	1
T Cell Maturation.....	1
TCR Structure .....	2
MHC .....	2
Historical Discoveries .....	2
MHC Structure.....	3
MHC and T Lymphocytes .....	3
MHC and Autoimmune Diseases.....	4
MHC Bias Pre-immune TCR Repertoire .....	4
TCR Repertoire.....	5
TCR Repertoire Diversity .....	5
Public TCR Repertoire.....	6
Treg Cells.....	7
Treg Identification .....	7
Treg Development Models .....	7
Treg Repertoire .....	8
Experimental Autoimmune Encephalomyelitis (EAE).....	9
High-throughput Sequencing (HTS).....	10
<b>CHAPTER 2. METHODOLOGY .....</b>	<b>11</b>
Mice and Materials .....	11
Mice .....	11
Monoclonal Antibodies.....	11
High-throughput Sequencing.....	11
EAE Immunization .....	11
Cell Isolation .....	12
Cell Counting.....	12
Cell Sorting .....	12
RNA Isolation and cDNA Transcription .....	13
DNA Preparation and Sequencing.....	13
Raw Data Trim.....	13
Retrogenic Mice Models.....	14
Molecular Subcloning.....	14
Retroviral Transduction .....	15
Generation of Retrogenic Mice.....	15
Clinical Evaluation.....	15
Chimeric Mice .....	16
Cell Proliferation Assay.....	16
Cytokine Analysis .....	16
Retroviral Transfection of CD4 <sup>+</sup> 4G4 Hybridoma Cell .....	16
Enzyme-linked Immunosorbent Assay (ELISA) .....	17



5'RACE.....	17
Statistics .....	18
<b>CHAPTER 3. RESULTS.....</b>	<b>19</b>
Introduction.....	19
Results.....	19
High Prevalence of Public TCR $\beta$ in the Autoimmune Repertoire.....	19
Functional Characterization of the CNS Public TCR $\beta$ in Retrogenic Mice Model...	42
<b>CHAPTER 4. PRELIMINARY EXPERIMENTS.....</b>	<b>57</b>
Introduction.....	57
Results.....	57
<b>CHAPTER 5. DISCUSSION .....</b>	<b>69</b>
Public TCR in Skewing Repertoire Response and Autoimmune Susceptibility .....	69
Functional Characterization of TCR $\alpha$ Repertoire in TCR $\beta$ 1 Retrogenic Mice Model.....	71
Cross Reactivity, Gut and CNS .....	72
Retrogenic Mice Models versus Transgenic Mice Models .....	73
Summary .....	74
<b>LIST OF REFERENCES .....</b>	<b>75</b>
<b>APPENDIX A. SUPPLEMENTAL TABLES .....</b>	<b>86</b>
<b>APPENDIX B. SUPPLEMENTAL FIGURES.....</b>	<b>89</b>
<b>VITA.....</b>	<b>92</b>

## LIST OF TABLES

Table 3-1.	Description of TRBV13-2 <sup>+</sup> TCR sequences acquired from control mice. ....	21
Table 3-2.	Description of TRBV13-2 <sup>+</sup> TCR sequences acquired from mice with early EAE. ....	22
Table 3-3.	Description of TRBV13-2 <sup>+</sup> TCR sequences acquired from mice with late EAE. ....	24
Table 3-4.	Highly shared CNS CDR3 $\beta$ sequences.....	36
Table 3-5.	TCR $\beta$ retrogenic mice.....	43
Table 3-6.	Distinct TCR $\alpha$ chains isolated from CNS CD4 <sup>+</sup> GFP-Foxp3 <sup>+</sup> and GFP-Foxp3 <sup>-</sup> T cells from TCR $\beta$ 1 mice with EAE.....	48
Table 4-1.	Fourteen reconstituted TCR $\alpha\beta$ with MOG <sub>35-55</sub> reactivity on hybridoma cells.....	60
Table A-1.	Annealing oligo sequences for CDR3 $\beta$ . ....	86

## LIST OF FIGURES

Figure 3-1. TCR TRBJ use during EAE.....	25
Figure 3-2. Association of CNS TCR with the memory T cell pool. ....	26
Figure 3-3. Representation of shared TRBV13-2 <sup>+</sup> TCR $\beta$ among CNS-infiltrating T cells.....	27
Figure 3-4. Models for the high frequency of shared CNS TCR $\beta$ . ....	29
Figure 3-5. Over-representation of unique public sequences in the CNS-infiltrating repertoire. ....	30
Figure 3-6. Over-representation of total public sequences in the CNS-infiltrating repertoire. ....	31
Figure 3-7. Over-representation of unique and total CNS-associated Foxp3 <sup>+</sup> and Foxp3 <sup>-</sup> public TCR $\beta$ in the pre-immune repertoire.....	32
Figure 3-8. Repertoire focusing in mice with EAE. ....	35
Figure 3-9. Formation of the public autoimmune TCR repertoire through biased recombination.....	41
Figure 3-10. Enforced public TCR $\beta$ expression leads to spontaneous autoimmune encephalomyelitis.....	45
Figure 3-11. Characterization of spontaneous EAE development in TCR $\beta$ 1 retrogenic mice. ....	46
Figure 3-12. TCR $\beta$ 1 <sup>+</sup> TCR recognize MOG <sub>35-55</sub> . ....	47
Figure 3-13. Spontaneous EAE was protected by the co-engrafted WT cells in chimeric retrogenic mice. ....	51
Figure 3-14. Public TCR $\beta$ 4, TCR $\beta$ 7 impose MOG-reactive TCR repertoires.....	52
Figure 3-15. Heightened public TCR $\beta$ 3 autoreactivity. ....	53
Figure 3-16. MOG <sub>35-55</sub> response and disease-free survival of retrogenic mice. ....	55
Figure 4-1. Pie charts of TRAV and TRAJ usage in TCR $\beta$ 1 CNS infiltrating T cells. ..	59
Figure 4-2. Titration assay for MOG <sub>35-55</sub> -specific TCR. ....	61
Figure 4-3. MOG <sub>35-55</sub> response and disease-free survival of TCR $\alpha\beta$ retrogenic mice. ..	62

Figure 4-4. Disease onset is associated with early CD4 T cell engraftment. ....	65
Figure 4-5. Treg analysis of retrogenic T cells. ....	66
Figure 4-6. Cross reactivity to MOG <sub>35-55</sub> mimicry. ....	68
Figure B-1. Diagram of two main plasmids. ....	89
Figure B-2. Gating strategy for surface staining on TCR $\beta$ 1 retrogenic mice. ....	90
Figure B-3. Gating strategy for Foxp3 intracellular staining on TCR $\beta$ 1 retrogenic mice. ....	91

## CHAPTER 1. INTRODUCTION

### T-cell Receptor

#### T Lymphocytes

A complete immune system involves different functional cell types, each of which plays a particular role during immune response. Among these cells, the lymphocytes occupy the central stage because they are the cells representing the specificity of immune response. T cells constitute a major division of lymphocytes, which express TCR on the cell surface. TCR is a heterodimer composed of two distinct chains,  $\alpha$  and  $\beta$  or  $\gamma$  and  $\delta$ . The  $\alpha$  and  $\beta$  heterodimers make up 95% of T-cells, while the  $\gamma$  and  $\delta$  heterodimers make up 5% of T-cells<sup>1</sup>. The  $\alpha\beta$  TCRs can be further divided into two sub-lineages based on their distinct cell surface co-receptors, CD4 and CD8. Here we just focus on CD4<sup>+</sup> T cells bearing  $\alpha\beta$  TCRs. CD4<sup>+</sup> T cells tend to differentiate into different functional cell subtypes secreting their typical cytokines as a consequence of priming. For example, Type 1 helper T cell (T<sub>h</sub>1) mainly produces interferon gamma (IFN- $\gamma$ ), Type 1 helper T cell (T<sub>h</sub>2) produces interleukin 4 (IL-4), IL-5, IL-13, T<sub>h</sub>17 help cell produces IL-17 and regulatory T cell (Treg) produces transforming growth factor beta (TGF- $\beta$ ) and IL-10.

#### T Cell Maturation

Pluripotent stem cells in bone marrow give rise to the T lineage precursors, and T lineage precursors will travel from the blood to thymus for a serial of early maturation events. In the thymic cortex, T lineage progenitors appear as CD4<sup>-</sup>CD8<sup>-</sup> double negative form. During this stage, TCR $\beta$  chain will first undergo rearrangement. If the rearrangement produces a productive TCR $\beta$  chain, it will pair with a surrogate  $\alpha$  chain, pre-T $\alpha$ , otherwise will lead to clonal deletion. Functional TCR $\beta$  chain rearrangement will be followed by a successful TCR $\alpha$  chain rearrangement and expression of CD4 and CD8 co-receptors for the next double positive stage. Somatic recombination events for TCR must be completed by the CD4<sup>+</sup>CD8<sup>+</sup> stage and the CD4<sup>+</sup>CD8<sup>+</sup> double positive population need to migrate to thymic medulla for further maturation. For positive selection, only the CD4<sup>+</sup>CD8<sup>+</sup> T cells with TCRs capable of low-affinity binding to a self-peptide-MHC (pMHC) on thymic epithelial cells can receive a signal to survive, otherwise they will be neglected and undergo apoptotic death<sup>2</sup>. Cells that undergo positive selection process will begin to commit to either the CD4<sup>+</sup> or CD8<sup>+</sup> single positive lineage. Relatively, low-affinity recognition of a self-pMHCI will lose CD4 and differentiate into CD8<sup>+</sup> T cells, while higher-affinity recognition of a self-pMHCII will lose CD8 and develop into CD4<sup>+</sup> T cells<sup>3</sup>. During the commitment stage, differential expression of the lineage associated transcription factors, as ThPOK or Runx3, will accompany the CD4<sup>+</sup> helper lymphocyte or CD8<sup>+</sup> cytotoxic T lymphocyte (CTL) function<sup>4</sup>. On the other hand, since the somatic recombination event is a totally random process, CD4<sup>+</sup> or CD8<sup>+</sup> T lymphocytes will by chance produce high-affinity TCR recognizing auto-antigens in the thymus. These cells

will undergo an elimination process and induce apoptotic cell death, which is referred as negative selection. In alternative, some cells bearing high affinity TCR to self-pMHC will induce the Foxp3 transcription expression, which causes the cells to differentiate into a specific subpopulation, natural regulatory T cells (nTreg). The TCR affinity for self-pMHC of Treg is considered at the high end of the positive selection range but at the low end of the negative selection range<sup>5</sup>, but Treg development is not well understood.

## **TCR Structure**

The TCR is a disulfide-linked heterodimer. Each single chain is organized as immunoglobulin (Ig) chains, consisting of a variable N terminal and a conserved C terminal. Although TCR shares similar structural features as B-cell receptor (BCR), the mechanism of antigen recognition is totally different. In contrast to recognizing intact molecules, TCR recognizes a complex consisting of a peptide, which is derived by proteolysis of the antigen and presented on a class I (MHC-I) or class II MHC (MHC-II) molecule by an antigen-presenting cell (APC).

The adaptive immune system will encounter a large variety of pathogen-derived antigens, which requires a corresponding TCR diversity. The TCR diversity is primarily localized to three complementarity determining regions (CDRs) on each chain. Among the six CDR loops, relatively conserved amino acids in the TCR CDR1 and CDR2 regions, encoded by the germ line V gene, are often used to bind exposed areas of the MHC  $\alpha$ -helix. However, CDR3 loops, made up at least partially of non-germ line encoded residues are hyper variety and are positioned to engage with MHC bound peptide directly. The contact induced by CDR1 and CDR2 imposes the usual diagonal mode of TCR binding on MHC. Meanwhile, this arrangement also allows flexibility in the pitch formed by CDR1 and CDR2, allowing the TCR to accommodate CDR3 loops and peptide ligands of different sequences and lengths and yet still bind the pMHC in approximately the same orientation. Characterization of CDR3 sequence variation therefore provides a good measure of TCR diversity in an antigen selected repertoire.

## **MHC**

### **Historical Discoveries**

The adaptive immune system consists of two components: antibody mediated humoral immunity and T cell mediated cellular immunity. In contrast to antibodies engaging with intact antigens, T cells function through interacting with the cell surface bound small peptides via their heterodimer T cell receptors. The task of displaying cell surface bound peptides for recognition by T cells is mediated by classical major histocompatibility complex<sup>6</sup>.

Studies about MHC associated immune response began from rejection of grafts and tumor transplantation more than seventy years ago<sup>7-9</sup>. MHC represents a special case as the immune responses are extraordinarily sensitive to the difference at the MHC. Discovery of MHC suggests a co-evolutionary development of the lymphocyte receptors which are somatically generated in the thymus, conferring them the ability to react well with the foreign MHC but no longer react with the host MHC<sup>10</sup>.

## MHC Structure

Until recently, great than 400 genes are mapped to the human or mouse *Mhc*. The mouse *Mhc* is referred as *H2* while in human it is referred as *HLA* (Human Leucocyte Antigen). In most cases we specifically refer the “MHC” molecules to the class I MHC and class II MHC based on their structural and functional properties. Both classes of MHC are heterodimers with similar structures which composed of three domains, one  $\alpha$ -helix/ $\beta$ -sheet ( $\alpha\beta$ ) superdomain that forms a peptide-binding site and two Ig-like domains. A fully assembled class I MHC molecule is composed of a polymorphic  $\alpha$  chain noncovalently attached to the nonpolymorphic  $\beta$ 2-microglobulin ( $\beta$ 2m). The peptide-binding cleft ( $\alpha$ 1 $\alpha$ 2 domain) is formed by the heavy chain only, and the light chain subunit,  $\beta$ 2-microglobulin associated with  $\alpha$ 3 of the heavy chain to stabilize the peptide binding. In contrast, a fully assembled class II MHC molecule is composed of a polymorphic  $\alpha$  chain noncovalently attached to a polymorphic  $\beta$  chain and the peptide-binding cleft is formed by two heavy chains ( $\alpha$ 1 $\beta$ 1). To present the peptide antigens on MHC molecules, a seven stranded  $\beta$ -sheet forms the floor of the binding groove and the sides are formed by two long  $\alpha$ -helices. Polymorphic residues cluster within and around the binding groove provide variation in structural and chemical properties, which accounts for the specific peptide-binding motifs for each MHC molecules<sup>11-13</sup>.

Although both MHCs form a vice-like groove with two flanking  $\alpha$ -helices and a  $\beta$ -sheets formed floor, the peptide binding groove ends are quite open in class II MHCs, which allows them to accommodate longer peptides. Generally, 8 to 10-mers peptides were presented by class I MHCs, whereas 10 to 30 residues or longer peptides were presented by class II MHCs. The anchor residues of the peptide are buried in specificity pockets that differ from allele to allele<sup>14,15</sup>, leaving the upwarding amino acid side chains bulging out of the groove for a direct interaction with the TCR. Termini sequences of the long peptides may also extend out the binding grooves and contribute to the TCR interaction.

## MHC and T Lymphocytes

MHC molecules convey their function and trigger T cell responses via binding the peptide antigens and presenting them for recognition by antigen-specific T lymphocytes. Class II MHCs present peptides that originate from proteolysis of extracellular antigens in endosomal-type compartments, whereas class I MHCs present peptides primarily derived from intracellular degradation of proteins in the cytosol. Recognition of MHC

molecules is T cell type restricted, as cytotoxic T cells preferentially engage with class I MHCs, whereas T-helper cells preferentially engage with class II MHCs.

## **MHC and Autoimmune Diseases**

Not only for transplant acceptance and immune responsiveness, the MHC is also the principal genetic locus conveying risk for a number of human diseases. More than 40 diseases have been linked to the MHC, many of which are autoimmune disease in nature<sup>16-19</sup>. Particular alleles of HLA class II loci, especially with DR and DQ are high risk alleles for autoimmune diseases<sup>20</sup>. For example, studies identify the association of the HLA-DRB1 locus in rheumatoid arthritis, as HLA-DR4 shared a common sequence motif within the DR $\beta$  chain, suggesting preferential antigen presentation of self-epitopes by these molecules<sup>21</sup>. In human type 1 diabetes, HLA genes are also thought to contribute as much as 50% of the genetic risk for type 1 diabetes. The disease incidence is significantly increased in patients with HLA-DR3-DQ2 and DR4-DQ8 haplotypes<sup>22,23</sup>. Studies also indicated the homozygosity for HLA-DRB1\*15:01 increases the probability of developing multiple sclerosis ~7-fold<sup>24,25</sup>. In contrast, few non-MHC alleles impart more than a 1.2-fold increase in risk<sup>26</sup>. The precise mechanisms underlying the association of most of these diseases with the particular MHC haplotypes are not well understood. Differential binding of self-antigen ligands may be one manner through which MHC variants alter risk. However, even on a single cell, thousands of different antigenic epitopes can bind to single MHC specificity. Therefore large numbers of tissue-restricted epitopes will associate with any MHC allele. As an alternative, MHC molecules have been hypothesized to primarily confer risk by modulating the selection and activation of pathologic effector and protective regulatory T cells<sup>27,28</sup>.

## **MHC Bias Pre-immune TCR Repertoire**

Despite the lack of direct evidence, the hypothesis that TCRs are evolutionarily selected to react with MHC is rational. The TCR specificity on developing thymocytes is screened through positive and negative selection<sup>29,30</sup>.

One model that MHCs bias the pre-immune T cell repertoire was proposed, from which a large number of CD4<sup>+</sup>CD8<sup>+</sup> thymocytes failed positive selection and died by neglect due to a lack of MHC specificity<sup>2</sup>. In addition, CD4, CD8, MHC-I and MHC-II knockout mice were utilized to analyze for the pre-selection repertoire. Mice without CD4 and CD8 still developed normal number of T cells, however, some of the cells could be activated by foreign cells lacking MHC molecules. These results implicate that CD4 and CD8 molecule is required for interacting with MHC during pre-selection stage, in effect forcing all selected T cells to have an affinity for MHC<sup>31</sup>.

Another model was proposed from the experiments performed on mice with impaired negative selection. TCR $\alpha$  and  $\beta$  chains expressed by the pMHCII-specific T cells from those mice contact MHC primarily with the germ line encoded CDR1 and



CDR2 regions, suggesting a co-evolutionary selection of TCR V domain and MHC molecules. This finding implies that many pre-selection CD4<sup>+</sup> CD8<sup>+</sup> thymocytes are deleted because of their intrinsic MHC specificity of TCRs and the only cells survive are those with TCRs containing CDR3 that interfere with CDR1 and CDR2 mediated MHC binding<sup>32</sup>.

Nevertheless, what we mentioned above doesn't exclude the role of CDR3 in mediating the pre-immune repertoire. CDR1 and CDR2 regions are located in the germ line-encoded V domains whereas the CDR3 regions are generated by the random V(D)J somatic recombination, which is responsible for interacting with peptide directly. Some CDR3 were found to interfere with TCR-pMHC interaction and lead CD4<sup>+</sup>CD8<sup>+</sup> T cell die by neglect, in contrast, other CDR3 attenuated the CDR1 and CDR2 mediated MHC binding and foster positive selection. Thus, the CDR1 and CDR2 domain of most TCR $\alpha$  and  $\beta$  chains can produce intrinsic MHC reactivity, CDR3 domain will sterically interfere to varying degrees with this reactivity, producing a repertoire of TCRs with a wide spectrum of affinities for self-MHC.

## **TCR Repertoire**

### **TCR Repertoire Diversity**

Similar to the rearrangement of Ig heavy and light chains, the diversity of TCR repertoire is generated from somatic recombination. The V(D)J somatic recombination introduces two types of diversity: combinatorial diversity and junctional diversity. A functional TCR $\alpha\beta$  heterodimer is generated through randomly arrange different gene segments, which refers to variable (V), diversity (D) and joining (J) gene segments to a constant region (C) in the case of TCR $\beta$  chains, or V-J-C in TCR $\alpha$  chains. In the human TCR loci, there are 42 TRBV, 2 TRBD, 12 TRBJ, 43 TRAV and 58 TRAJ functional gene segments, whereas in mouse TCR loci, there are 35 TRBV, 2 TRBD, 12 TRBJ, 71 TRAV and 51 TRAJ functional gene segments<sup>33</sup>. The lymphocyte specific V(D)J recombinase will recognize the conserved recombination signal sequences located adjacent to V,D,J exons, delete intervening DNA and ligate the segments. Therefore, the amount of combinatorial diversity is decided by the possible number of combinations of the germline V, J, D gene segment numbers. In addition, the combinatorial diversity is further enhanced by the juxtaposition of two different, randomly generated TCR $\alpha$  and TCR $\beta$  chain. On the other hand, the largest contribution to the diversity is coming from junctional diversity, which involves removal or addition of nucleotides between VD, DJ, or VJ junctions. Removal of nucleotides by nucleases may lead to the generation of novel amino acid sequences or to out-of-frame nonfunctional products, while DNA polymerase mediated asymmetric breaks repair or TdT mediated nucleotide addition will generate non-germ line coded sequences<sup>34</sup>.

Theoretically, these events will produce a potential repertoire diversity of up to 10<sup>15</sup> different TCRs in mice<sup>1</sup> and 10<sup>18</sup> in humans<sup>35</sup>. Given that only ~3% of T cells will

survive after thymic selection, this leaves more than  $10^{13}$  possible TCR diversity for mice and  $10^{16}$  for humans in the periphery if the full repertoire could form<sup>36</sup>. However, the estimated numbers of T cell clonotypes are only about  $10^6$  in mice<sup>37</sup> and  $10^7$  in humans<sup>1</sup> in the peripheral circulation, several orders of magnitude less than the theoretical maximal diversity.

## Public TCR Repertoire

Unlike antibodies, which can engage antigens in highly variable manners, TCR $\alpha\beta$  heterodimers associate with pMHC in largely stereotypical orientations that require significant energy contributions from both the TCR $\alpha$  and  $\beta$  chains<sup>6</sup>. Considering this, public TCR $\alpha$  or  $\beta$  chains would not be expected to bias TCR recognition, as each public TCR $\alpha$  or  $\beta$  chain may associate with a vast array of distinct  $\alpha$  or  $\beta$  chains that contribute roughly equally to recognition. However, it has also been shown that certain TRAV and TRBV chains are preferentially employed in specific responses<sup>38-41</sup>. In some extreme cases, certain TCR sequences are broadly shared between individuals, and therefore can be referred to as a 'public' repertoire<sup>42-44</sup>.

What is the underlying mechanism of TCR bias? Biased TCR repertoire may result from different factors. First, a number of analyses were performed on public CD8<sup>+</sup> T cell responses to persistent infections such as human HIV<sup>45,46</sup>, Epstein-Barr virus (EBV)<sup>47,48</sup> and cytomegalovirus (CMV)<sup>49-51</sup>, suggesting chronic antigenic stimulation can impose the selective expansion of T cell clonotypes with optimal TCR structural features<sup>49,51</sup> in immune responses. Nevertheless, chronic viral antigenic stimulation is not necessarily required for promoting biased TCR usage, since it is also found in acute viral infection<sup>52-55</sup> or after immunization<sup>39,56-59</sup>. The other evidence of biased TCR usage was also be found associated with autoimmune disease such as multiple sclerosis<sup>56,60,61</sup> and type 1 diabetes<sup>62</sup> or alloreactivity<sup>63</sup>.

The other events influencing the TCR bias may happen either in the pre-selected repertoire or during thymic selection. A model of convergent recombination was proposed by Venturi *et al.*, as a process whereby multiple recombination events 'converge' to produce the same nucleotide sequence and multiple nucleotide sequences 'converge' to encode the same amino-acid sequence. This process enables some TCR sequences to be produced more frequently than others during somatic recombination<sup>44</sup>. On the other hand, studies indicated that CDR1 and CDR2 domains of TCR V regions are 'hard-wired' with an inherent propensity to recognize conserved features in the MHC  $\alpha$ -helices, thymic selection may shape the TCR repertoire with intrinsic TCR reactivity to self-MHC. The consequence of this bias towards MHC can result in a preferential usage of certain V regions in the TCR repertoire<sup>64,65</sup>.

## Treg Cells

### Treg Identification

As we mentioned above, both positive and negative selection shape the pre-immune TCR repertoire based on TCR affinities<sup>66</sup>. Besides that, a specialized lineage of CD4<sup>+</sup> T cells with TCR affinities for self-MHC will differentiate into regulatory T cells. Tregs play an essential role in mediate peripheral tolerance<sup>67,68</sup>. Tregs derived from thymus are referred to as natural Treg cells (nTreg), whereas Tregs generated in secondary lymphoid organs by foreign antigen stimulation are referred as induced Tregs (iTreg)<sup>69</sup>.

It was proposed more than 40 years that a distinct subset of T cells generated from thymus is responsible for immune suppression<sup>70</sup>. The first evidence came from mouse neonatal thymectomy studies, mice thymectomized on the third day after birth (d3Tx) of neonatal mice developed organ specific autoimmune disease. However, the autoimmune disease could be totally prevented by thymus transplantation between days 10 and 15 of life. This observation suggests thymocytes may contain a subset of suppressor cells which are exported from the thymus later than autoreactive T-cells<sup>71</sup>. Furthermore, Sakaguchi and his colleagues identified and characterized this subset of suppressor CD4<sup>+</sup> T-cells their constitutively expressed CD4 and IL-2 receptor  $\alpha$  chain (CD25)<sup>72,73</sup>. However, CD25 is highly expressed on both activated CD4 and CD8 T cells, compromising its usefulness as a Treg restricted marker<sup>74</sup>. A major advance in the study of Treg was derived from the discovery of a genetic mutation in humans, immunodysregulation, polyendocrinopathy and enteropathy, X linked syndrome (IPEX). The mutation genetic locus encodes a forkhead winged-helix transcription factor family member Foxp3<sup>75</sup>. Similar as studies on scurfy mice, Foxp3-gene knockouts resulted in complete loss of Treg cells and severe autoimmune disease<sup>76</sup>. The most important thing is that expression of Foxp3 is specifically restricted to Treg lineage and required for Treg cell development in the thymus<sup>74,77-80</sup>. Foxp3-GFP knocked in mice were developed by Rudensky *et al.*, permitting ready identification and isolation of Foxp3<sup>+</sup> Treg by cell sorting<sup>81</sup>. Treg cells make up approximately 10%-15% of mouse CD4<sup>+</sup> lymphocytes, and approximately 5%-10% of CD4<sup>+</sup>CD8<sup>-</sup> thymocytes<sup>74</sup>.

### Treg Development Models

The common view about Treg origin is that the majority of Tregs are generated in the thymus as a distinct T cell subpopulation, bearing with high-affinity TCR-peptide-MHC interactions. Studies were conducted using several double transgenic mice models. When TCR transgenic mice bearing a TCR specific for a determinant (S1) derived from influenza hemagglutinin (HA) were crossed to mice expressing the HA transgene, the transgenic T cells developed a large portion of Tregs rather than deletion. In contrast, thymocytes bearing TCRs with low affinity to S1 reduced the percentage of Treg, which suggested that the selection of Treg appeared to require a TCR with high affinity for self-

pMHC<sup>82-84</sup>. But why only 50% of the exported thymocytes developed into Tregs rather than 100% in that mice model is not clear, implying there is a “niche” size for Treg cell development<sup>85</sup>. An alternative model for the differentiation for thymic Treg was proposed by van Santen *et al.*<sup>86</sup>. In experiments where the transgenic TCR was confronted with their specific pMHC ligand in the thymus, the percentage of Treg cells increased without a change in absolute numbers. Thus, selective survival might be an alternative explanation for Treg differentiation.

Mature nTregs are emigrants from the thymus, however, it is not the only place for the generation of Foxp3<sup>+</sup> Treg cells. In some extrathymic condition, Foxp3<sup>+</sup> T cells can be induced from peripheral non-Treg cells, referred as adaptive Tregs or induced Tregs (iTregs), which acquire similar suppressor phenotype and function as nTreg<sup>87</sup>. *In vivo*, cell transfer experiment demonstrated that approximately 5% splenic CD4<sup>+</sup>CD25<sup>-</sup> T cells were converted to CD4<sup>+</sup>CD25<sup>+</sup> suppressor cells in RAG -knockout recipient mice which expressed transgenic antigens<sup>88</sup>. TGF- $\beta$  is a pivotal factor for Treg generation *in vitro* through triggering the Smad2/3 signal pathway<sup>89</sup>. In addition, the vitamin A metabolite retinoic acid (RA), which is produced by a subset of DCs in the gut-associated lymphoid tissue, is able to inhibit IL-6 mediated T<sub>H</sub>17 cell induction. In the presence of TGF- $\beta$ , RA facilitates the conversion of Foxp3<sup>-</sup> T cells to Foxp3<sup>+</sup> Treg cells<sup>90,91</sup>. Furthermore, low doses stimulation in sub-immunogenic conditions can induce Treg generation in the periphery particularly to self-components that do not lead to tolerance in the thymus<sup>87,92</sup>. That may explain why majority iTreg is generated in the gut-associated lymphoid tissue since it is enriched for commensal bacteria antigens, and CD103<sup>+</sup> DCs, which serve as the main source for RA and TGF- $\beta$ <sup>93,94</sup>.

## Treg Repertoire

How can Treg precursors commit to Treg lineage instead of negative selection if they possess high-affinity TCR-peptide-MHC interactions? By using GFP-Foxp3 knock-in mice, Hsieh *et al.* was able to reveal the selection of T cells into the Treg lineage at the transition from DP to SP, indicating commitment of Treg lineage and negative selection at the same stage<sup>95</sup>. In addition, double transgenic mice model revealed that the proportion of regulatory T cells declined with decreased TCR affinity and the affinity range permissive for Treg development overlaps considerably with the range promoting negative selection<sup>96</sup>. However, Treg cell development is accompanied by deletion of T cells sharing the same TCR, and the relative proportions of cells undergoing either negative selection or commitment to Tregs change with the doses of agonist peptide/MHC<sup>96</sup>. These results suggest that Treg commitment may be due to other intrinsic and extrinsic factors besides TCR affinity.

What factors decide the commitment to Treg lineage instead of non-Treg lineage? TCR repertoire analysis has been applied on Foxp3 deficient mice. The same TCR as used by suppressive Treg cells in normal mice could be used by pathogenic autoimmune T conventional cells (Tconv), suggesting normal mice might have a population of self-reactive Tconv that express the Treg self-reactive TCR repertoire<sup>95</sup>. Very few studies

have addressed in detail either the TCR repertoire of Treg or their antigen specificity due to the limitation of methods. TCR repertoire analysis has been shown great potential to compare the TCR repertoire between Treg and Tconv. TCR repertoire analysis in pre immune mice demonstrated that naturally arising Tconv and Treg cells share a portion of TCRs that, depending on the experimental model and evaluation method, varies from 10% – 42%<sup>97-99</sup>. Not only to investigate the TCR repertoire in thymus, has TCR repertoire analysis also been utilized to survey the interconversion between Treg and Tconv repertoire at the loci of inflammation. In one diabetes model, only limited Treg and Tconv cell overlap was found in islets, suggesting that these cell types were not interconverting at the site of inflammation<sup>100</sup>. Meanwhile, Liu *et al.* performed repertoire analyses and functional assessments of isolated TCRs from TCR $\alpha$  retrogenic mice immunized with MOG-EAE. The result demonstrated that that ontogenically distinct Treg and Tconv cell repertoires with convergent specificities for autoantigen respond during autoimmunity<sup>101</sup>. In addition, high-throughput sequencing and global analysis were further conducted on normal MOG-EAE mice, showing differences in sequence and physical characteristics distinguish Treg and Tconv TCR<sup>102</sup>.

### **Experimental Autoimmune Encephalomyelitis (EAE)**

As the most predominant autoimmune disorder of the central nervous system (CNS), multiple sclerosis (MS) affects approximate 2.5 million people worldwide<sup>103</sup>. Over the last eighty years, scientists developed EAE models to elucidate the pathogenesis of the disease or to test new therapeutic approaches<sup>104</sup>. EAE is a demyelinating disease of the CNS, with T cell and macrophages dominating the inflammatory response, causing destruction of axonal myelin sheath in the CNS and further neuronal damage<sup>105</sup>. Disease is most commonly induced in susceptible mice strains by immunization with immunodominant epitopes of myelin proteins such as MBP<sub>1-9</sub> (myelin basic protein)<sup>106</sup>, PLP<sub>139-151</sub> (proteolipid protein)<sup>107</sup>, or MOG<sub>35-55</sub> (myelin oligodendrocyte glycoprotein)<sup>108</sup> together with complete Freund's adjuvant and pertussis toxin. Activated encephalitogenic T cells then infiltrate into the CNS and initiate disease. Mice usually develop an acute episode of paralysis following by a spontaneous resolution. The disease symptoms of EAE reflect the anatomical location of the inflammatory lesions, which is similar to MS. However, the pathology of MS is quite heterogeneous since abnormal CD4<sup>+</sup> T-cells, CD8<sup>+</sup> T-cells, B-cells and activated microglia/macrophages are correlated for the lesion development in MS patients<sup>105</sup>. Though there is no single EAE model, which can mimic MS as a whole, this will not preclude the study about the self-limiting nature of this CNS disease model. Foxp3<sup>+</sup> regulatory T cells (Treg) are the effective suppressors responsible for disease resolution a regulatory network capable of suppressing vigorous auto-reactive response<sup>109-111</sup>. This model therefore provides a good basis to investigate regulatory mechanisms in CNS autoimmune disease.

## High-throughput Sequencing (HTS)

The adaptive immune system generates a large pool of T cell clonotypes to fight against innumerable pathogenic antigens. The germ line genome is limited in size, however, the immune system compensates this by introducing the V(D)J somatic recombination. Focused on TCR, the receptor diversity is focused on a small segment of the TCR $\alpha$  and  $\beta$  chain genes, the CDR3 region, which directly engage with peptide-MHC complex<sup>6</sup>. On average, it is grossly estimated that there are 20 - 200 T cells for each single clonotype in the periphery<sup>112</sup>, however, the frequencies vary dramatically due to a cell's specificity and immunologic history<sup>113</sup>. Analyses of the TCR repertoire may provide insight into the nature and dynamics of these immune responses<sup>114-116</sup>. Traditional sequencing method may no longer meet the needs to investigate TCR repertoire systematically due to low time cost efficiency and limited sample size<sup>97,101</sup>. Advances in high-throughput sequencing have enabled the development of a powerful new technology for probing the adaptive immune system<sup>115,117</sup>. First of all, high-throughput immunosequencing allows millions T cell receptor sequences can be read in parallel from a single sample. The dynamics of an adaptive immune response, which is based on clonal expansion and contraction, can be monitored in real time at high sensitivity and the global properties of the adaptive immune repertoires can be studied. Second, the highly variable CDR3 regions, which serve as tag for TCR are pretty short (~15-60 nt), making them amenable to rapid interrogation. Third, HTS has been successfully employed in many global adaptive immune repertoire property analyses where there is immune compromise, suggesting a potential clinical utility. Those areas cover the aging immune system<sup>118</sup>, immunotherapy<sup>119</sup> and autoimmune disease<sup>120</sup>, etc. On the other hand, public clonotypes are associated with human disease or common pathogens within a specific HLA context<sup>121</sup>. Identification of public clonotypes in patients provides a potential diagnostic application.

## CHAPTER 2. METHODOLOGY

### Mice and Materials

#### Mice

C57BL/6J (B6), B6.129P2-*Tcrb*<sup>tm1Mom</sup>/J (TCR $\beta$ <sup>-/-</sup>), B6.SJL-*Ptprc*<sup>a</sup> *Pep3*<sup>b</sup>/BoyJ (CD45.1) and B6.129P2-*Rag1*<sup>tm1Mon</sup>/J (Rag1<sup>-/-</sup>) mice were purchased from The Jackson Laboratory (Bar Harbor, ME). GFP-Foxp3 mice on a B6 background were obtained from Dr. A. Rudensky (NYU)<sup>74</sup>. Mice were bred under specific-pathogen-free conditions, and animal experiments were carried out in compliance with Institutional Animal Care and Use Committee guidelines.

#### Monoclonal Antibodies

Red blood cells were lysed prior to staining. Fc receptors were blocked with mice CD16/CD32 antibody specific for Fc $\gamma$  R III/I (Miltenyi Biotec, San Diego, CA). Cell surface staining was performed for 20 min at 4°C in PBS containing 0.1% sodium azide and 2% (vol/vol) fetal bovine serum (FBS). Monoclonal antibodies (Ab) specific for CD4 (clone RM4-5), CD8 (clone 53-6.7), TCR $\beta$  (clone H57-597), CD44 (clone 1M7), CD45RB (clone C363.16A), CD69 (clone H1-2F3), CD45.1 (clone A20) or CD45.2 (clone 104) were from BD Biosciences (San Jose, CA). For intracellular staining, cells were first stained with surface markers, fixed, permeabilized and stained for intracellular Foxp3 (clone FJK-16s) with the Foxp3 Staining Buffer Set (eBioscience, San Diego, CA). For cytokine staining, cells were first treated with 1x Cell Stimulation Cocktail (eBioscience) at 37°C for 4 hr, stained for surface markers in the presence of 10  $\mu$ g mL<sup>-1</sup> Monensin (eBioscience), followed by fixation and permeabilization and staining for IL-17A (clone eBio17B7, eBioscience) and IFN- $\gamma$  (clone XMG1.2, BD Biosciences). Flow cytometric analysis was performed on an LSRFortessa (BD Biosciences) and analyzed by using FlowJo software (Tree Star, Ashland, OR).

### High-throughput Sequencing

#### EAE Immunization

MOG<sub>35-55</sub> peptide (MEVGWYRSPFSRVVHLYRNGK) was synthesized by St. Jude Hartwell Center for Biotechnology and HPLC purified prior to use. EAE was induced and scored as described<sup>102</sup>. In brief, B6 mice were s.c. immunized with 100  $\mu$ g of MOG<sub>35-55</sub> peptide in complete Freund's adjuvant containing 0.4 mg *Mycobacterium tuberculosis* H37RA (Difco, Lawrence, KS). Two hundred nanograms of pertussis toxin (List Biological Laboratories, Campbell, CA) was administered i.v. on day 0 and day 2.

Clinical scoring was: 1, limp tail; 2, hind limb paresis or partial paralysis; 3, total hind limb paralysis; 4, hind limb paralysis and body or front limb paresis or paralysis; 5, moribund.

### **Cell Isolation**

Mice were sacrificed by CO<sub>2</sub> asphyxiation and the spleens, lymph nodes, thymi were removed and collected individually in 6cm diameter dishes. Cells from these tissues were squeezed through the 70µm nylon mesh by gently mashing with the rubber end of a plunger from a 3cc syringe. A single cell suspension was created and harvest into a 50ml conical tube. Usually red blood cells need to be lysed for splenic cells.

For CNS tissue, the mice were anesthetized by intraperitoneal administration of a lethal dose of Avertin (0.5ml of 2.5%, Sigma-Aldrich, St. Louis, MO). After complete anesthetization, the mice were placed on a polystyrene board and pinned down. The mice abdomen and chest were opened. The right atrium of the heart was cut open, and a 271/2 g needle was immediately inserted into the left ventricle slowly perfused with PBS. After PBS perfusion, the brain and spinal cord were gently collected. The CNS tissue was gently mashed through a 70µm nylon cell strainer with the rubber end of a plunger. The cell suspension was spun down at 1500 rpm for 10 minutes and resuspended in 15ml of 37.5% Percoll (GE Healthcare Bio-Sciences, Piscataway, NJ). After centrifuging at 1500 rpm for 10 minutes with soft break, supernatant was gently discarded. The cell pellets were washed with PBS and then spun down again.

### **Cell Counting**

Cell numbers were automatically calculated by Beckman cell coulter. As an alternative, adequately diluted cell suspension was thoroughly mixed with trypan blue and read on hemocytometer chamber. The total number of live cells was counted in the four corner squares. The cell concentration per ml was calculated as following equation.

$$\text{Cells per ml} = \text{the average count per square} \times \text{the dilution factor} \times 10^4$$

### **Cell Sorting**

T cells were isolated from spleen, CNS, and thymus as described. Splenic and CNS cells were stained with CD4 Ab and flow cytometrically sorted into CD4<sup>+</sup> GFP-Foxp3<sup>+</sup> (Treg) and CD4<sup>+</sup> GFP-Foxp3<sup>-</sup> (Tconv) populations. Some splenic Tconv cells were further sorted into CD4<sup>+</sup>CD44<sup>hi</sup>CD45RB<sup>lo</sup> (memory/effector) and CD4<sup>+</sup>CD44<sup>lo</sup>CD45RB<sup>hi</sup> (naïve) populations. Thymic T cells were stained with CD4, CD8, and TCR Abs and sorted into CD4<sup>+</sup>CD8<sup>+</sup>TCR<sup>lo</sup> double positive, CD4<sup>+</sup>CD8<sup>-</sup>Foxp3<sup>-</sup>, and CD4<sup>+</sup>CD8<sup>-</sup>Foxp3<sup>+</sup> single positive T cell populations. Flow cytometric sorting used a Reflection (Sony Biotechnology, Champaign, IL) sorter.



## RNA Isolation and cDNA Transcription

Sorted cell populations were lysed, and total RNA was isolated using the RNeasy Kit (Qiagen, Valencia, CA). cDNA was produced using the Omniscript RT Kit (Qiagen) according to the manufacturer's instructions. cDNA was amplified with C $\beta$  (5'-GGGTGGAGTCACATTTCTCAGATC-3') and Vb8.2 (5'-CCCCCTCTCAGACATCAGTGTAC-3') specific primers using the High Fidelity PCR System (Roche, Indianapolis, IN). The ~200-bp PCR product was purified by agarose gel electrophoresis and column purification (QIAquick Gel Extraction Kit, Qiagen).

## DNA Preparation and Sequencing

DNA end repair was performed according to our previous protocol<sup>102</sup>. First, incubate the PCR products from cDNA transcription with 15U T4 DNA polymerase (NEB, Beverly, MA), 50U T4 polynucleotide kinase (NEB), 0.4 mM 2'-deoxynucleoside 5'-triphosphate, 1x T4 ligase buffer with 10 mM 2'-deoxyadenosine triphosphate (Promega, Madison, WI), and 5U Klenow enzyme (Promega) for 30 min at 20°C. The product was subsequently purified by using the QIAquick PCR Purification Kit (Qiagen). To add adenosine tags on the DNA 3' ends, purified DNA was incubated with 25U Klenow fragment (NEB), 1x Klenow buffer, and 0.2 mM 2'-deoxyadenosine triphosphate for 30 min at 37°C. The product was purified by using the MinElute Reaction Cleanup Kit (Qiagen) and concentrated to 10  $\mu$ l volume. Next, sequencing adapters were ligated onto the DNA products, adding 3 mM Index PE adapter Oligo Mix, 5  $\mu$ l Quick DNA ligase (NEB), and 1x ligase buffer, and incubated for 15 min at 20°C. To remove unligated adapters, the product was purified using the QIAquick Gel Extraction Kit (Qiagen). Samples were each divided into 3, and InPE 1.0 and 2.0 (Illumina®, San Diego, CA) and Index primers were next linked to the DNA, using the Phusion DNA Polymerase Kit (Finnzymes Oy, Espoo, Finland) with the following PCR condition: 19 cycles at 98°C 10 sec, 65°C 30 sec, 72°C 30 sec. The PCR products were purified using the QIAquick PCR purification kit, as above. Each sample was divided into 3, and equimolar quantities of each sequenced over three lanes of a flow cell with an Illumina® Genome Analyzer IIx sequencer using a 125 bp (plus 6 bp barcode) recipe to obtain single-end reads that cover the entire CDR3 $\beta$  region.

## Raw Data Trim

Raw data was demultiplexed and filtered using CASAVA 1.6.0. The data was subsequently trimmed for the presence of adapter sequences using CLC Genomics WorkBench v4.0. The Illumina® 125-bp reads were then scanned for V $\beta$  and J $\beta$  sequence homology immediately external to the C and F residues bordering the CDR3 using cross\_match <http://www.phrap.org/>. To identify CDR3 sequences, reads were filtered based on the cross\_match results using the following criteria: (i) 100% sequence

identity for both V $\beta$  and J $\beta$  mapping; (ii) translated amino acid sequence between V $\beta$  and J $\beta$  is in the correct frame and reveals a translated product (no stop codon); (iii) the deduced CDR3 amino acid sequences between the V $\beta$  and J $\beta$  sequences begin with the conserved C and end with a FGXG, FAXG or HGXG motif. The deduced CDR3 nt sequences were then scanned using the Phred quality score cutoffs of 0, 10, 20 or 30, and reads with CDR3 nt sequence containing at least one low quality base at a given cutoff level were filtered out

## Retrogenic Mice Models

### Molecular Subcloning

The backbone construct is MSCV-IRES-GFP<sup>122</sup>, which was further designed for the sake of our experiments<sup>101,123</sup>. To generate the TCR $\beta$ 1-GFP construct which expresses single TCR $\beta$  chain, the TRBV13-2<sup>+</sup> TCR $\beta$  segment was PCR amplified from 1MOG244.2<sup>123</sup> (forward primer: 5'-GCCGAATTCGCCACCATGTCTAACAACACTGCCTTC-3'; reverse primer: 5'-GGGTAGCCAACTCGAGAATGAG-3') and subcloned into EcoRI/XhoI sites in the IRES-GFP retroviral vector. The TCR $\beta$ 1-CDR3-J $\beta$  segment was created by annealing a pair of complementary oligos synthesized by St. Jude Hartwell Center (sense oligo: 5'-TCGAGTTGGCTACCCCTCTCAGACATCAGTGTACTTCTGTGCCAGCGGTGAGACTGGGGGAACTATGCTGAGCAGTTCTTCGGACCAGGGACACGACTCACCGTCCTAGAA-3'; anti-sense oligo: 5'-GATCTTCTAGGACGGTGAGTCGTGTCCCTGGTCCGAAGAACTGCTCAGCATAGTTTCCCCCAGTCTCACCGCTGGCACAGAAGTACACTGATGTCTGAGAGGGGGTAGCCAAC-3'). This was subcloned into the XhoI/BglII cloning sites of 1MOG244.2 vector to synthetically recreate TCR $\beta$ 1. Other TCR $\beta$  constructs were similarly constructed synthetically and the oligo sequences were in **Table A-1**. pMOTII plasmid (gift from Dr. D. Vignali; SJCRH) contained the entire OTII TCR (V $\alpha$ 2-2A-V $\beta$ 5.1) cassette. OTII TCR $\beta$  sequence was PCR amplified (forward primer: 5'-GCCGAATTCGCCACCATGTCTAACAACACTGCCTTC-3'; reverse primer: GTCACATTTCTCAGATCTTCTAG-3'), digested with EcoRI/BglII, and then subcloned into the EcoRI/BglII sites of TCR $\beta$ 1-GFP (**Figure B-1a**).

To reconstitute a polycistronic MSCV construct expressing the unique TCR $\alpha$  of 1MOG244.2 and the TCR $\beta$ 1  $\beta$  chain, 1MOG244.2 and TCR $\beta$ 1-GFP constructs were both digested with EcoRI/XhoI. The digested fragment from 1MOG244.2, which included an entire TCR $\alpha$  chain, a *T. asigna* 2A sequence and the TRBJ 13-2 segment, was ligated with the cut TCR $\beta$ 1-GFP vector, generating a new plasmid named as 244.2 $\alpha$ -TCR $\beta$ 1 $\beta$ -GFP (**Figure B-1b**). The other polycistronic constructs expressing different TCR $\alpha$  chain but fixed TCR $\beta$ 1  $\beta$  chain were reconstituted on 244.2 $\alpha$ -TCR $\beta$ 1 $\beta$ -GFP. The secondary BglII behind the CDR3 $\beta$  was destroyed without disturbing the amino acid sequences by using Quick change site directed mutagenesis kit (Agilent Technologies, Santa Clara,

CA). Different TCR $\alpha$  chains including TRAV and CDR3 $\alpha$  were amplified and subcloned into the EcoRI/BglII cloning sites of 244.2 $\alpha$ -TCR $\beta$ 1 $\beta$ -GFP.

### **Retroviral Transduction**

Retrovirus was produced as described<sup>123</sup>. Ten micrograms of retroviral construct and packing plasmid were cotransfected into 293 T cells using the calcium phosphate transfection method, and the cells were incubated in DMEM supplemented with 10% fetal bovine serum (Atlanta Biologicals, Lawrenceville, GA), 100 U mL<sup>-1</sup> penicillin, 100  $\mu$ g mL<sup>-1</sup> streptomycin, and 292  $\mu$ g mL<sup>-1</sup> L-glutamine (Invitrogen Life Technologies) at 37°C for 36 hr. Supernatant was collected twice a day for 72 hr and used to infect GP+E86 retroviral producer cells in the presence of 8  $\mu$ g mL<sup>-1</sup> polybrene (Sigma-Aldrich, St. Louis, MO).

### **Generation of Retrogenic Mice**

Donor TCR $\beta$ <sup>-/-</sup> mice received 0.15 mg 5-fluorouracil g<sup>-1</sup> body weight i.p. (APP Pharmaceuticals, Schaumburg, IL). After 48 hr, bone marrow cells were harvested from the femurs of the mice and cultured in complete Click's medium (Invitrogen, Grand Island, NY) supplemented with 20% fetal bovine serum (FBS), 20 ng mL<sup>-1</sup> mIL-3, 50 ng mL<sup>-1</sup> hIL-6, and 50 ng mL<sup>-1</sup> mSCF (Pepro Tech, Rocky Hill, NJ) for 48 hr. Next, the hematopoietic progenitor cells (HPCs) were collected and cocultured for another 48 hr with irradiated (1200 rads) GP+E86 retrovirus producer cells in complete Click's medium supplemented as above and with 6  $\mu$ g mL<sup>-1</sup> polybrene. Then, the HPCs were harvested, re-suspended in PBS supplemented with heparin (10 U per recipient mouse, Sigma-Aldrich), and injected i.v. into the sublethally irradiated (450 rad) Rag1<sup>-/-</sup> recipients at a ratio of two recipient mice per bone marrow donor. Transduction efficiency was confirmed by flow cytometry for GFP expression. Engraftment was analyzed on day 28 after HPC transplantation.

### **Clinical Evaluation**

Cohorts of retrogenic mice were generated and clinically monitored for  $\geq 120$  days after HPC transfer. Mice were processed and submitted for histopathologic examination either during the peak disease or after 120 days if healthy. Full necropsy including CNS tissues was processed on at least three mice for each cohort for concurrent inflammatory and degenerative lesions. Paraffin-embedded tissue samples were stained with hematoxylin and eosin (H&E) and, where appropriate, CD3. The severity of spontaneous EAE was scored by using the predetermined qualitative and semiquantitative criteria: 0, lesions absent, 1, minimal to mild inconspicuous lesions, 2, conspicuous lesions, 3, prominent multifocal lesions, 4, marked coalescing lesions.

## Chimeric Mice

HPCs from CD45.1<sup>-</sup>CD45.2<sup>+</sup> TCR $\beta$ <sup>-/-</sup> mice were transfected with TCR $\beta$ 1 retrovirus as described above. Retrogenic HPCs were harvested and diluted with CD45.1<sup>+</sup>CD45.2<sup>-</sup> syngeneic B6 bone marrow cells, and subsequently injected into irradiated (450Rads) CD45.1<sup>+</sup>CD45.2<sup>-</sup> Rag1<sup>-/-</sup> mice at a ratio of two recipient mice per bone marrow donor. Engraftment was analyzed at day 28 after HPC transplantation. Disease incidence was monitored for at least 60 days.

## Cell Proliferation Assay

Splenic cells were isolated from retrogenic mice and CD4<sup>+</sup> T cells were purified with anti-CD4 Ab (L3T4) coated microbeads (Miltenyi Biotec, San Diego, CA) and enriched using MACS separation columns (Miltenyi Biotec). Purified CD4<sup>+</sup> T cells were co-cultured at  $5 \times 10^4$  per well in 96-well plates with  $2 \times 10^5$  irradiated (3500 rad) syngeneic splenic APCs and stimulated with 100  $\mu\text{g ml}^{-1}$  MOG<sub>35-55</sub> peptide for 72 hr, pulsed with 1  $\mu\text{Ci}$  <sup>3</sup>H-thymidine (PerkinElmer, Boston, MA), and harvested 16 hr later for scintillation counting. To further assess the dividing cell fraction, the Cell Trace violet cell proliferation kit (Invitrogen) was used according to the manufacturer's instruction. Cells were labeled with 5  $\mu\text{M}$  CellTrace<sup>TM</sup> violet prior to culture with the indicated stimuli for 72 hr. The cells were then stained with surface markers and 7-AAD (BD Biosciences) and viable CD4 T cell proliferation was measured by dye dilution. As a positive control, 1  $\mu\text{L}$  Mouse T-Activator CD3/CD28 Dynabeads (Invitrogen) were added to positive control wells to at a 1:1 bead-to-cell ratio.

## Cytokine Analysis

Culture supernatants were collected at 48 hr and analyzed for IL-2, IL-4, IL-10, IFN- $\gamma$ , and IL-17A using the Milliplex MAP mouse cytokine/chemokine immunoassay kit (Millipore, Billerica, MA) on a Luminex (Bio-Rad) instrument. For intracellular cytokine staining, cells were cultured with 1x Cell Stimulation Cocktail (eBioscience) at 37°C for 4 hr, stained for surface markers in the presence of 10  $\mu\text{g ml}^{-1}$  monensin (eBioscience), followed by fixation and permeabilization, and intracellular staining with IL-17A and IFN- $\gamma$  Abs.

## Retroviral Transfection of CD4<sup>+</sup>4G4 Hybridoma Cell

Transfected GP+E86 retroviral producer cell lines were expanded in 75ml flasks. Twelve milliliter of retroviral supernatant was harvested from each day confluent GP+E86 producer cells. To transfect hybridoma cells,  $1 \times 10^6$  TCR-deficient CD4<sup>+</sup> 4G4 hybridoma cells<sup>101</sup> were resuspended in 3 ml retroviral supernatant in the presence of 6  $\mu\text{g/ml}$  polybrene. The cell suspension was centrifuged at 1800 rpm, 8°C for 90 minutes. The infected cells were then cultured at 37°C for 48hrs and cytometrically sorted twice

for the GFP<sup>high</sup>TCR<sup>high</sup> population and expanded. The purity of the GFP<sup>high</sup>TCR<sup>high</sup> 4G4 cells was confirmed by flow cytometry (BD FACSCalibur).

### **Enzyme-linked Immunosorbent Assay (ELISA)**

In 96 well flat bottom plates,  $1 \times 10^5$  hybridoma cells were co-cultured with  $3 \times 10^5$  (3500 rad) irradiated syngeneic splenic APCs in the presence of indicated stimuli for 24 hr. Purified CD3 antibody was pre-mounted in positive control wells. Culture supernatant was harvested for IL-2 ELISA assay (BD PharMingen). Purified anti-IL-2 capture antibody (clone MQ1-17H12) was diluted to 2 µg/ml in binding solution. 100 µl of the diluted antibody solution was added per well of a 96-well ELISA plate (Nunc Maxisorb). The plate was sealed and incubated overnight at 4°C. The capture antibody solution was discarded, and non-specific binding was blocked by adding 200 µl of blocking buffer per well (BD Bioscience), and incubated at RT for at least 2hrs. After wash with PBS/Tween (PBS and 0.1% Tweens) for 3 times, 100 µl of culture supernatants were added to the each sample well, meanwhile a series of nine 2-fold dilutions of recombination mouse IL-2 standard (from 5000pg/ml to 19.5pg/ml) was added to standard curve wells. The plate was sealed and incubated at 4°C overnight. After washing with PBS/Tweens for 4 times, 100 µl diluted biotinylated anti-IL-2 detection antibody (1 µg/ml) was added and incubated at RT for 1 hour. Again after washing with PBS/Tween for 4 times, 100 µl diluted peroxidase labeled anti-biotin (Vector laboratories, Burlingame, CA) was added and incubated at RT for 30 minutes. The plate was washed for 5 times and 100 µl of ABTS substrate solution with hydrogen peroxide was added for color development. After color developed for 5-10 min, the optical density value was read on a microplate reader instrument (Bio-Rad) setting to 405nm.

### **5'RACE**

T cells were isolated from the CNS of TCRβ1 retrogenic mice with disease scores  $\geq 3$ . RNA was isolated and 5' RACE performed using the 5'/3' RACE Kit, 2nd Generation (Roche, Indianapolis, IN) following the manufacturer's instructions. Briefly, full strand cDNA was synthesized from mRNA by using specific primer 1 (5'-GGAGTCAAAGTCGGTGAACAG-3'). The mRNA template was degraded by Transcriptor Reverse Transcriptase. PolyA was added to the 3' end of the cDNA, and the tailed cDNA was PCR amplified using the Oligo (dT) anchor primer (5'-GACCACGCGTATCGATGTCGACTTTTTTTTTTTTTTTTV-3') and a nested specific primer 2 (5'-CCTGAGACCGAGGATCTTTTAAC-3'). A second PCR reaction was performed with the PCR anchor primer (5'-GACCACGCGTATCGATGTCGAC-3') and a nested specific primer 3 (5'-CAGGTTCTGGGTTCTGGAT-3'). PCR products were subsequently cloned with TOPO TA (Invitrogen). Bacterial clones were randomly selected for Sanger sequencing, and sequences identified using the IMGT database (<http://www.imgt.org/>).

## Statistics

Means and SDs were calculated in Excel or PRISM. Plots demonstrate mean  $\pm$  1 SD. Two-tailed student t-tests were applied to compare any two groups and ANOVA for three or more groups. For multiple comparisons, significance is only shown for indicated groups. A  $p < 0.05$  was considered statistically significant. Kaplan Meier curves were calculated in PRISM.

## CHAPTER 3. RESULTS

### Introduction

Despite the theoretical diversity of the TCR repertoire, a small fraction of  $\alpha$  and  $\beta$  monomers are shared by most individuals, or public<sup>42,44</sup>. Public TCR largely result from recombinatorial biases in TCR  $\alpha$  and  $\beta$  chain formation, and in some studies were found to be prevalent in autoimmune and other responses<sup>43,124-126</sup>. Unlike antibodies, which can engage antigens in highly variable manners, TCR $\alpha\beta$  heterodimers associate with pMHC in largely stereotypical orientations that require significant energy contributions from both the TCR  $\alpha$  and  $\beta$  chains<sup>6</sup>. Considering this, public TCR  $\alpha$  or  $\beta$  chains would not be expected to bias TCR recognition, as each public  $\alpha$  or  $\beta$  may associate with a vast array of distinct  $\beta$  or  $\alpha$  chains that contribute roughly equally to recognition. However, it has also been shown that certain TRAV and TRBV chains are preferentially employed in specific responses<sup>38-41</sup>, and in one case structural data identified a binding “hotspot” between a single TRBV and antigen-MHC ligand explaining this preference<sup>124</sup>.

Considering this, we hypothesized that public  $\alpha$  or  $\beta$  chains, which are fixed not only for the V region, but for J and CDR3 sequences may modulate a TCR $\alpha\beta$  heterodimer’s likelihood of productively engaging autoantigen. Because public TCR chains are shared throughout a population and, due to their preferential formation, often present at high frequency<sup>127</sup>, they may in theory also broadly influence autoimmune susceptibility.

Here we use a model of CNS autoimmune disease, experimental autoimmune encephalomyelitis, to identify the role of public TCR chains in disease susceptibility, coupling high-throughput analyses of the TCR $\beta$  repertoire with functional studies and the transgenic expression of 15 disease-associated public and private TCR $\beta$ . Analyses of >18 million TCR $\beta$  from Foxp3<sup>+</sup> regulatory and Foxp3<sup>-</sup> conventional T cells from different organs and time points identified a high prevalence of public TCR within the autoimmune response, consistent with previous lower resolution analyses in other models.

### Results

#### High Prevalence of Public TCR $\beta$ in the Autoimmune Repertoire

##### Demographic information of the sequenced TCR $\beta$ repertoires

To understand the composition and dynamics of autoimmune effector and regulatory repertoires, we analyzed CD4<sup>+</sup> Foxp3<sup>-</sup> (Tconv) and Foxp3<sup>+</sup> (Treg) TRBV13-2<sup>+</sup> TCR $\beta$  in mice with myelin oligodendrocyte glycoprotein (MOG)<sub>35-55</sub>-induced EAE and healthy controls. TRBV13-2 is the dominant TCR $\beta$  in MOG-specific T cells<sup>128</sup>.

Saturation sequencing was performed using high-throughput techniques, with  $>18 \times 10^6$  TCR studied<sup>43,102,117,129,130</sup>, either from control mice (**Table 3-1**), EAE immunized mice with early disease (**Table 3-2**) or EAE immunized mice with late disease (**Table 3-3**).

### **TRBJ utilization**

TRBJ utilization, an indicator of the heterogeneity of the sequenced populations, was compared in Tconv and Treg from the CNS and spleens of mice with EAE and spleens of controls and analyzed by one-way ANOVA. The results demonstrated that TRBJ utilization was diverse and similar among these sample groups, not matter the comparison was for unique sequences, which represented clonotype diversity, or total sequences, which represented both diversity and abundance. Only a slightly increased frequency for TRBJ 2.1 usage was seen in Tconv and Treg from the CNS with early EAE (**Figure 3-1**).

### **CNS infiltrating TCR repertoires mapped onto splenic TCR repertoire**

When we performed routine phenotypic staining on the CNS infiltrating T cells, we found the majority of CNS infiltrating Tconv cells had activated, memory/effector T cell phenotype with high level CD69 and CD44 expression. Therefore we tried to trace the cell origin by comparing the TCR $\beta$  repertoires of CNS Tconv cells with the splenic memory and naïve TCR $\beta$  repertoires. The results demonstrated that the splenic sequences identified in the CNS were heavily biased toward the memory/activated subset (77.7 $\pm$ 9.0% of unique, 99.0 $\pm$ 0.7% of total TCR $\beta$  sequences acquired) (**Figure 3-2**), indicating that the CNS was infiltrated by highly diverse, activated T cell populations from the periphery.

### **Over representation of shared TRBV13-2<sup>+</sup> TCR $\beta$ among CNS-infiltrating T cells**

Due to the limited size of the CNS infiltrates, relatively small numbers of unique sequences were identified in the CNS repertoires (**Table 3-2** and **Table 3-3**). Of these, 9.2% of the unique Foxp3<sup>-</sup> CNS sequences present in mice with early EAE (d 15-18) were shared by  $\geq 2$  of 9 mice (**Figure 3-3a**). However, the shared sequences comprised 50.8% of total CNS sequences acquired, indicating a high prevalence of the shared TCR $\beta$ . Similarly, in 3 mice analyzed with late disease (d 26), 8.1% of unique sequences were shared, but these comprised 49.6% of total CNS Foxp3<sup>-</sup> sequences (**Figure 3-3d**). Progressively smaller numbers of unique Foxp3<sup>-</sup> TCR $\beta$  were shared in the CNS by increasing numbers of mice (**Figure 3-3b, e**). Meanwhile, we noticed the shared TCR $\beta$  had a pattern to be over-represented due to clonal expansion. For example, 0.05% of unique CD4<sup>+</sup> Foxp3<sup>-</sup>-derived TCR $\beta$  sequences were identified in  $\geq 7$  of the 9 early EAE CNS, but comprised  $>1.5\%$  of total sequences acquired. Therefore, we calculated the frequency of identification of each unique amino acid sequence relative to that of an average sequence in the same CNS. The representation ratio increased along with the increasing number of shared mice, suggesting these shared TCR $\beta$  were heavily utilized (**Figure 3-3c, f**). A similar pattern of high shared TCR representation was evident with CNS-infiltrating Treg cells (**Figure 3-3g-l**).



**Table 3-1. Description of TRBV13-2<sup>+</sup> TCR sequences acquired from control mice.**

Mouse	Organ	Cell type	Total sequences acquired	Unique CDR3 aa sequences acquired	Unique CDR3 nt sequences acquired
1	Spleen	Foxp3 <sup>-</sup>	281,344	73,570	106,280
	Spleen	Foxp3 <sup>+</sup>	440,281	23,277	29,429
2	Spleen	Foxp3 <sup>-</sup>	62,062	27,752	36,092
	Spleen	Foxp3 <sup>+</sup>	111,605	14,542	17,415
3	Spleen	Foxp3 <sup>-</sup>	290,060	66,792	94,807
	Spleen	Foxp3 <sup>+</sup>	270,998	19,853	24,702
	Thymus	CD4 <sup>+</sup> CD8 <sup>+</sup> TCR <sup>lo</sup>	256,784	61,634	76,304
4	Spleen	Foxp3 <sup>-</sup>	438,870	52,958	74,596
	Spleen	Foxp3 <sup>+</sup>	351,528	24,441	31,038
	Thymus	CD4 <sup>+</sup> CD8 <sup>+</sup> TCR <sup>lo</sup>	393,817	75,945	95,070
5	Thymus	CD4 <sup>+</sup> CD8 <sup>+</sup> TCR <sup>lo</sup>	216,474	47,159	58,864
6	Thymus	CD4 <sup>+</sup> CD8 <sup>+</sup> TCR <sup>lo</sup>	280,972	52,659	65,831

Splenocytes were flow sorted for CD4, TCR and GFP-Foxp3 as indicated. The CD4<sup>+</sup>CD8<sup>+</sup>TCR<sup>lo</sup> thymic population was CD5 and CD69 negative, indicative of a pre-selection population. Numbers listed are of sequences available for analysis after culling based on sequence quality metrics.

**Table 3-2. Description of TRBV13-2<sup>+</sup> TCR sequences acquired from mice with early EAE.**

Mouse	EAE day	Disease score	Organ	Cell type	Total sequences acquired	Unique CDR3 aa sequences acquired	Unique CDR3 nt sequences acquired
1	15	3	CNS	Foxp3 <sup>-</sup>	156,144	2,874	3,421
			CNS	Foxp3 <sup>+</sup>	87,181	4,132	4,713
			Spleen	Foxp3 <sup>-</sup>	63,835	29,305	38,439
			Spleen	Foxp3 <sup>+</sup>	24,836	6,735	7,580
2	15	3	CNS	Foxp3 <sup>-</sup>	46,981	2,449	2,728
			CNS	Foxp3 <sup>+</sup>	49,642	1,439	1,658
			Spleen	Foxp3 <sup>-</sup>	97,675	37,439	52,648
			Spleen	Foxp3 <sup>+</sup>	867,145	18,941	24,258
3	16	3	CNS	Foxp3 <sup>-</sup>	103,407	3,513	3,999
			CNS	Foxp3 <sup>+</sup>	82,018	2,664	3,138
			Spleen	Foxp3 <sup>-</sup>	77,028	30,955	39,967
			Spleen	Foxp3 <sup>+</sup>	71,488	11,741	13,828
4	16	3	CNS	Foxp3 <sup>-</sup>	186,996	3,497	4,041
			CNS	Foxp3 <sup>+</sup>	264,020	3,417	4,189
			Spleen	Foxp3 <sup>-</sup>	388,207	55,115	78,185
			Spleen	Foxp3 <sup>+</sup>	53,833	6,701	7,545
8	18	3	Spleen	Foxp3 <sup>-</sup>	380,377	50,920	70,037
			Spleen	Foxp3 <sup>+</sup>	421,907	17,770	22,336
9	18	2	Spleen	Foxp3 <sup>-</sup>	327,583	62,579	89,502
			Spleen	Foxp3 <sup>+</sup>	315,408	15,389	19,027
10	15	3	CNS	Foxp3 <sup>-</sup>	274,619	2,687	3,506
			CNS	Foxp3 <sup>+</sup>	87,560	2,240	2,628
			Spleen	CD45Rb <sup>hi</sup> CD44 <sup>lo</sup> Fo xp3 <sup>-</sup>	304,477	41,969	57,395
				CD45Rb <sup>lo</sup> CD44 <sup>hi</sup> Fo xp3 <sup>-</sup>	39,229	4,961	5,527
11	15	4	Spleen	Foxp3 <sup>+</sup>	310,883	11,828	14,484
			CNS	Foxp3 <sup>-</sup>	591,007	1,700	2,261
			CNS	Foxp3 <sup>+</sup>	53,291	911	1,073
			Spleen	CD45Rb <sup>hi</sup> CD44 <sup>lo</sup> Fo xp3 <sup>-</sup>	135,721	31,439	41,642
				CD45Rb <sup>lo</sup> CD44 <sup>hi</sup> Fo xp3 <sup>-</sup>	396,380	10,393	12,541
12	18	3	Spleen	Foxp3 <sup>+</sup>	133,339	10,502	12,490
			CNS	Foxp3 <sup>-</sup>	109,483	1,410	1,726

**Table 3-2. (Continued).**

Mouse	EAE day	Disease score	Organ	Cell type	Total sequences acquired	Unique CDR3 aa sequences acquired	Unique CDR3 nt sequences acquired
13	18	4	CNS	Foxp3 <sup>+</sup>	88,279	1,508	1,857
			Spleen	CD45Rb <sup>hi</sup> CD44 <sup>lo</sup> Fo xp3 <sup>-</sup>	133,687	35,012	47,045
			Spleen	CD45Rb <sup>lo</sup> CD44 <sup>hi</sup> Fo xp3 <sup>-</sup>	192,803	12,083	14,474
			Spleen	Foxp3 <sup>+</sup>	317,907	14,737	18,525
			CNS	Foxp3 <sup>-</sup>	288,981	1,429	1,915
			CNS	Foxp3 <sup>+</sup>	42,867	1,172	1,362
			Spleen	CD45Rb <sup>hi</sup> CD44 <sup>lo</sup> Fo xp3 <sup>-</sup>	335,855	65,789	95,606
			Spleen	CD45Rb <sup>lo</sup> CD44 <sup>hi</sup> Fo xp3 <sup>-</sup>	225,451	11,932	14,176
			Spleen	Foxp3 <sup>+</sup>	290,023	14,003	17,136
			CNS	Foxp3 <sup>-</sup>	224,925	3,240	4,061
14	18	4	CNS	Foxp3 <sup>+</sup>	385,327	4,077	5,305
			Spleen	CD45Rb <sup>hi</sup> CD44 <sup>lo</sup> Fo xp3 <sup>-</sup>	304,862	46,495	64,598
			Spleen	CD45Rb <sup>lo</sup> CD44 <sup>hi</sup> Fo xp3 <sup>-</sup>	351,771	16,385	20,123
			Spleen	Foxp3 <sup>+</sup>	464,759	19,879	25,604

Cells were flow sorted for CD4, TCR, and, as indicated, GFP-Foxp3, CD45Rb, and CD44.

**Table 3-3. Description of TRBV13-2<sup>+</sup> TCR sequences acquired from mice with late EAE.**

Mouse	EAE day	Disease score	Organ	Cell type	Total sequences acquired	Unique CDR3 aa sequences acquired	Unique CDR3 nt sequences acquired
5	26	1	CNS	Foxp3 <sup>-</sup>	12,038	1,322	1,399
			CNS	Foxp3 <sup>+</sup>	25,388	3,097	3,362
			Spleen	Foxp3 <sup>-</sup>	291,902	61,300	90,429
			Spleen	Foxp3 <sup>+</sup>	299,258	13,610	16,711
6	26	2	CNS	Foxp3 <sup>-</sup>	40,212	3,629	4,039
			CNS	Foxp3 <sup>+</sup>	130,450	9,942	11,581
			Spleen	Foxp3 <sup>-</sup>	2,735,563	140,052	220,739
			Spleen	Foxp3 <sup>+</sup>	123,832	15,375	18,333
7	26	3	CNS	Foxp3 <sup>-</sup>	48,451	3,455	3,776
			CNS	Foxp3 <sup>+</sup>	1,439	809	828
			Spleen	Foxp3 <sup>-</sup>	1,247,903	88,487	132,053
			Spleen	Foxp3 <sup>+</sup>	177,834	11,042	12,892

Cells were flow sorted for CD4, TCR and the presence or absence of GFP-Foxp3.

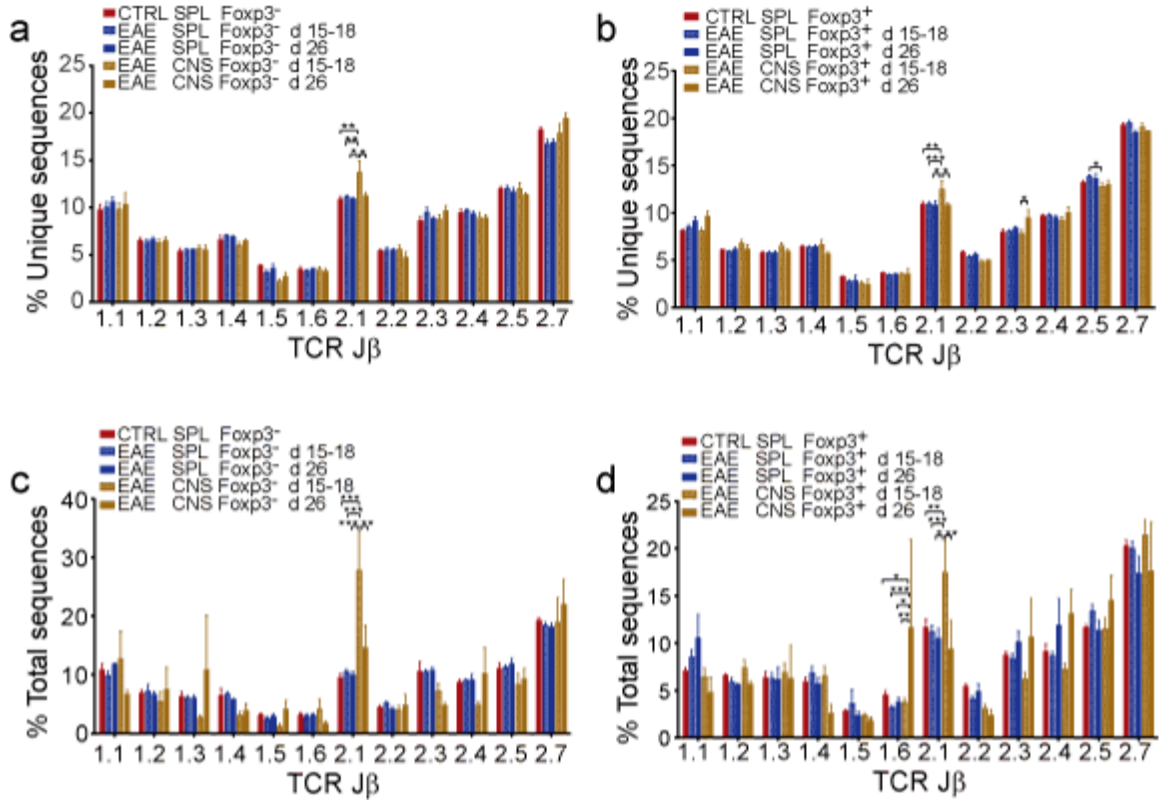


**Figure 3-1. TCR TRBJ use during EAE.**

TRBV13-2<sup>+</sup> TCRβ repertoires were determined in the spleens of pre-immune mice (n=4) and spleens and CNS of mice with early (d 15-18, n=9) or late (d 26, n=3) EAE. TRBJ use was tabulated for acquired sequences as an indicator of repertoire diversity. Mean+1 s.d. percent of unique (a, b) or total (c, d) TRBJ use by CD4<sup>+</sup>GFP-Fxp3<sup>-</sup> (a, c) and CD4<sup>+</sup>GFP-Fxp3<sup>+</sup> (b, d) derived TCRβ from individual mice is plotted.

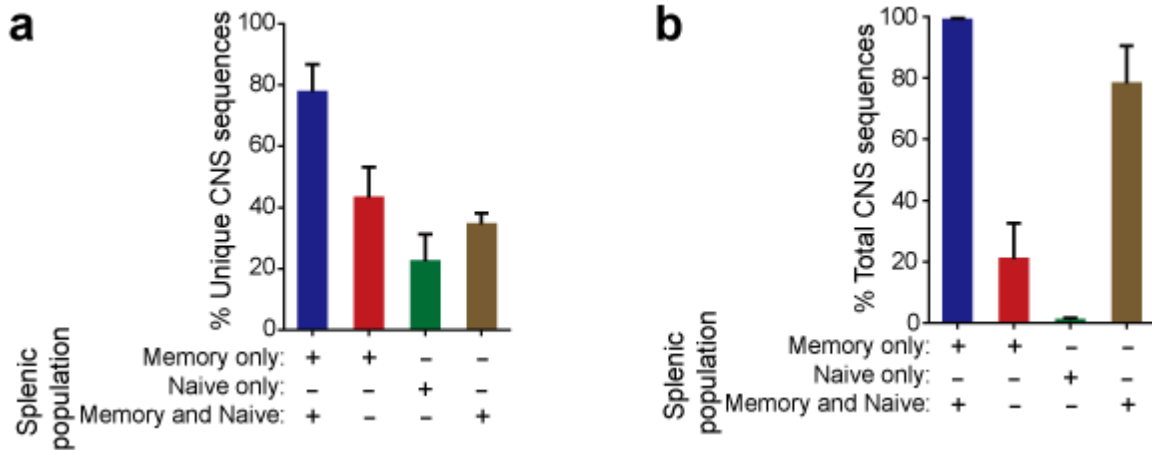


**Figure 3-2. Association of CNS TCR with the memory T cell pool.**

CNS TCR $\beta$  sequences from sorted CD45Rb<sup>hi</sup>CD44<sup>lo</sup> or CD45Rb<sup>lo</sup>CD44<sup>hi</sup> T cells from the spleens of the same mice (n=5) were compared to determine the association of CNS-infiltrating sequences with the naïve and memory populations. (a) Percent of unique CNS sequences that were identified exclusively in the splenic memory or naïve populations, or in both memory and naïve populations are plotted. (b) Percent of total CNS sequences acquired were mapped as in (a).

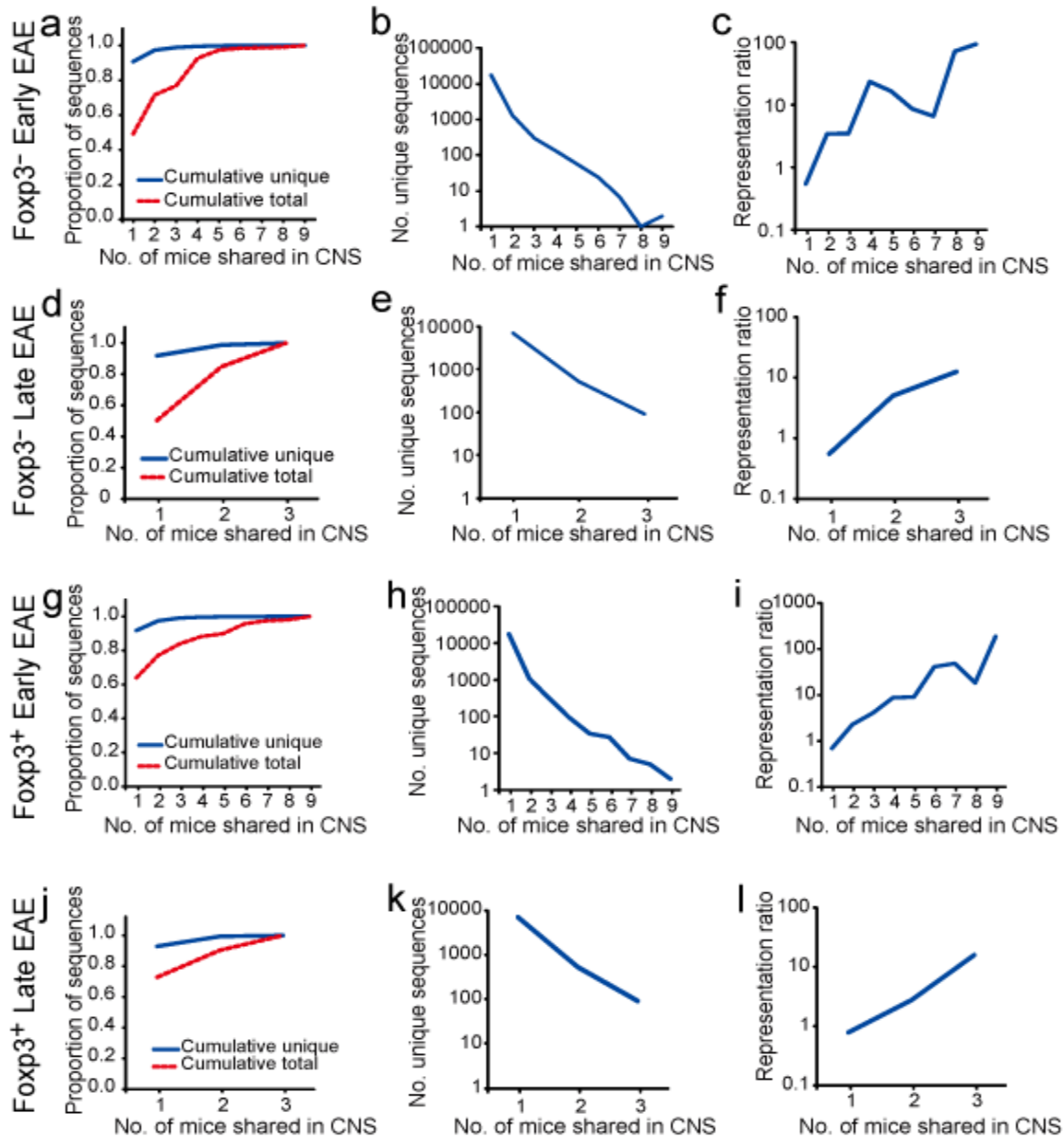


**Figure 3-3. Representation of shared TRBV13-2<sup>+</sup> TCR $\beta$  among CNS-infiltrating T cells.**

CNS TRBV13-2<sup>+</sup> Tconv and Treg TCR $\beta$  repertoires from mice with early (d 15-18, n=9; a-c, g-i) or late (d 26, n=3, d-f, j-l) EAE were determined by high-throughput sequencing. (a, d, g, j) The proportion of unique TCR $\beta$  amino acid sequences and total TCR $\beta$  sequences acquired that were cumulatively identified in the indicated number of mice is plotted. (b, e, h, k) The number of unique amino acid sequences shared in the CNS of the indicated number of mice with early or late EAE is plotted. (c, f, i, l) The frequency of identification of each unique amino acid sequence relative to that of an average sequence in the same CNS, was calculated. The mean of this, or representation ratio, for sequences shared by the indicated number of mice with early or late EAE is plotted.

### **Preferential deployment of public versus private TCR $\beta$ to the autoimmune repertoire**

The prevalence of the shared TCR $\beta$  in the CNS repertoire did not indicate that shared sequences were preferentially employed. Public sequences uninvolved in the autoimmune response may have been present at similarly high frequencies, leading to their proportionately high utilization<sup>131</sup>. There, TCR from cells involved and uninvolved in the CNS response could be directly compared. We proposed one model that if TCR engaged in the CNS response were randomly deployed from the public and private peripheral repertoires, then splenic sequences identified and not identified in the CNS would be expected to be similarly public (**Figure 3-4 Model 1**). We also proposed an alternative model that if public TCR $\beta$  were preferentially incorporated into the CNS response, the splenic sequences also seen in the CNS should be enriched in public sequences (**Figure 3-4 Model 2**). To assess this and establish the extent to which CNS-infiltrating T cells are public, we analyzed the more abundant TCR $\beta$  sequences in the spleen.

### **EAE splenic TCR $\beta$ mapped onto CNS TCR $\beta$ repertoires**

To test our hypothesized models, we were able to map the splenic TCR $\beta$  sequences from the mice with EAE onto CNS TCR $\beta$  repertoires. Splenic TCR $\beta$  sequences also seen in the CNS were markedly more likely to be shared than sequences not observed in the CNS. For example, 28.5% of the unique CNS Foxp3<sup>-</sup> sequences from mice with early disease were identified in all spleens analyzed compared with 2.7% of non-CNS sequences, indicating that many CNS sequences are derived from the public repertoire (**Figure 3-5a**). Pairwise analysis of the sharing of CNS and non-CNS sequences between individual mice verified this finding (**Figure 3-5c**). Results were similar in mice with late disease (**Figure 3-5b, c**) and for Foxp3<sup>+</sup> T cells (**Figure 3-5d-f**).

When we analyzed the total splenic TCR $\beta$  sequences, the results above enumerating unique TCR $\beta$  sequences acquired was replicated tabulating, and this also showed a dramatically enhanced sharing of CNS compared with non-CNS sequences (**Figure 3-6**).

### **Over-representation of CNS T cell-associated TCR $\beta$ in the pre-immune public repertoire**

Our previous analysis of the preferential recruitment and expansion of public splenic T cells was derived from the context of CNS inflammation. To circumvent the distortion from immune responses, we proposed that CNS infiltrating TCR $\beta$  should be disproportionately public in pre-immune mice too. To test this, we mapped splenic TCR $\beta$  sequences from mice with EAE onto pre-immune repertoires. For all samples analyzed, either Foxp3<sup>-</sup> or Foxp3<sup>+</sup> and early or late disease, substantially more CNS-infiltrating than non-infiltrating TCR $\beta$  sequences were identified as public in the pre-immune repertoire (**Figure 3-7**). This again was true both for unique and total TCR $\beta$  sequences analyzed. Together, these data support a heavily biased public TCR $\beta$  usage in the EAE



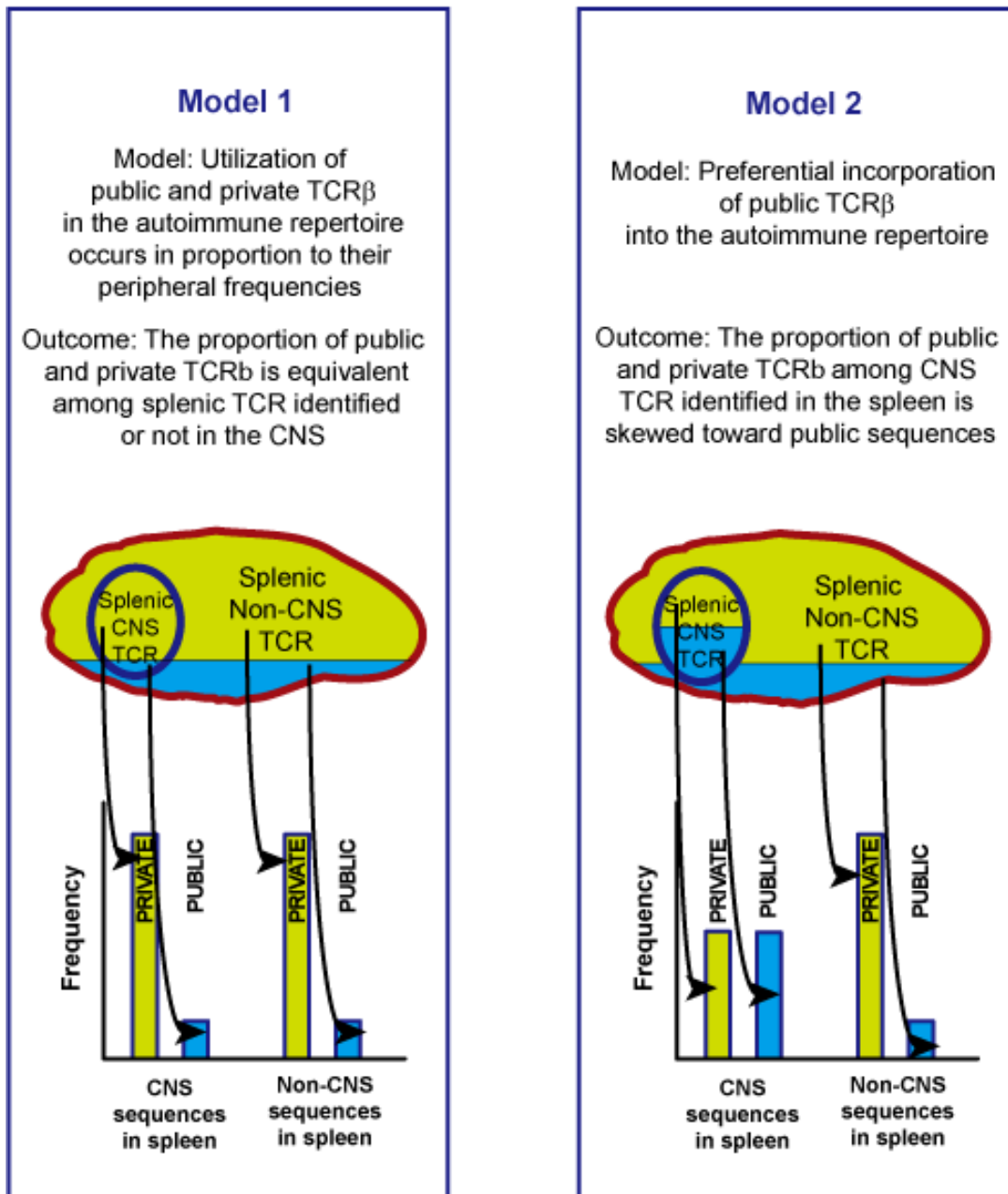


**Figure 3-4. Models for the high frequency of shared CNS TCR $\beta$ .**

In model 1, the high frequency of shared CNS TCR $\beta$  is explained by a generally high frequency of public relative to private TCR $\beta$ . In this model, T cells are randomly recruited to and expand within the autoimmune repertoire. Splenic TCR $\beta$  that are present within the CNS repertoire will show similar proportions of public sequences as TCR $\beta$  that are uninvolved in the autoimmune process. In model 2, public TCR $\beta$  are disproportionately recruited to and/or expand within the autoimmune response. In this case, there is a greater representation of public TCR $\beta$  among splenic sequences identified within the CNS than those unassociated with CNS autoimmunity.

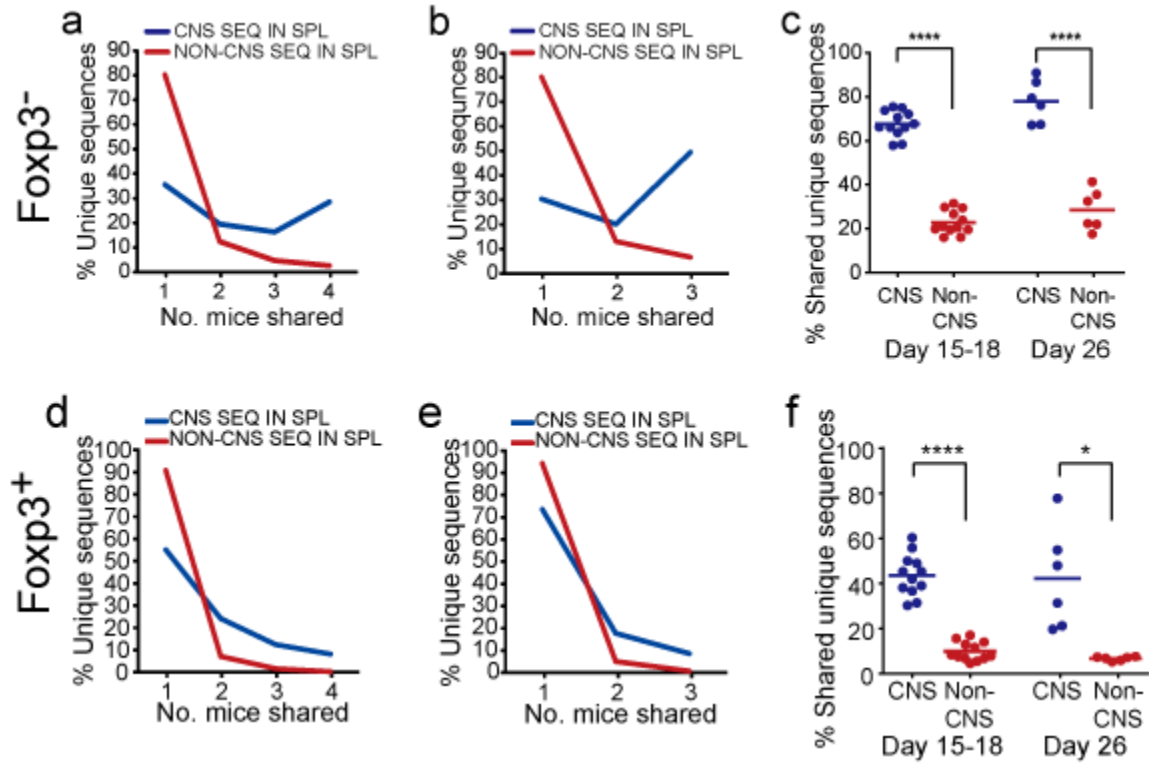


**Figure 3-5. Over-representation of unique public sequences in the CNS-infiltrating repertoire.**

Splenic CD4<sup>+</sup> GFP-Foxp3<sup>-</sup> and GFP-Foxp3<sup>+</sup> TRBV13-2<sup>+</sup> TCRβ repertoires from mice with early (d 15-18; n=4) or late (d 26; n=3) EAE were segregated into sequences identified or not within the CNS. Percent of unique TCRβ sequences that were shared by the indicated number of mice with early (a, d) and late (b, e) disease is shown. (c, f) The overlap of the repertoire from each mouse was compared pairwise with that of every other mouse in a cohort.

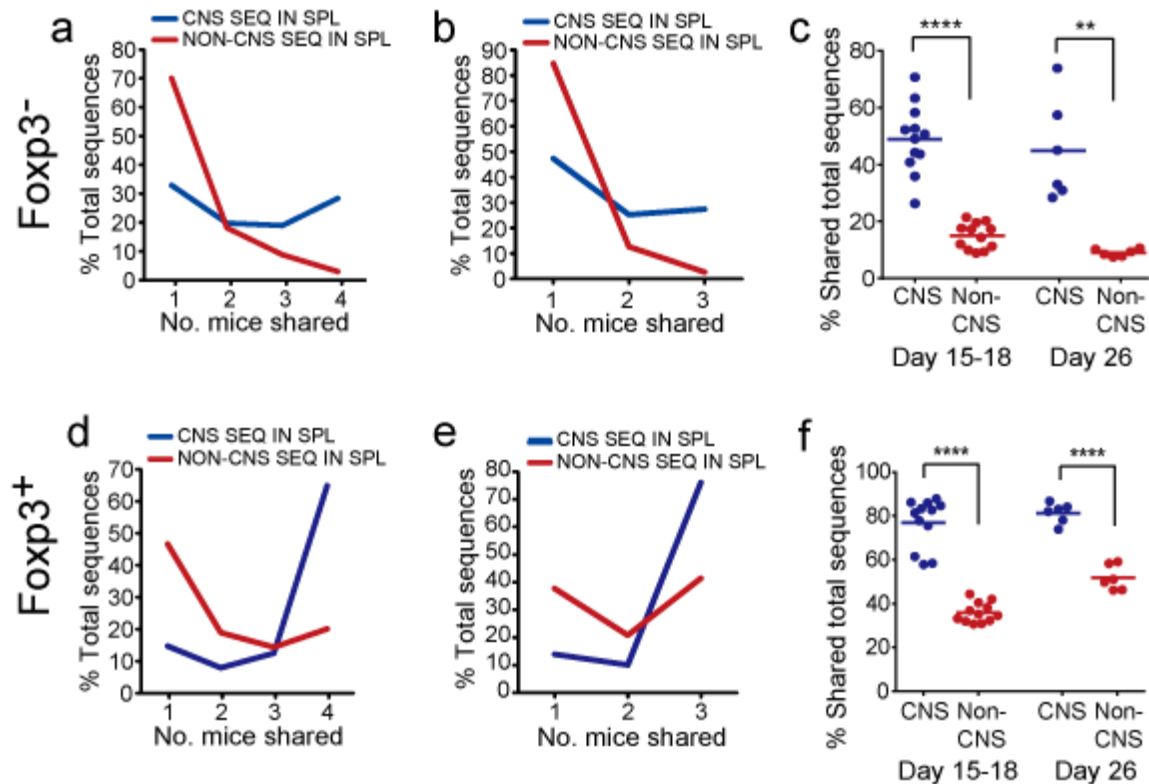
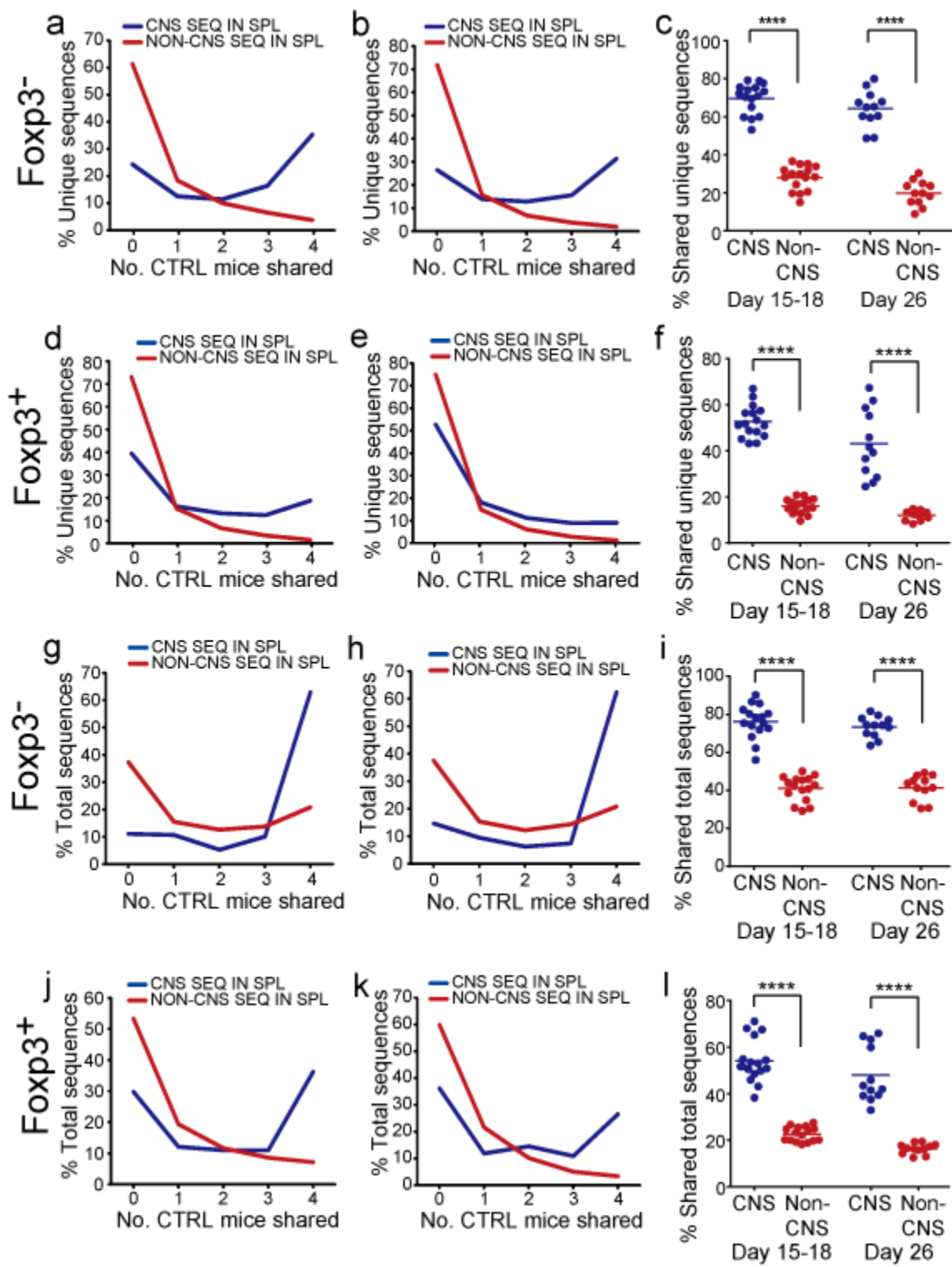


**Figure 3-6. Over-representation of total public sequences in the CNS-infiltrating repertoire.**

Analyses were performed on the same data sets as in **Figure 3-5**, however overlap among total, rather than unique, TCR $\beta$  sequences acquired was assessed. For this, frequencies were normalized so total sequence number was effectively equal in each mouse. This ensured that the weighting of each mouse in calculations was equivalent. Percent of total TCR $\beta$  sequences that were shared by the indicated number of mice with early (a, d) and late (b, e) disease is shown. (c, f) The overlap of the repertoire from each mouse was compared pairwise with that of every other in a cohort.

**Figure 3-7. Over-representation of unique and total CNS-associated Foxp3<sup>+</sup> and Foxp3<sup>-</sup> public TCRβ in the pre-immune repertoire.**

Splenic TRBV13-2<sup>+</sup> TCRβ amino acid repertoires from CD4<sup>+</sup>GFP-Foxp3<sup>-</sup> and GFP-Foxp3<sup>+</sup> T cells of mice with early (d 15-18; n=4) or late (d 26, n=3) EAE were mapped onto the splenic CD4<sup>+</sup>GFP-Foxp3<sup>-</sup> or CD4<sup>+</sup>GFP-Foxp3<sup>+</sup> repertoires from pre-immune mice (CTRL; n=4). Percent of unique CD4<sup>+</sup>GFP-Foxp3<sup>-</sup> sequences that were or were not identified in the CNS from mice with early (a) or late (b) EAE and also present in the CD4<sup>+</sup>GFP-Foxp3<sup>-</sup> repertoires of the indicated number of pre-immune spleens is plotted. (c) As in (a, b), but the overlap of repertoires from individual mice with EAE and individual pre-immune mice is plotted. (d-f) Analyses are equivalent to (a-c), but assessing unique sequence overlap between CD4<sup>+</sup>GFP-Foxp3<sup>+</sup> repertoires. (g-l) Parallel analyses of total CD4<sup>+</sup>GFP-Foxp3<sup>-</sup> and CD4<sup>+</sup>GFP-Foxp3<sup>+</sup> sequences acquired from mice with early or late EAE and pre-immune mice. As in **Figure 3-5**, sequence events were normalized for comparisons of total sequence overlap between mice, effectively equalizing the total number of sequences in each mouse.



repertoire, with this preference traceable to the pre-immune repertoire.

### **Temporal focusing of the public TCR repertoire**

To determine whether the extent of sharing of autoimmune repertoires differed in early and late EAE, we next compared CNS repertoires from individual mice. Overlap of CNS sequences was lowest when pairs of d 15-18 mice were compared with each other. Repertoire overlap increased when d 15-18 mice were compared with d 26 mice, and was greatest when d 26 mice were compared (**Figure 3-8a, b**). Splenic TCR overlap, unlike that of CNS TCR, did not change with disease stage (**Figure 3-8c, d**). Therefore the extent of sharing increases specifically with time in the disease-associated repertoire. That mice with early disease shared more of their CNS repertoire with late disease mice than with each other further indicates a temporal focusing of the shared CNS repertoire.

### **Recombinatorial bias and oligoclonality in autoimmune repertoire formation**

Considering the relatedness of the d 15-18 and d 26 repertoires, we combined the 12 CNS data sets we acquired to identify common TCR $\beta$  sequences. Forty eight TCR $\beta$  were identified in  $\geq 10$  of the 12 CNS repertoires (**Table 3-4**). These receptors were oligoclonal with multiple nt sequences used for each CNS amino acid sequence cumulatively (range 2-59, median=13) and within single mice (mean  $2.8 \pm 1.3$ ). Consistent with their oligoclonal presence, in individual CNS  $46.7 \pm 19.9\%$  of the 48 public TCR $\beta$  were identified in both the Foxp3<sup>+</sup> and Foxp3<sup>-</sup> lineages compared with  $2.9 \pm 1.9\%$  of private sequences ( $p < 10^{-5}$ ).

### **Biased rearrangement of public TCR $\beta$ in the thymus of pre-immune mice**

Given that the prevalence of CNS public sequences can be traced into splenic repertoire of pre-immune mice. We questioned whether these public TCR $\beta$  originated from the thymus with high probability of forming. Indeed, public TCR have been proposed for a high probability of forming in the thymus due to a process called biased recombination<sup>44,132,133</sup>. To assess this in the autoimmune public repertoire, we analyzed pre-selection CD4<sup>+</sup>CD8<sup>+</sup>TCR<sup>lo</sup> (DP) repertoires in pre-immune mice<sup>131</sup>. Nucleotide sequence diversity of each of the 48 public TCR $\beta$  was compared with that of paired private TCR $\beta$  from the same mouse with identical V $\beta$ , J $\beta$  and CDR3 length, and similar identification frequencies ( $>0.25 - <4$  fold). The public sequences displayed markedly greater pre-selection nt variability than control private sequences ( $6.2 \pm 2.9$  vs  $1.1 \pm 0.1$  nt sequences) (**Figure 3-9**), indicating that these have an increased probability of forming and the pre-selection recombinatorial biases foster disease-associated public repertoire formation.

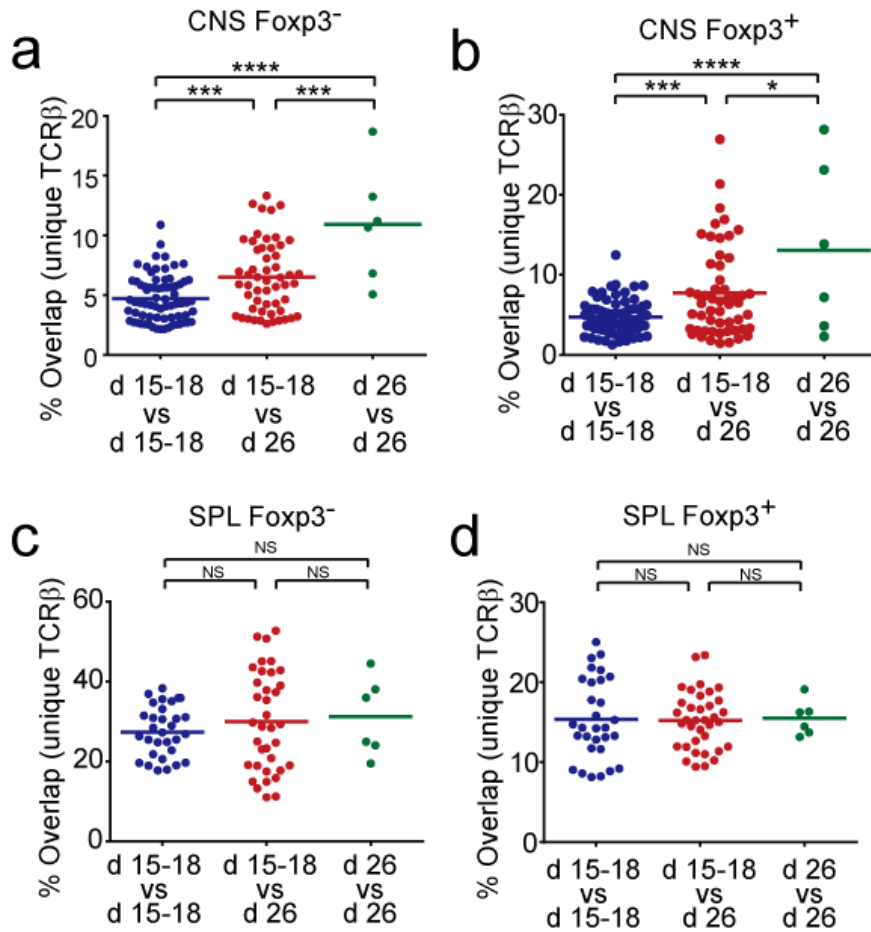


**Figure 3-8. Repertoire focusing in mice with EAE.**

CNS TCRβ repertoires of CD4<sup>+</sup>GFP-Foxp3<sup>-</sup> and Foxp3<sup>+</sup> T cells were compared between individual mice with early and late disease to determine changes in the overlap between repertoires with disease progression. Percent CNS CD4<sup>+</sup>GFP-Foxp3<sup>-</sup> (a) and Foxp3<sup>+</sup> (b) CNS TCRβ repertoire overlap between individual mice with early disease, mice with early versus late disease, and mice with late disease is plotted. Comparable analyses were performed on splenic CD4<sup>+</sup>GFP-Foxp3<sup>-</sup> (c) and CD4<sup>+</sup>GFP-Foxp3<sup>+</sup> (d) TCRβ repertoires.

**Table 3-4. Highly shared CNS CDR3 $\beta$  sequences.**

CDR3 $\beta$ sequence	CNS shared	CNS shared (Foxp3 <sup>-</sup> )	CNS shared (Foxp3 <sup>+</sup> )	Foxp3 <sup>-</sup>			Foxp3 <sup>+</sup>		
				Mean (%)	Median (%)	Range (%)	Mean (%)	Median (%)	Range (%)
ASGETGGNYAEQF	12	12	12	0.986	0.235	(0.017- 5.375)	1.818	1.774	(0.008- 4.346)
ASGQDTQY	12	10	11	0.086	0.014	(<0.001- 0.591)	0.150	0.018	(0.002- 0.978)
ASGDRYEQY	12	12	8	0.248	0.221	(0.008- 0.626)	0.047	0.009	(0.001- 0.290)
ASGEYEQY	12	7	11	0.102	0.008	(0.001- 0.605)	0.166	0.069	(0.006- 0.940)
ASGDNYNSPLY	12	8	10	0.015	0.009	(<0.001- 0.060)	0.061	0.008	(<0.001- 0.281)
ASGDAGNTLY	12	7	10	0.093	0.020	(<0.001- 0.351)	0.158	0.089	(0.002- 0.772)
ASGDSYNSPLY	11	9	10	0.182	0.024	(0.005- 1.359)	0.061	0.010	(0.001- 0.221)
ASGEDTQY	11	11	7	0.299	0.015	(<0.001- 3.081)	0.029	0.012	(0.002- 0.139)
ASGYEQY	11	8	9	0.013	0.009	(0.002- 0.044)	0.609	0.047	(0.009- 5.187)
ASGETANSDYT	11	6	10	0.019	0.006	(0.001- 0.087)	0.872	0.592	(0.001- 3.136)
ASGDSSGNTLY	11	7	9	0.006	0.006	(<0.001- 0.017)	0.140	0.019	(<0.001- 0.503)
ASGEAGGNYAEQF	11	7	9	0.003	0.002	(<0.001- 0.009)	0.086	0.009	(0.001- 0.662)



Table 3-4. (Continued).

CDR3 $\beta$ sequence	CNS shared	CNS shared (Foxp3 <sup>-</sup> )	CNS shared (Foxp3 <sup>+</sup> )	Foxp3 <sup>-</sup>			Foxp3 <sup>+</sup>		
				Mean (%)	Median (%)	Range (%)	Mean (%)	Median (%)	Range (%)
ASGDAGNSDYT	11	7	8	0.534	0.082	(0.002- 3.315)	0.065	0.023	(0.001- 0.175)
ASGDRGYEQY	11	6	8	0.008	0.003	(0.001- 0.033)	0.164	0.039	(0.001- 0.583)
ASGDNSGNTLY	10	10	9	0.084	0.010	(<0.001- 0.577)	0.119	0.054	(<0.001- 0.664)
ASGDAGGSYEQY	10	8	10	0.217	0.059	(0.001- 1.221)	0.067	0.040	(0.001- 0.225)
ASGDDEQY	10	10	8	0.065	0.010	(<0.001- 0.481)	0.091	0.010	(<0.001- 0.352)
ASGDAGYEQY	10	8	9	0.033	0.025	(0.004- 0.103)	0.176	0.073	(0.001- 0.860)
ASGDEQY	10	8	9	0.009	0.003	(0.001- 0.033)	0.189	0.045	(0.010- 1.091)
ASGDQDTQY	10	9	8	0.014	0.006	(<0.001- 0.042)	0.050	0.013	(0.002- 0.267)
ASGDAETLY	10	6	10	0.016	0.006	(0.001- 0.059)	0.104	0.019	(<0.001- 0.619)
ASGGTGGNYAEQF	10	6	10	0.003	0.001	(<0.001- 0.013)	0.099	0.048	(0.002- 0.343)
ASGDAGGYEQY	10	8	8	0.013	0.015	(<0.001- 0.030)	0.069	0.068	(<0.001- 0.219)
ASGDWGSAETLY	10	8	8	0.016	0.006	(0.001- 0.050)	0.031	0.006	(<0.001- 0.169)

Table 3-4. (Continued).

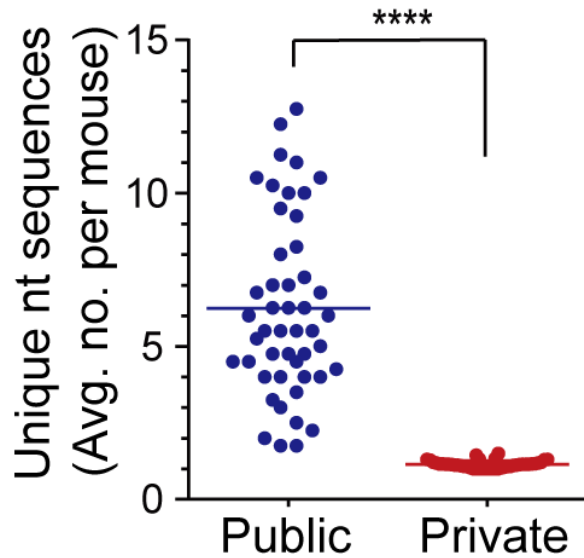
CDR3 $\beta$ sequence	CNS shared	CNS shared (Foxp3 <sup>-</sup> )	CNS shared (Foxp3 <sup>+</sup> )	Foxp3 <sup>-</sup>			Foxp3 <sup>+</sup>		
				Mean (%)	Median (%)	Range (%)	Mean (%)	Median (%)	Range (%)
ASGPYEQY	10	7	8	0.143	0.008	(0.001- 0.913)	0.277	0.043	(0.001- 1.681)
ASGDSAETLY	10	8	7	0.007	0.008	(0.001- 0.017)	0.146	0.032	(<0.001- 0.659)
ASGDSYEQY	10	8	7	0.037	0.013	(0.001- 0.123)	0.018	0.012	(0.001- 0.069)
ASGGTGGYEYQY	10	9	6	0.035	0.008	(0.001- 0.204)	0.020	0.011	(0.002- 0.069)
ASGDRGNTEVF	10	7	8	0.031	0.002	(0.001- 0.134)	0.011	0.002	(<0.001- 0.070)
ASGDRGSGNTLY	10	9	6	0.027	0.005	(0.001- 0.130)	0.014	0.003	(<0.001- 0.069)
ASGDADTQY	10	7	7	0.042	0.030	(<0.001- 0.149)	0.017	0.001	(0.001- 0.059)
ASGGGQNYAEQF	10	9	5	0.054	0.038	(0.002- 0.143)	0.005	0.003	(0.002- 0.012)
ASGDAGSQNTLY	10	6	8	0.013	0.012	(0.002- 0.024)	0.045	0.017	(0.001- 0.179)
ASGDAGEQY	10	8	6	0.019	0.008	(<0.001- 0.091)	0.028	0.008	(0.001- 0.112)
ASGDAGGQNTLY	10	7	7	0.006	0.004	(<0.001- 0.017)	0.030	0.027	(0.002- 0.073)
ASGDGYEQY	10	7	7	0.004	0.003	(0.001- 0.008)	0.031	0.006	(0.001- 0.143)

Table 3-4. (Continued).

CDR3 $\beta$ sequence	CNS shared	CNS shared (Foxp3 <sup>-</sup> )	CNS shared (Foxp3 <sup>+</sup> )	Foxp3 <sup>-</sup>			Foxp3 <sup>+</sup>		
				Mean (%)	Median (%)	Range (%)	Mean (%)	Median (%)	Range (%)
ASGDPGGYEYQY	10	6	8	0.014	0.005	(0.001- 0.062)	0.016	0.009	(0.001- 0.069)
ASGDAGGQDTQY	10	8	6	0.005	0.004	(<0.001- 0.015)	0.020	0.011	(0.001- 0.078)
ASGDVEYQY	10	5	8	0.020	0.006	(<0.001- 0.079)	0.105	0.026	(<0.001- 0.386)
ASGDEDTQY	10	8	5	0.011	0.007	(0.001- 0.033)	0.084	0.005	(0.001- 0.325)
ASGDAWGGYEYQY	10	5	8	0.049	0.041	(0.002- 0.125)	0.040	0.009	(0.001- 0.210)
ASGEGTGGYEYQY	10	8	5	0.060	0.009	(<0.001- 0.311)	0.002	0.001	(<0.001- 0.008)
ASGDNYEYQY	10	8	5	0.005	0.003	(0.001- 0.017)	0.016	0.006	(0.002- 0.048)
ASGDAGTGGYEYQY	10	8	5	0.013	0.005	(0.001- 0.052)	0.005	0.003	(0.001- 0.015)
ASGEQGYEYQY	10	5	7	0.180	0.002	(0.001- 0.700)	0.028	0.008	(0.001- 0.140)
ASGDGGNQDTQY	10	8	4	0.045	0.028	(0.008- 0.167)	0.004	0.005	(0.001- 0.008)
ASGDWGSSYEYQY	10	5	6	0.089	0.008	(0.001- 0.376)	0.039	0.016	(<0.001- 0.168)
ASGGQNTVEF	10	6	5	0.002	0.002	(<0.001- 0.005)	0.018	0.004	(0.001- 0.043)

**Table 3-4. (Continued).**

Sequences for 48 TRBV13-2<sup>+</sup> CDR3 $\beta$  from TCR $\beta$  identified as highly shared in the CNS are listed. The number of mice in which the sequences were identified (n=12 total) in Foxp3<sup>-</sup> and Foxp3<sup>+</sup> T cells is listed, as is the mean, median, and range of the percent of total CNS sequences acquired with the indicated amino acid sequence.



**Figure 3-9. Formation of the public autoimmune TCR repertoire through biased recombination.**

To determine the diversity of the public autoimmune repertoire in pre-selection thymocytes, nucleotide (nt) sequences identified for 48 highly public CNS TCR $\beta$  amino acid sequences were assessed in sorted pre-selection CD4<sup>+</sup>CD8<sup>+</sup>TCR<sup>lo</sup> thymocytes from healthy mice (n=4). The mean number of unique nt sequences per thymus for each of the 48 sequences is plotted. For each CNS sequence, paired control private sequences were identified in each mouse with the same TRBV, TRBJ, and CDR3 $\beta$  length, and similar frequency (>0.25-<4 fold) as the public sequence for comparison. Mean unique nt sequences is similarly plotted.

## Functional Characterization of the CNS Public TCR $\beta$ in Retrogenic Mice Model

### Spontaneous autoimmunity mediated by a public TCR $\beta$

Autoantigen-specific T cells are readily identifiable in the T cell repertoire of healthy individuals<sup>133-135</sup>. The preferential use of public TCR $\beta$  during EAE suggested a role for direct evidence. To better define the impact of public TCR $\beta$ , we generated retroviral transgenic (retrogenic) mice that enforced the expression of the most common public TCR $\beta$  sequence, TCR $\beta$ 1 (**Table 3-5**)<sup>101,123,136</sup>.

### Phenotypic characterization of TCR $\beta$ 1 retrogenic mice

Impressively, TCR $\beta$ 1 retrogenic mice developed spontaneous EAE with very early T cell engraftment at ~4 wk (**Figure 3-10a**). Indeed, numbers of T cells infiltrating the CNS at this time were similar to numbers in the spleen (**Figure 3-10b**). CD4<sup>+</sup>Foxp3<sup>-</sup>, CD4<sup>+</sup>Foxp3<sup>+</sup>, and CD8<sup>+</sup> T cells engrafted (**Figure B-2, B-3**), and the CD69 activation marker was expressed on 31 $\pm$ 5% and 81 $\pm$ 5% of splenic and CNS T cells from diseased mice respectively (**Figure 3-10a-d, Figure B-2**). Mortality was >50% (**Figure 3-10a**). TCR $\beta$ 1<sup>+</sup> T cells proliferated strongly to MOG<sub>35-55</sub> and CNS and splenic cells demonstrated T<sub>h</sub>1 and T<sub>h</sub>17 subset differentiation and a histologic pattern consistent with optico-spinal encephalomyelitis (**Figure 3-10c-f, Figure 3-11e-g**). Notably, disease in mice retrogenic for just the TCR $\beta$ 1 monomer was markedly accelerated, increased in incidence, and more severe than our prior results with retrogenic mice expressing five different disease-associated private MOG-specific TCR $\alpha\beta$  heterodimers<sup>101</sup>.

### TCR $\beta$ 1 imposes MOG<sub>35-55</sub> specificity on TCR $\alpha\beta$ heterodimers

TCR $\beta$ 1 retrogenic mice were enforced to express a single TCR $\beta$  chain (TCR $\beta$ 1) pairing with endogenous random TCR $\alpha$  chains. The corresponding TCR repertoire would be limited but diverse enough for a wide spectrum of TCR specificity. Referred to our observation, we hypothesized that single TCR $\beta$ 1 might dominate MOG<sub>35-55</sub> recognition on TCR with diverse TCR $\alpha$ . To establish pairing requirements, we co-expressed TCR $\beta$ 1 with 7 TCR $\alpha$  chains isolated from non-TCR $\beta$ 1 TCR. We reconstituted the TCR $\alpha\beta$  heterodimers and enforced the expression on CD4 4G4 hybridoma cell lines. *In vitro*, MOG<sub>35-55</sub> stimulation assay showed two of the hybrid TCR responded to MOG<sub>35-55</sub>, indicating that TCR $\beta$ 1 can drive MOG responsiveness with random TCR $\alpha$  chain (**Figure 3-12**). TCR $\alpha$  cDNA was further isolated from CNS-infiltrating T cells from 3 TCR $\beta$ 1 mice by 5' RACE and subcloned. These were heterogeneous and did not overlap between mice (**Table 3-6**), indicating that TCR $\beta$ 1 is associated with many TCR $\alpha$ .

### Protective role of the co-engrafted wide type (WT) cells in chimeric retrogenic mice

To determine whether non-transgenic T cells impede spontaneous EAE mediated by TCR $\beta$ 1, we generated chimeric retrogenic mice, mixing wild type CD45.1<sup>+</sup>CD45.2<sup>-</sup> and smaller numbers of congenic TCR $\beta$ 1-transduced CD45.1<sup>-</sup>CD45.2<sup>+</sup> hematopoietic

**Table 3-5. TCR $\beta$  retrogenic mice.**

TCR name	TRBJ	CDR3 sequence	CNS shared (Total, n=12)	CNS shared (Foxp3 <sup>-</sup> )	CNS shared (Foxp3 <sup>+</sup> )	SPL Shared (Total, n=9)	SPL shared (Foxp3 <sup>-</sup> )	SPL shared (Foxp3 <sup>+</sup> )
<b>CNS shared, Public (group 1)</b>								
TCR $\beta$ 1	2-1	ASGETGGNYAEQF	12	12	12	9	9	9
TCR $\beta$ 2	2-7	ASGDRYEY	12	12	8	9	9	9
TCR $\beta$ 3	2-7	ASGYEQY	11	8	9	9	9	9
TCR $\beta$ 4	1-2	ASGETANSDYT	11	6	10	9	9	9
TCR $\beta$ 5	2-7	ASGDAGGSYEQY	10	8	10	9	9	9
TCR $\beta$ 6	2-7	ASGDGEY	9	4	9	9	9	9
<b>CNS non-shared, Public (group 2)</b>								
TCR $\beta$ 7	2-1	ASGEQQGTEQF	1	1	1	3	3	1
TCR $\beta$ 8	2-7	ASGDGLGGSYEQY	1	1	0	9	9	5
TCR $\beta$ 9	1-6	ASGDVRGYNSPLY	1	0	1	2	1	1
TCR $\beta$ 10	1-2	ASGDGTSNSDYT	1	0	1	9	9	2
<b>Private (group 3)</b>								
TCR $\beta$ 11	2-5	ASGIGDTQY	1	0	1	1	1	1
TCR $\beta$ 12	2-7	ASGDAGTGYEYF						
TCR $\beta$ 13	2-4	ASGDWGGEDTLYF						
TCR $\beta$ 14	2-4	ASGDETGGAYEQYF						
TCR $\beta$ 15	2-3	ASGGGLGGTSAETLYF						
<b>Control</b>								
OT-II	2-4	ASSLGGESQNTLYF						

**Table 3-5. (Continued).**

TRBV13-2<sup>+</sup> TCR  $\beta$  chains that were shared in total, Foxp3<sup>-</sup>, and Foxp3<sup>+</sup> populations in the CNS and spleen of the indicated number of mice were transduced into TCR $\beta$ <sup>-/-</sup> HPC and retrogenic mice generated. For TCR $\beta$  chains identified in a single mouse, the percent of total TRBV13-2<sup>+</sup> TCR sequences in the CNS bearing the indicated sequence is listed in parentheses. For shared CNS sequences, frequency means, medians, and ranges are provided in **Table 3-1**. Sequences  $\beta$ 12-15 were isolated from primary TRBV13-2<sup>+</sup> MOG<sub>35-55</sub>-specific T cell hybridomas in our laboratory, and were not observed in any of the mice evaluated for the repertoire analyses here. OT-II $\beta$  comprises the TCR $\beta$  chain from the ovalbumin<sub>323-229</sub>-specific OT-II TCR, and was assessed as a negative control.



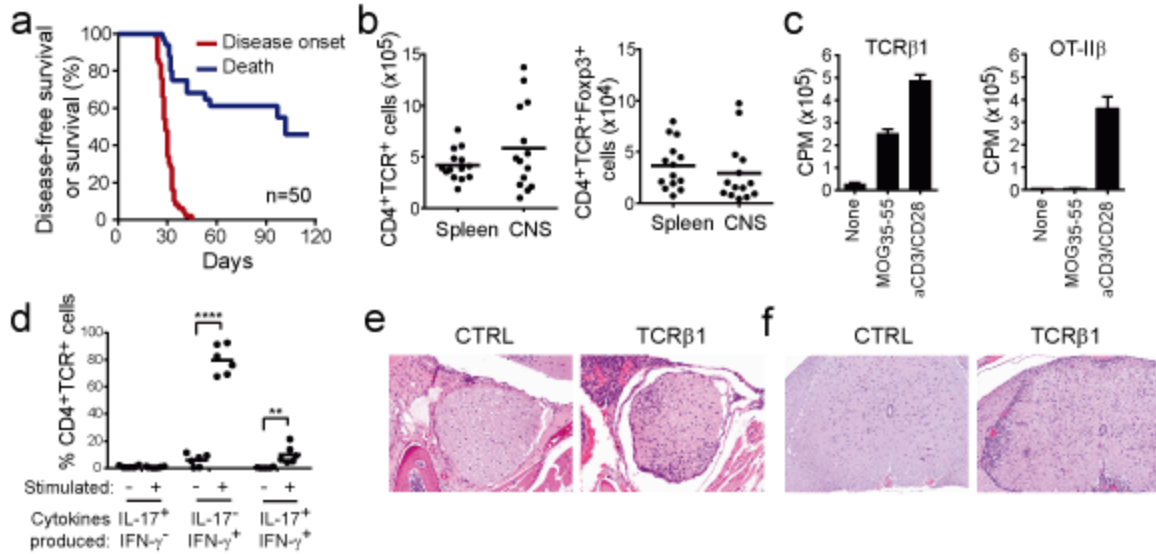


**Figure 3-10. Enforced public TCRβ expression leads to spontaneous autoimmune encephalomyelitis.**

Retrogenic mice were generated by transducing TCRβ<sup>-/-</sup>, GFP-Foxp3 HPCs with TCRβ1. (a) Kaplan Meier analysis of survival and disease-free survival. (b) Absolute numbers of CD4<sup>+</sup>TCR<sup>+</sup> and CD4<sup>+</sup>TCR<sup>+</sup>GFP-Foxp3<sup>+</sup> T cells in spleens and CNS of TCRβ1 mice with EAE. (c) Proliferation of splenic T cells from TCRβ1 or control retrogenic mice expressing an OT-II TCR (ovalbumin-specific)-derived β chain in response to MOG<sub>35-55</sub> or mitogen measured by <sup>3</sup>H-thymidine incorporation. (d) Percent of CNS-infiltrating T cells expressing IL-17, IFN-γ, or both IL-17 and IFN-γ in the absence or presence of *ex-vivo* restimulation, as determined by intracellular cytokine staining, is plotted. (e, f) Histologic analyses of the CNS of TCRβ1 retrogenic mice showing a mixed infiltrate of lymphocytes, macrophages, and granulocytes, gliosis and perivascular cuffing in the septum, meninges, and optic nerve (e) and white tracts of the lumbar spinal cord (f) in day 28 TCRβ1 mice but not control retrogenic mice.

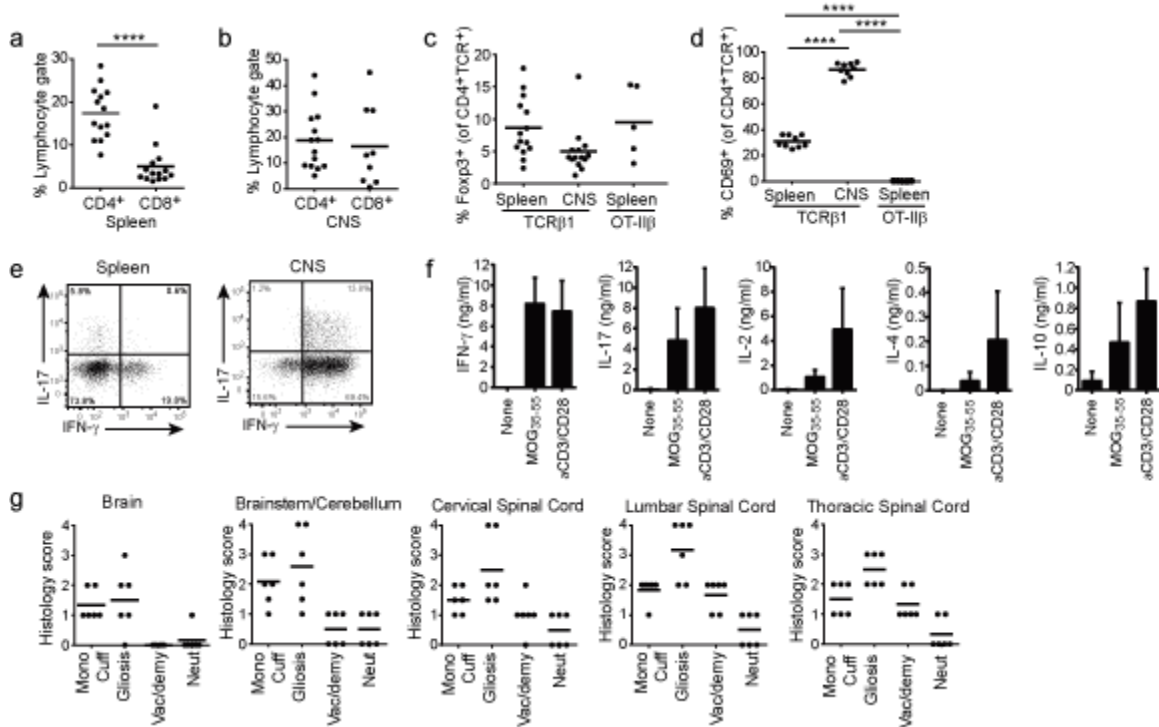


**Figure 3-11. Characterization of spontaneous EAE development in TCRβ1 retrogenic mice.**

Percent of CD4<sup>+</sup>TCR<sup>+</sup> and CD8<sup>+</sup>TCR<sup>+</sup> T cells within the lymphocyte gate in day 30-35 TCRβ1 mice in the spleen (a) and CNS (b). \*\*\*\*,  $p < 0.0001$ . (c) The percent of CD4<sup>+</sup>TCR<sup>+</sup> lymphocytes expressing GFP-Foxp3 in the spleens and CNS of TCRβ1 and control OT-II TCRβ retrogenic mice is plotted. Groups are NS by ANOVA. (d) The percent of activated CD4<sup>+</sup>TCR<sup>+</sup> T cells was determined by CD69 activation marker expression in the spleen and CNS and compared with results in the spleens of OT-II TCRβ mice. (e) Splenic and CNS T cells from TCRβ1 mice with EAE were stimulated *ex vivo* with mitogen and IFN-γ and IL-17 production measured by intracellular staining. Representative data is shown. Summary data is provided in figure 6d. (f) Splenocytes from TCRβ1 mice with EAE were stimulated with myelin MOG<sub>35-55</sub> and secretion of the indicated cytokines measured by bead array. (g) Major organs from TCRβ1 mice with EAE were analyzed histologically. Inflammation was localized to the CNS. Scoring of the indicated CNS regions was performed by a blinded reviewer as described under Methodology.

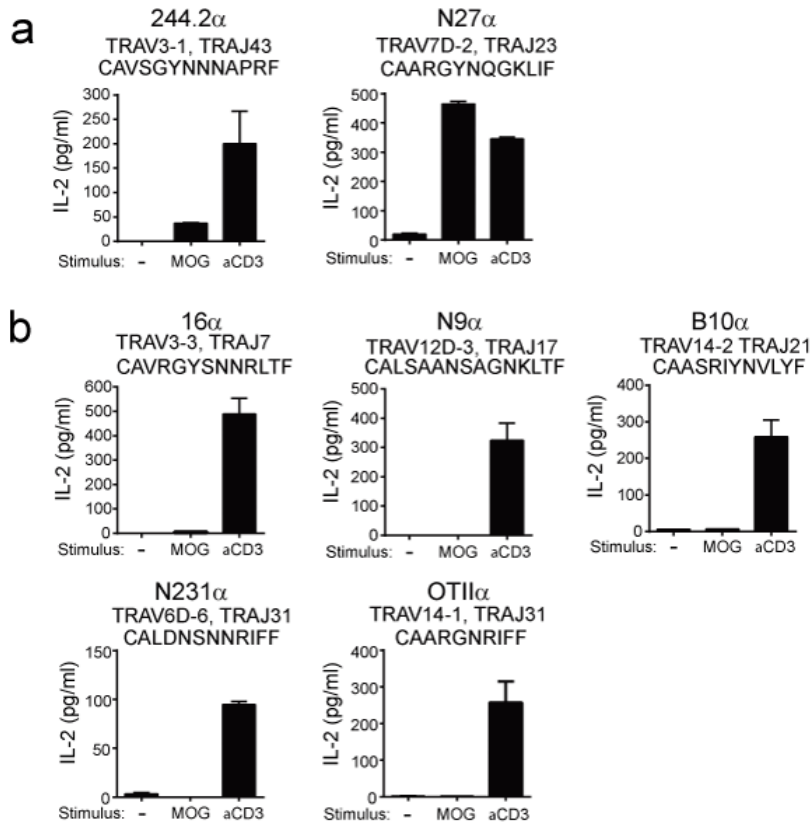


**Figure 3-12. TCR $\beta$ 1<sup>+</sup> TCR recognize MOG<sub>35-55</sub>.**

To determine the pairing requirements of the TCR $\beta$ 1 chain for MOG<sub>35-55</sub> recognition, we linked to it 7 TCR $\alpha$  chains derived from alternative (non-TCR $\beta$ 1) TCR in polycistronic retroviral constructs. TCR $\alpha$  chains and TCR $\beta$ 1 were separated by the *T. asigna* 2A sequence to support stoichiometric production of each chain, and cloned into the IRES-GFP retroviral vector. Retrovirus was transduced into 4G4 TCR $\alpha\beta$ -deficient cells that we had transfected to express CD4. TCR $\alpha\beta$ <sup>+</sup> cells were flow cytometrically sorted, and stimulated with MOG<sub>35-55</sub> or anti-CD3. IL-2 production was measured by ELISA at 24 hr. (a) TCR $\alpha$  chains that when paired with TCR $\beta$ 1 conferred MOG<sub>35-55</sub> responsiveness. (b) TCR $\alpha$  chains that did not confer MOG<sub>35-55</sub> responsiveness.

**Table 3-6. Distinct TCR $\alpha$  chains isolated from CNS CD4<sup>+</sup>GFP-Foxp3<sup>+</sup> and GFP-Foxp3<sup>-</sup> T cells from TCR $\beta$ 1 mice with EAE.**

Mouse	Source	Cell type	TRAV	TRAJ	CDR3
<b>5'RACE clones:</b>					
1	CNS	Foxp3 <sup>-</sup>	TRAV13-2	TRAJ26	CAPPAHAQGLTF
1	CNS	Foxp3 <sup>-</sup>	TRAV13D-1	TRAJ37	CALITGNTGKLIF
1	CNS	Foxp3 <sup>-</sup>	TRAV14-2	TRAJ26	CAARTYAQGLTF
1	CNS	Foxp3 <sup>-</sup>	TRAV14D-3	TRAJ31	CAARKNSNNRIFF
1	CNS	Foxp3 <sup>-</sup>	TRAV4D-3	TRAJ49	CAAVTGYQNFYF
1	CNS	Foxp3 <sup>-</sup>	TRAV4D-4	TRAJ42	CAASGGSNAKLTF
1	CNS	Foxp3 <sup>-</sup>	TRAV4D-4	TRAJ57	CAAGQGGSAKLIF
1	CNS	Foxp3 <sup>-</sup>	TRAV4N-3	TRAJ27	CAAGGYTGKLTF
1	CNS	Foxp3 <sup>-</sup>	TRAV6D-6	TRAJ57	CALGDRGSAKLIF
1	CNS	Foxp3 <sup>-</sup>	TRAV7-1	TRAJ21	CAVRKRSNYNVLYF
1	CNS	Foxp3 <sup>-</sup>	TRAV7-2	TRAJ23	CAASMDYNQGKLIF
1	CNS	Foxp3 <sup>-</sup>	TRAV7-3	TRAJ34	CAVSPQSSNTNKVVF
1	CNS	Foxp3 <sup>-</sup>	TRAV7-4	TRAJ12	CAASGRTGGYKVVVF
1	CNS	Foxp3 <sup>-</sup>	TRAV7-4	TRAJ21	CAASARSNYNVLYF
1	CNS	Foxp3 <sup>-</sup>	TRAV7-6	TRAJ33	CAASNYQLIW
1	CNS	Foxp3 <sup>-</sup>	TRAV8-1	TRAJ39	CATPYNNAGAKLTF
1	CNS	Foxp3 <sup>-</sup>	TRAV9N-2	TRAJ35	CVLSSGFASALTF
1	CNS	Foxp3 <sup>-</sup>	TRAV9N-2	TRAJ35	CVLSAGFASALTF
1	CNS	Foxp3 <sup>-</sup>	TRAV9N-3	TRAJ39	CAVSAINAGAKLTF
2	CNS	Foxp3 <sup>-</sup>	TRAV12-2	TRAJ33	CALSARVNYQLIW
2	CNS	Foxp3 <sup>-</sup>	TRAV14D-1	TRAJ57	CAASPQNQGGSAKLIF
2	CNS	Foxp3 <sup>-</sup>	TRAV6-2	TRAJ17	CVLGDRRSAGNKLTF
2	CNS	Foxp3 <sup>-</sup>	TRAV6-3	TRAJ45	CAMSGADRLTF
2	CNS	Foxp3 <sup>-</sup>	TRAV7-4	TRAJ9	CAAGISNMGYKLTF
2	CNS	Foxp3 <sup>-</sup>	TRAV7-4	TRAJ9	CAARISNMGYKLTF
3	CNS	Foxp3 <sup>-</sup>	TRAV19	TRAJ24	CAVPASLGKLQF
3	CNS	Foxp3 <sup>-</sup>	TRAV4D-3	TRAJ21	CAAGGYNVLYF
3	CNS	Foxp3 <sup>-</sup>	TRAV7-3	TRAJ27	CAANTGKLTF
3	CNS	Foxp3 <sup>-</sup>	TRAV7D-3	TRAJ37	CAVGGNTGKLIF
1	CNS	Foxp3 <sup>+</sup>	TRAV13D-1	TRAJ39	CALVMNNNAGAKLTF
1	CNS	Foxp3 <sup>+</sup>	TRAV4D-3	TRAJ50	CAARSSSSFSKLVF
1	CNS	Foxp3 <sup>+</sup>	TRAV4D-3	TRAJ42	CAAGGSNAKLTF
1	CNS	Foxp3 <sup>+</sup>	TRAV4D-4	TRAJ57	CAAALNQGGSAKLIF
1	CNS	Foxp3 <sup>+</sup>	TRAV4D-4	TRAJ57	CAAGQGGSAKLIF
1	CNS	Foxp3 <sup>+</sup>	TRAV4N-3	TRAJ47	CAAVPMDYANKMIF
1	CNS	Foxp3 <sup>+</sup>	TRAV7-2	TRAJ9	CAASWMGYKLTF
1	CNS	Foxp3 <sup>+</sup>	TRAV7-3	TRAJ22	CAVSASSGSWQLIF
1	CNS	Foxp3 <sup>+</sup>	TRAV7-3	TRAJ22	CAVSMSFGSWQLIF
1	CNS	Foxp3 <sup>+</sup>	TRAV7-4	TRAJ12	CAASGRTGGYKVVVF
1	CNS	Foxp3 <sup>+</sup>	TRAV7D-3	TRAJ22	CAVSISGSWQLIF

**Table 3-6. (Continued).**

<b>Mouse</b>	<b>Source</b>	<b>Cell type</b>	<b>TRAV</b>	<b>TRAJ</b>	<b>CDR3</b>
2	CNS	Foxp3 <sup>+</sup>	TRAV12-3	TRAJ39	CALRRGNAGAKLTF
2	CNS	Foxp3 <sup>+</sup>	TRAV7-6	TRAJ32	CAVLGSSGNKLIF
2	CNS	Foxp3 <sup>+</sup>	TRAV9D-3	TRAJ32	CALSPYGSSGNKLIF
2	CNS	Foxp3 <sup>+</sup>	TRAV9D-3	TRAJ32	CALSPYESSGNKLIF
3	CNS	Foxp3 <sup>+</sup>	TRAV21	TRAJ49	CILKTGYQNFYF
3	CNS	Foxp3 <sup>+</sup>	TRAV6-5	TRAJ49	CILKTGYQNFYF
<b>Additional TRAV4 amplification clones:</b>					
3	CNS	Foxp3 <sup>+</sup>	TRAV4D-3	TRAJ33	CAAPDSNYQLIW
3	CNS	Foxp3 <sup>+</sup>	TRAV4D-3	TRAJ57	CAARQGGSAELIF
3	CNS	Foxp3 <sup>+</sup>	TRAV4D-3	TRAJ40	CAAPGNYKYVF
3	CNS	Foxp3 <sup>+</sup>	TRAV4D-3	TRAJ39	CAAGGDNAGAKLTF
3	CNS	Foxp3 <sup>+</sup>	TRAV4D-3	TRAJ50	CAAIASSSFSKLVF
3	CNS	Foxp3 <sup>+</sup>	TRAV4D-4	TRAJ57	CAAENQGGSAKLIF

TCR $\alpha$  were isolated by 5'RACE except for a subset of Foxp3<sup>+</sup> clones from mouse 3 that were isolated with TRAV4 and TCR C $\alpha$ -specific primers.

progenitor cells (HPCs). Approximately 40% of mice were protected from disease (**Figure 3-13a**). TCR $\beta$ 1<sup>+</sup> cells were a minority, though less frequent in mice protected from than developing EAE (**Figure 3-13c**). When EAE developed, symptoms were milder and mortality diminished, consistent with a protective role for the co-engrafted WT cells. We anticipated that TCR $\beta$ 1 imposes MOG-recognition on T cells, and that this should occur even in healthy animals. To test this, we analyzed disease-free chimeric mice. TCR $\beta$ 1<sup>+</sup>CD45.2<sup>+</sup> but not WT CD45.1<sup>+</sup> T cells from unprimed disease-free mice proliferated strongly to MOG<sub>35-55</sub> (**Figure 3-13b, d-e**). An estimated 15.6 $\pm$ 7.8% of the initial population of CD45.2<sup>+</sup> T cells responded to MOG<sub>35-55</sub> compared to 49.2 $\pm$ 12.3% to control  $\alpha$ CD3/CD28.

### **Public but not private TCR $\beta$ confer myelin specificity and provoke spontaneous autoimmunity**

TCR $\beta$ 1 is to our knowledge the first example of a single TCR chain endowing a heterogeneous population of T cells with overt spontaneous autoreactivity. To more comprehensively define the impact of public TCR $\beta$  in autoimmune susceptibility, we generated 14 additional TCR $\beta$  retrogenic mice using five additional TCR $\beta$  identified in  $\geq$ 9 CNS and all spleens (group 1), four in a single CNS at high frequency and shared in splenocytes to varying extents (group 2), and five that were wholly private (group 3; **Table 3-5**). A majority of CNS-infiltrating T cells in MOG-EAE recognize the MOG<sub>35-55</sub> epitope<sup>137</sup>. To minimize the possibility that TCR selected for analysis were derived from non-specific bystander T cells, group 2 and 3 TCR $\beta$  were either derived from high frequency CNS-infiltrating clones or private TCR $\alpha\beta$  sequences demonstrated to recognize MOG<sub>35-55</sub> autoantigen. For each TCR $\beta$ , mice were monitored for  $\geq$ 120 days or until the development of clinical disease, at which time all major organs were assessed grossly and histologically. T cells from disease-free mice were assayed for MOG<sub>35-55</sub>-specific responsiveness.

Of the additional group 1 TCR $\beta$ , none developed spontaneous EAE, though 2 of the 5 mice showed autoimmune features. Unprimed T cells from TCR $\beta$ 4 mice proliferated strongly in response to MOG<sub>35-55</sub> as measured both by <sup>3</sup>H-thymidine incorporation and membrane-associated dye dilution assays (**Figure 3-14a-c**). Therefore, like TCR $\beta$ 1, this TCR $\beta$  endows a large proportion of disparate TCR $\alpha\beta$  with specificity for the MOG<sub>35-55</sub> autoantigen. Meanwhile, T cells from TCR $\beta$ 7 (group 2) proliferated weakly to MOG<sub>35-55</sub>. This was detectable by <sup>3</sup>H-thymidine incorporation but not the less sensitive dye dilution assay (**Figure 3-14d**). However, mice expressing the 5 private group 3 TCR $\beta$  did not show any evidence for myelin reactivity.

Notably, TCR $\beta$ 3 T cells did not respond to MOG<sub>35-55</sub>. However, with early engraftment these mice developed spontaneous alopecia and esophagitis (**Figure 3-15**). This was associated with prominent T cell infiltrates in these locations. TCR $\beta$ 3 implicated that some CNS-associated public TCR $\beta$  may provoke alternative types of spontaneous autoimmunity. Except TCR $\beta$ 1 and TCR $\beta$ 3, there was no other histologic or clinical evidence of disease in mice expressing any of the other 4 group 1 CNS public

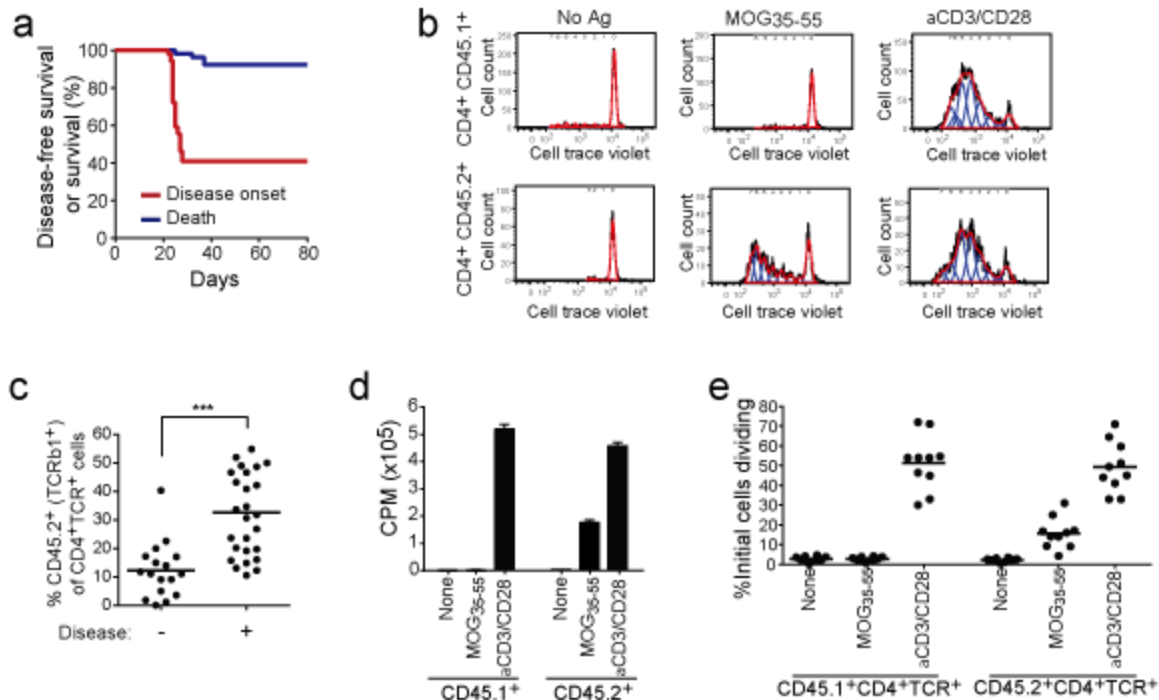


**Figure 3-13. Spontaneous EAE was protected by the co-engrafted WT cells in chimeric retrogenic mice.**

Chimeric retrogenic mice were generated by transducing wild type (WT) CD45.1<sup>+</sup>CD45.2<sup>-</sup> and congenic TCRβ1-transduced CD45.1<sup>-</sup>CD45.2<sup>+</sup> hematopoietic. (a) Disease-free and overall survival of mice chimeric for WT (CD45.1<sup>+</sup>) and TCRβ1 (CD45.2<sup>+</sup>) T cells are plotted. (b) *Ex-vivo* proliferation of CD4<sup>+</sup>CD45.1<sup>+</sup> (TCRβ1<sup>-</sup>) and CD4<sup>+</sup>CD45.2<sup>+</sup> (TCRβ1<sup>+</sup>) T cells from a representative 8 wk disease-free retrogenic mouse was measured by CellTrace<sup>TM</sup> Violet dilution 72 hr after stimulation. (c) Peripheral blood samples were collected at day 28 from mice chimeric for TCRβ1<sup>+</sup> and TCR<sup>WT</sup> T cells. The percent of CD4<sup>+</sup>TCR<sup>+</sup>CD45.2<sup>+</sup> (TCRβ1<sup>+</sup>) T cells among total CD4<sup>+</sup>TCR<sup>+</sup> T cells in chimeric mice developing or not developing EAE is plotted. (d) CD4<sup>+</sup>TCR<sup>+</sup>CD45.2<sup>+</sup> (TCRβ1<sup>+</sup>) and CD4<sup>+</sup>TCR<sup>+</sup>CD45.1<sup>+</sup> (TCR<sup>WT</sup>) T cells were flow cytometrically sorted from 8 wk chimeric mice without current or historical signs of EAE. The cells were stimulated as indicated and proliferation measured on day 3 by <sup>3</sup>H-thymidine incorporation. (e) T cells from 8 wk disease-free chimeric mice were labeled with CellTrace<sup>TM</sup> Violet and stimulated as indicated. At 72 hr, proliferation of CD4<sup>+</sup>TCR<sup>+</sup>CD45.2<sup>+</sup> and CD45.1<sup>+</sup> cells was determined as in figure 6h. The magnitude of each division peak was divided by 2<sup>x</sup>, where x=division peak number, to estimate numbers of parental cells whose progeny populated an individual peak. Based on this, the percent of total parental cells that had divided was calculated and is plotted.

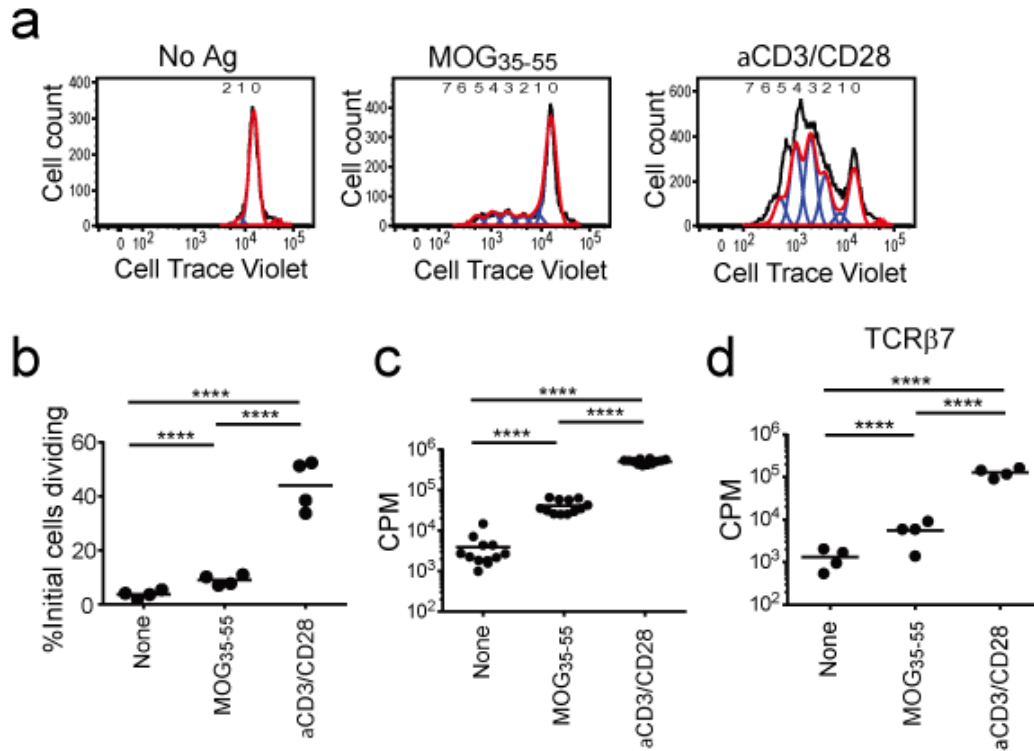


**Figure 3-14. Public TCRβ4, TCRβ7 impose MOG-reactive TCR repertoires.**

(a) Proliferation of T cells from unprimed and disease-free retrogenic TCRβ4 mice was measured by dye dilution 72 hr after stimulation as indicated. (b) The percent of initial cells dividing in response to the indicated stimulus was calculated by dividing each division peak by  $2^n$ , where  $n$ =division number, to estimate initial cell numbers forming each peak. (c) Proliferative response of purified TCRβ4 T cells measured using  $^3\text{H}$ -thymidine incorporation. Circles indicate means of triplicates from individual mice. (d) T cells from TCRβ7 retrogenic mice were isolated and stimulated as indicated. Proliferative response was measured at 72 hr by  $^3\text{H}$ -thymidine incorporation. Circles indicate means of triplicates from individual mice.



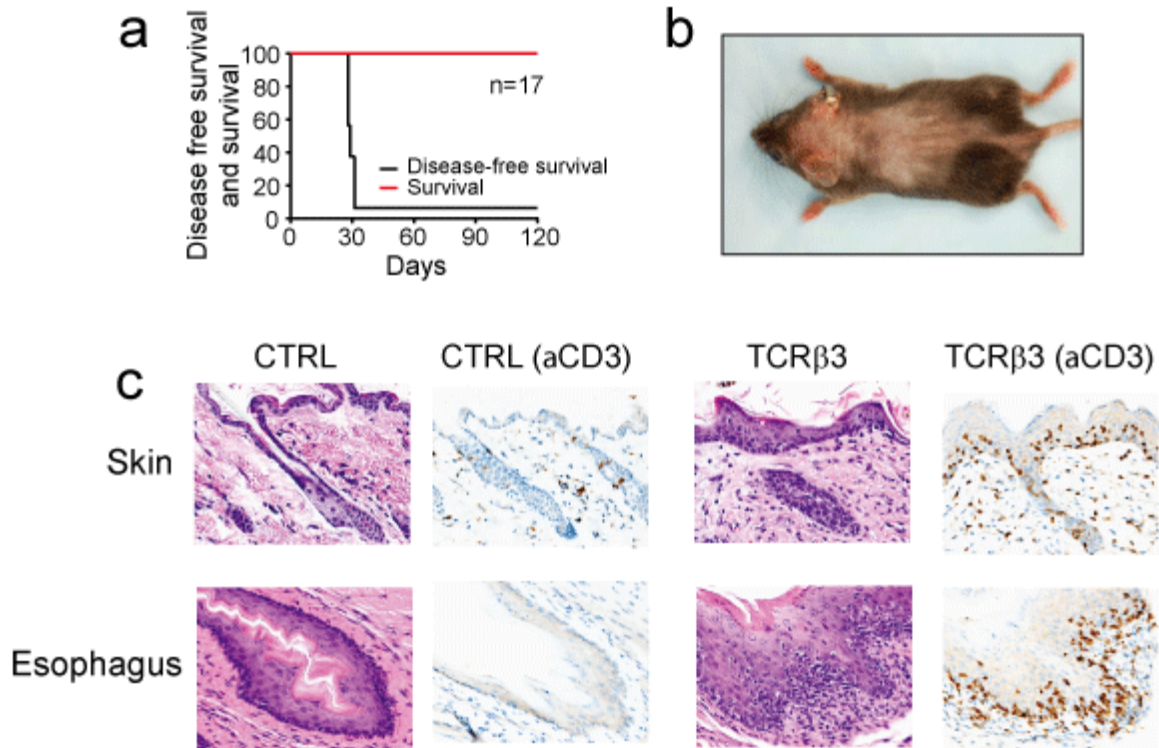


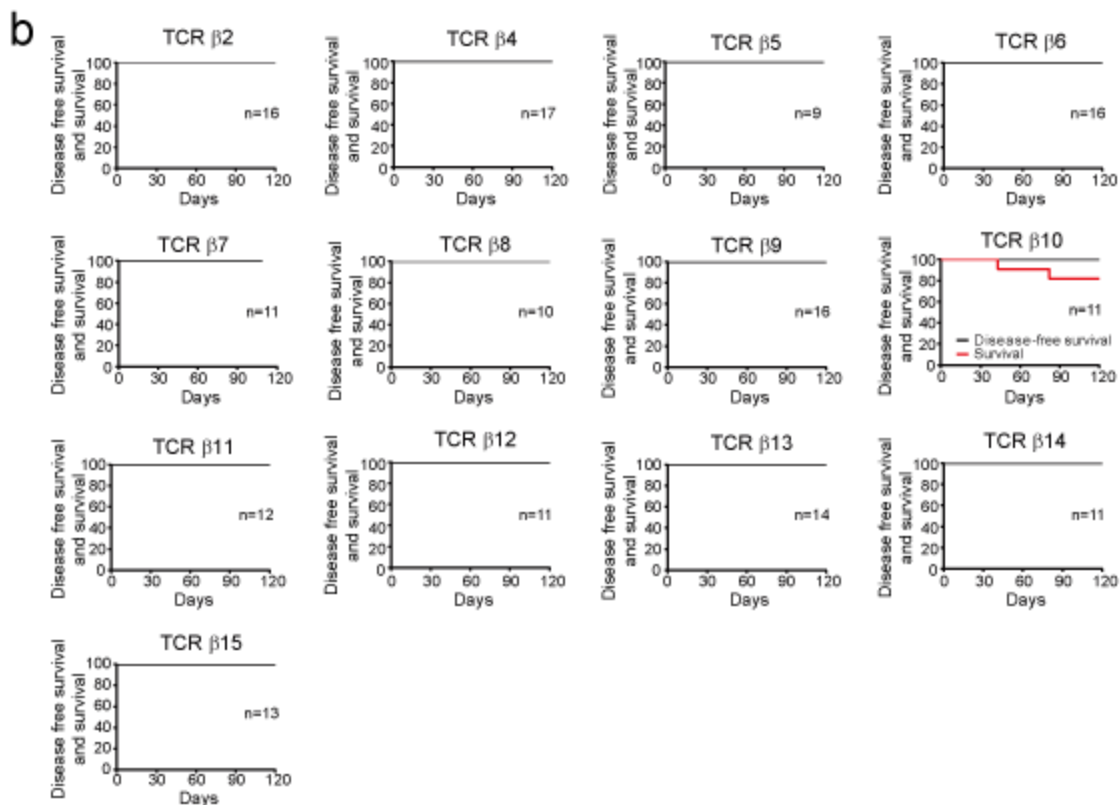
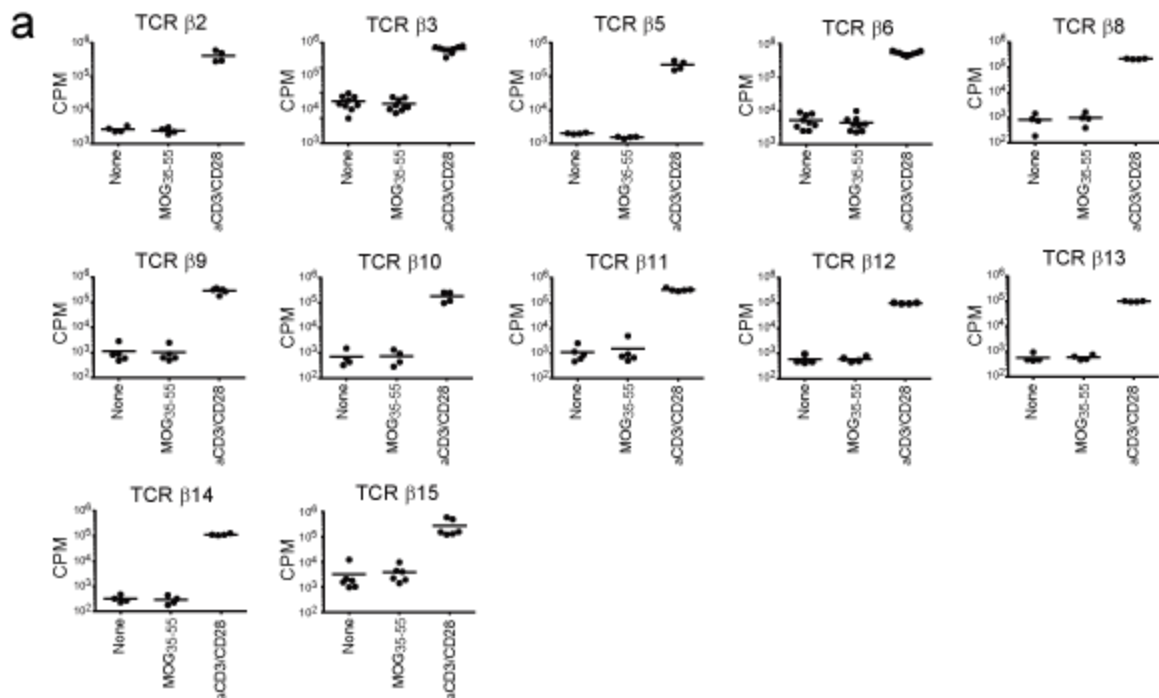
**Figure 3-15. Heightened public TCRβ3 autoreactivity.**

(a) Kaplan-Meier analysis of alopecia-free and overall survival in TCRβ3 retrogenic mice. (b) The dorsal surface of a representative TCRβ3 mouse demonstrates extensive alopecia areata. (c) Premature catagen and inflammatory infiltrates in the follicular and interfollicular epidermis, and inflammatory infiltrates associated with diffuse thickening and hypercellularity of the squamous esophageal epithelium of a day 30 TCRβ3 mouse. Immunohistochemistry for CD3<sup>+</sup> cells demonstrates markedly increased T cell numbers compared with a healthy control (CTRL) retrogenic mouse.

TCR $\beta$ , or the 4 group 2 TCR $\beta$  that were identified in a single CNS but public in the spleen. Mice expressing the 5 private group 3 TCR $\beta$  were also absent of clinical or histologic disease (**Figure 3-16**).

**Figure 3-16. MOG<sub>35-55</sub> response and disease-free survival of retrogenic mice.**

MOG<sub>35-55</sub> specific proliferation, disease-free survival, and overall survival is plotted for group 1 (TCR $\beta$  1-6), group 2 (TCR $\beta$  7-10), and group 3 (TCR $\beta$  11-15) mice not otherwise shown in other figures. (a) T cell proliferation to MOG<sub>35-55</sub>. CD4<sup>+</sup> T cells were purified from splenocytes from the indicated disease-free retrogenic mice and cultured for 3 days in the presence of syngeneic irradiated splenic APCs in the absence of additional stimulation or with 100  $\mu\text{g ml}^{-1}$  MOG<sub>35-55</sub> or  $\alpha\text{CD3/CD28}$ . Cultures were pulsed with <sup>3</sup>H-thymidine at 72 hr and <sup>3</sup>H incorporation measured. Circles indicate means of triplicates from individual mice. No significant differences were identified between unstimulated and MOG<sub>35-55</sub> stimulated samples for the mice shown. (b) Kaplan Meier analysis of disease free and overall survival of the indicated retrogenic mice is shown. Disease-free and overall survival was 100% over the 120 day observation period for all mice plotted except TCR $\beta$ 10, of which 2 died without overt preceding illness or apparent cause.



## CHAPTER 4. PRELIMINARY EXPERIMENTS

### Introduction

Though TCR repertoire analysis has proved to be a powerful tool in investigating the relationship between Treg and Tconv cells, the disparity of the results conducted from those experiments were affected by different mice model and sample size of the TCR repertoire, and it is limited in that inferences are made by population shifts in the absence of knowledge about antigen specificity. To better clarify the relationship between Treg cells and Tconv cells, the best way is to study the specificity and responsiveness of Treg and Tconv in the context of specific antigens. Our lab developed a retrogenic mouse model of EAE in which the TCR $\alpha$  chain locus was fixed by the enforced expression of a TCR $\alpha$  from a myelin oligodendrocyte glycoprotein (MOG)-specific T cell. TRBV13-2 is expressed by almost half of MOG-specific T cells in MOG-EAE, and we focused on this disease-associated repertoire<sup>101</sup>.

However, as we discussed in Chapter 3, public TCR $\beta$  distort repertoire response characteristics and foster reactivity to specific autoantigens. We can benefit from retrogenic mice models with enforced expression of disease-associated public TCR $\beta$  chains and investigate the Tconv and Treg TCR repertoires. To begin with, we will focus on the TCR $\beta$ 1 retrogenic mice for several reasons. First, it is the most commonly shared TCR $\beta$ 1 in immunized mice and pre-immune mice. Second, it is presented on both Treg and Tconv population, narrowing our TCR fine specificity analysis on the pairing TCR $\alpha$  repertoire. Third, TCR $\beta$ 1 mice develop spontaneous EAE by imposing a high frequency of MOG-reactive TCR repertoire, implying the close association between TCR $\beta$ 1 derived repertoire with MOG-EAE.

### Results

We favor a model where the public TCR $\beta$ 1, which pairs with degenerate TCR $\alpha$  but still retains auto-reactivity, however, we cannot rule out the possibility that this public TCR $\beta$ 1 may impose a biased TCR $\alpha$  pairing. Biased TCR $\alpha$  usage was observed on CNS infiltrating cells in MOG-EAE mice, V $\alpha$ 9-J $\alpha$ 23 and V $\alpha$ 9-J $\alpha$ 31. However, there lacks evidence to show whether this biased TCR $\alpha$  usage is TCR $\beta$ 1 related<sup>126</sup>.

First we need to identify the TCR $\alpha$  repertoire in TCR $\beta$ 1 retrogenic mice. Mice were sacrificed around day 30 post bone marrow transplant during their peak disease, and CNS T cells were isolated. The number of specific V $\alpha$  antibodies are very limited, only V $\alpha$  2, V $\alpha$ 3.2, V $\alpha$ 5, V $\alpha$ 8.3 and V $\alpha$ 11 specific antibodies are commercialized. Flow cytometric phenotyping of the isolated CNS T cells by using these V $\alpha$  antibodies failed to show any enriched TRAV usage compared with MOG-induced EAE mice (data not shown). Since V $\alpha$  nucleotide sequences are much more conservative than V $\beta$ , to discriminate different V $\alpha$  subtype, full length TCR $\alpha$  cDNA were generated by using 5' RACE. CNS infiltrating T cells from TCR $\beta$ 1 were sorted into Treg and Tconv population.

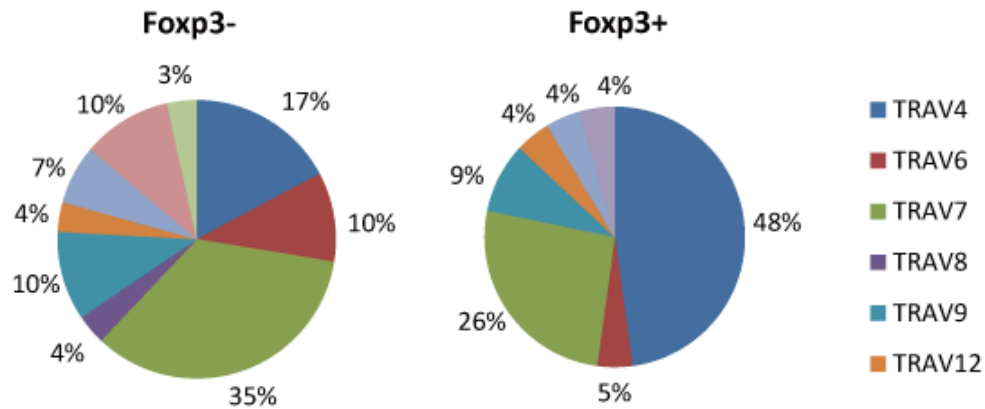
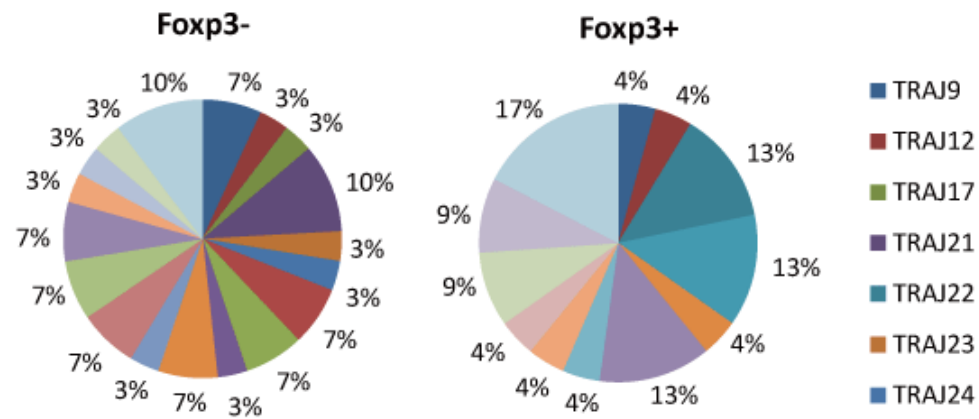
cDNA were synthesized, amplified by using 21 V $\alpha$  and C $\alpha$  specific primers, and TA subcloned into the pCR2.1 vector to create a cDNA library of TCR $\alpha$  chains. cDNA containing plasmids will be randomly selected and sequenced. V $\alpha$ , J $\alpha$ , and CDR3 $\alpha$  regions will be interpreted by IMGT-V-QUEST (<http://imgt.cines.fr>).

Overall, 52 unique TCR $\alpha$  chains were identified from three mice (**Table 3-6**), among which 29 were Tconv derived whereas 23 were Treg derived. The CDR3 $\alpha$  sequences of those oligoclone types were heterogeneous and did not overlap between mice, indicating that TCR $\beta$ 1 is associated with diverse TCR $\alpha$ . However, TRAV4 and TRAV7 utilization were enriched in either Foxp3<sup>-</sup> Tconv cells (TRAV4: 17%, TRAV7: 35%) or Foxp3<sup>+</sup> Treg cells (TRAV4: 48%, TRAV7: 26%), but we didn't find any evident enriched TRBJ usage (**Figure 4-1**).

Though we identified a number of TCR $\alpha$  from TCR $\beta$ 1 CNS infiltrating cells, and TCR $\beta$ 1 was able to impose TCR MOG<sub>35-55</sub> reactivity by paring with degenerate TCR $\alpha$ , however, what antigen these T cells recognized *in vivo* was still unknown. They can be either a MOG responder, a MOG non-responder but react to other cryptic self-antigen in CNS<sup>138</sup>, or a just circulating bystander during the CNS inflammation. Therefore we first tested their MOG<sub>35-55</sub> specificity in CD4 4G4 hybridoma T cell lines. Fourteen out of fifty-two TCR reconstituted hybridoma cell lines demonstrated low to high MOG<sub>35-55</sub> reactivity (**Table 4-1**). Next, we further tested their fine specificity of all MOG<sub>35-55</sub> reactive TCR in peptide titration assay. In either Treg or Tconv population, TCR were identified with high, moderate, and low sensitivity for MOG<sub>35-55</sub> stimulation (**Figure 4-2**). Nine out of eleven TCR with TRAV4 V region mediated moderate to high MOG<sub>35-55</sub> response, no matter it was Treg or Tconv derived. In contrast, the other 2 TRAV4 TCR were able to mediate very low MOG<sub>35-55</sub> response, both of which were Treg derived. In addition, 2 TRAV7 TCR mediated low to moderate MOG<sub>35-55</sub> response, both of which were Tconv derived. The only 1 TRACV13 TCR mediated high MOG<sub>35-55</sub> response, and it was from Tconv.

To find out whether MOG<sub>35-55</sub> specificity *in vitro* was correlated with the pathogenesis *in vivo*, retrogenic mice were made with enforced expression of particular MOG<sub>35-55</sub> specific TCR $\alpha\beta$ . Mice were followed for disease development for at least 80 days post bone marrow transfer. For most of the Tconv derived TCR (**Figure 4-3a**), mice progressed spontaneous EAE symptoms with early T cell engraftment, only PUN308 was observed for decreased incidents due to its poor engraftment. For those Treg derived TCR (**Figure 4-3b**), PUN342 could induce severe spontaneous EAE, but Br11, Br17, Br25, Br41, Br47 were observed with sporadic or no disease incidents which were associated with low T cell engraftment. For PUN355 and PUN376, those TCRs showed low MOG<sub>35-55</sub> reactivity, no disease was observed even with good engraftments.

From these preliminary experiments, it seems impossible to simply correlate any TRAV usage, T cell type, CDR3 $\alpha$  sequences or MOG<sub>35-55</sub> specificity with pathogenesis *in vivo*. PUN003 and PUN005 were Tconv derived with low MOG reactivity, but were still able to induce spontaneous EAE otherwise high MOG reactive PUN308 was on the

**a****b**

**Figure 4-1. Pie charts of TRAV and TRAJ usage in TCR $\beta$ 1 CNS infiltrating T cells.**

CNS infiltrating T cells were isolated from TCR $\beta$ 1 retrogenic mice. cDNA was synthesized, subcloned, and followed by Sanger sequencing (a) TRAV usage in Tconv or Treg (b) TRAJ usage in Tconv or Treg.

**Table 4-1. Fourteen reconstituted TCR $\alpha\beta$  with MOG<sub>35-55</sub> reactivity on hybridoma cells.**

Constructs	Derived cell type	TRAV	TRAJ	CDR3 $\alpha$	TRBV	TRBJ	CDR3 $\beta$
<b>PUN002</b>	Foxp3 <sup>-</sup>	TRAV4D-3	TRAJ21	AAGGYNVLYF	TRBV13-2	TRBJ2-1	ASGETGGNYAEQF
<b>PUN003</b>	Foxp3 <sup>-</sup>	TRAV7-3	TRAJ27	AANTGKLTF	TRBV13-2	TRBJ2-1	ASGETGGNYAEQF
<b>PUN005</b>	Foxp3 <sup>-</sup>	TRAV7D-3	TRAJ37	AVGGNTGKLIF	TRBV13-2	TRBJ2-1	ASGETGGNYAEQF
<b>PUN307</b>	Foxp3 <sup>-</sup>	TRAV4D-4	TRAJ42	AASGGSNAKLTF	TRBV13-2	TRBJ2-1	ASGETGGNYAEQF
<b>PUN308</b>	Foxp3 <sup>-</sup>	TRAV4D-3	TRAJ49	AAVTGYQNFYF	TRBV13-2	TRBJ2-1	ASGETGGNYAEQF
<b>PUN323</b>	Foxp3 <sup>-</sup>	TRAV13D-1	TRAJ37	ALITGNTGKLIF	TRBV13-2	TRBJ2-1	ASGETGGNYAEQF
<b>PUN342</b>	Foxp3 <sup>+</sup>	TRAV4D-3	TRAJ42	AAGGSNAKLTF	TRBV13-2	TRBJ2-1	ASGETGGNYAEQF
<b>PUN355</b>	Foxp3 <sup>+</sup>	TRAV4D-4	TRAJ57	AAGQGGSACLIF	TRBV13-2	TRBJ2-1	ASGETGGNYAEQF
<b>PUN376</b>	Foxp3 <sup>+</sup>	TRAV4D-3	TRAJ50	AARSSSSFSKLVF	TRBV13-2	TRBJ2-1	ASGETGGNYAEQF
<b>BR11</b>	Foxp3 <sup>+</sup>	TRAV4D-3	TRAJ33	AAPDSNYQLIW	TRBV13-2	TRBJ2-1	ASGETGGNYAEQF
<b>BR17</b>	Foxp3 <sup>+</sup>	TRAV4D-3	TRAJ57	AARQGGSACLIF	TRBV13-2	TRBJ2-1	ASGETGGNYAEQF
<b>BR25</b>	Foxp3 <sup>+</sup>	TRAV4D-3	TRAJ40	AAPGNYKYVF	TRBV13-2	TRBJ2-1	ASGETGGNYAEQF
<b>BR41</b>	Foxp3 <sup>+</sup>	TRAV4D-3	TRAJ39	AAGGDNAGAKLTF	TRBV13-2	TRBJ2-1	ASGETGGNYAEQF
<b>BR47</b>	Foxp3 <sup>+</sup>	TRAV4D-3	TRAJ50	AAIASSSFSKLVF	TRBV13-2	TRBJ2-1	ASGETGGNYAEQF

Identified TCR $\alpha$  sequences from 5' RACE were reconstituted with TCR $\beta$ 1 and transduced into CD4 4G4 hybridoma cells. All the hybridoma cell lines were treated with 100ug/ml MOG<sub>35-55</sub> in the presence of syngeneic APCs. IL-2 production was measured by ELISA at 24 hr. Fourteen out of total fifty-two unique TCR $\alpha$  chains were further tested for their fine specificity.



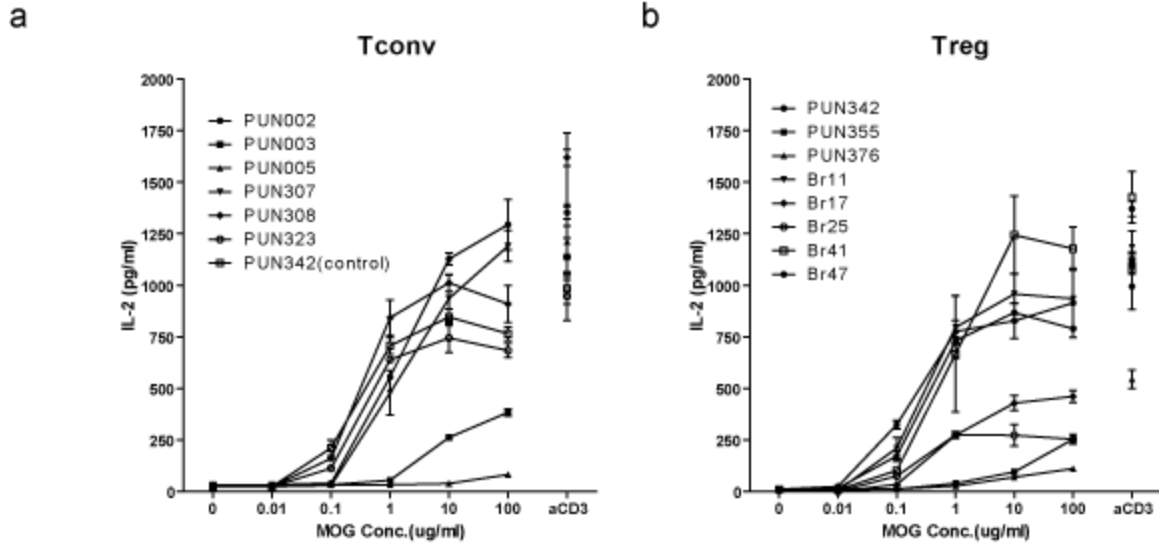


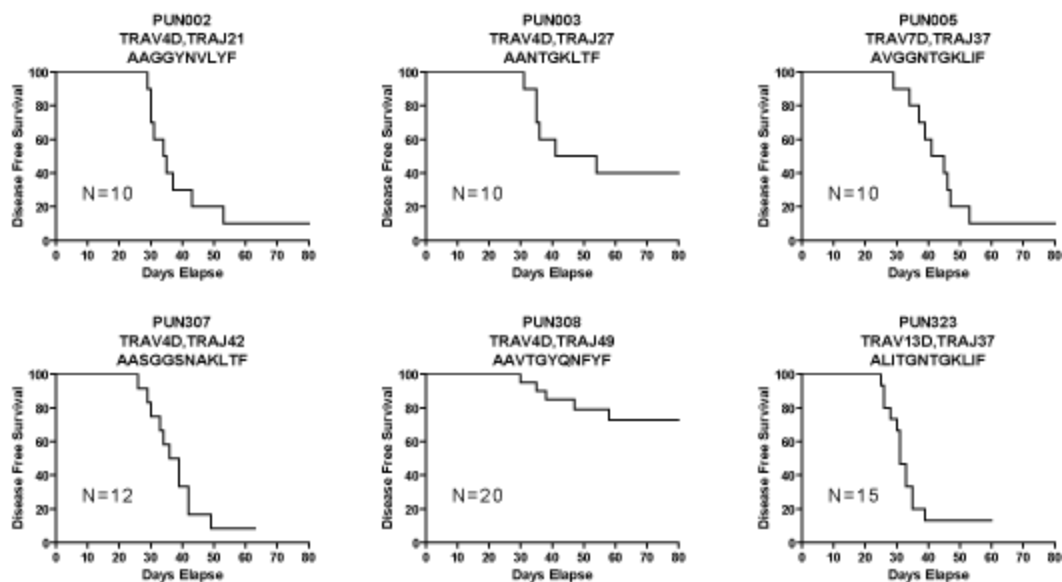
**Figure 4-2. Titration assay for MOG<sub>35-55</sub>-specific TCR.**

TCR reconstituted 4G4 CD4 hybridoma cells were tested for their fine specificity to MOG<sub>35-55</sub> stimulation *in vitro*. IL-2 production was analyzed by ELISA assay for different cell lines bearing either Tconv (a) or Treg (b) T-cell derived TCR, stimulated with varied doses of MOG<sub>35-55</sub> peptide in the presence of syngeneic APCs. PUN342 line is Treg derived TCR, used as an inner control for comparability. Data shown is representative of 3 independent experiments with at least 2 independent transductions of each TCR.

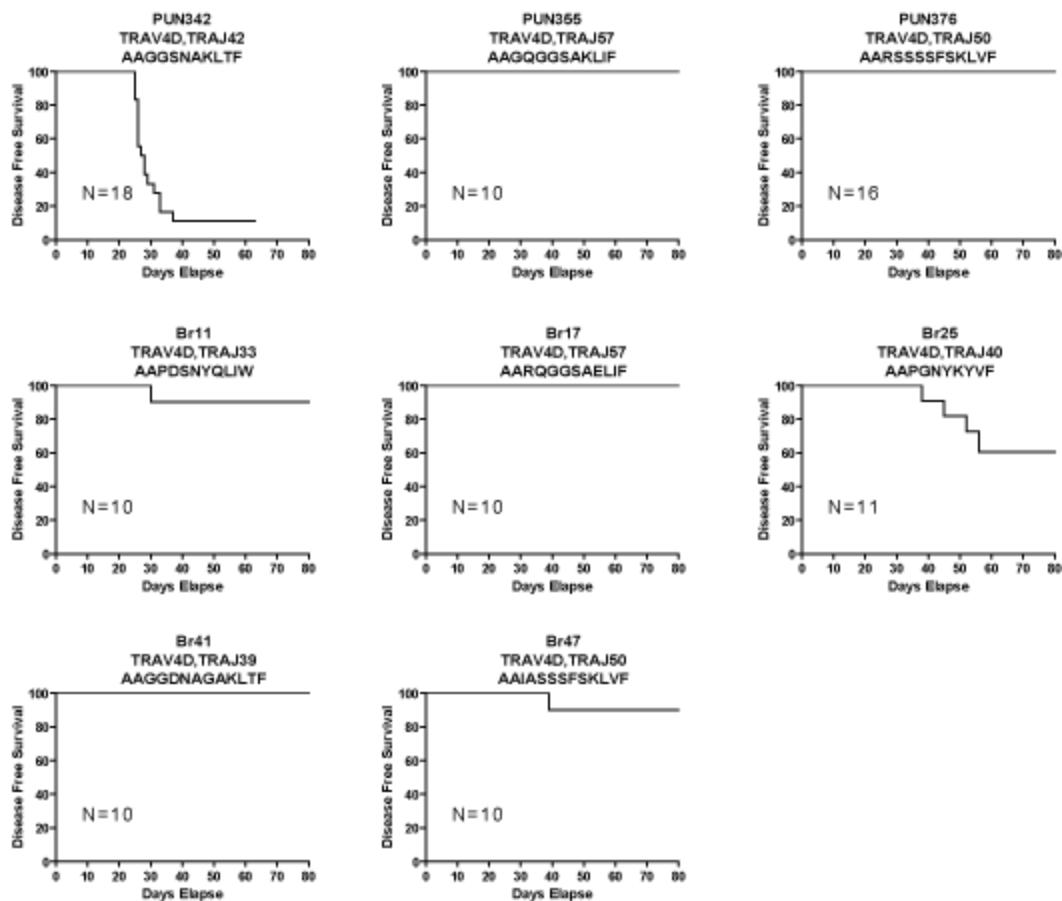
**Figure 4-3. MOG<sub>35-55</sub> response and disease-free survival of TCR $\alpha\beta$  retrogenic mice.**

Kaplan Meier analysis of disease free of the indicated TCR $\alpha\beta$  retrogenic mice is shown. TCR $\beta$ 1 was enforced expression with different TCR $\alpha$  identified from 5'RACE. Disease development was followed in these retrogenic mice at least 80 days post bone marrow transfer. Sick mice were sacrificed and analyzed before moribund. (a) Retrogenic mice with Tconv derived TCR $\alpha\beta$  .(b) Retrogenic mice with Treg derived TCR $\alpha\beta$ . Data was collected from at least 2 batches of retrogenic mice. Total mice number was indicated.

**a**



**b**



opposite, indicating it was not a solely MOG<sub>35-55</sub> specificity dependent pattern. The situation seems more complicated for Treg derived TCR, high MOG reactive PUN342 could induce disease while low MOG reactive PUN355 and PUN376 could not, even though PUN342 possess Tregs during the early disease ( $4.47 \pm 4.24\%$  in CNS,  $7.70 \pm 7.74\%$  in Spleen). On the other hand, several other Treg derived TCRs (Br11, Br17, Br25, Br41, Br47) were observed with poor early T cell engraftment resulting in the sporadic or no disease incidents. Interestingly, we noticed the CDR3 $\alpha$  sequences of PUN342 and PUN307 are almost identical except one extra “S” residue on the 3<sup>rd</sup> position of PUN342. They were identified from distinct T cell population, however, both of them share similar MOG<sub>35-55</sub> specificity and pathogenesis. This “S” residue can be tolerated due to the degeneracy of TCR specificity against MOG<sub>35-55</sub>-MHC ligand, but it may provide some clues for T cell lineage commitment in the thymus.

Retrogenic mice developed spontaneous EAE around day 30 post bone marrow transfer, for which early engraftment of those MOG<sub>35-55</sub> specific T cells seems essential for disease onset<sup>123</sup>. To investigate the relationship between early engraftment level and disease, the data from retrogenic mice of Tconv derived TCR $\alpha\beta$  were pooled together, and disease onset day showed an inverse correlation against the CD4 T cell frequency in blood lymphocytes on day 28, the higher level CD4 T cell frequency, the earlier the disease (**Figure 4-4**). Treg derived TCR was not analyzed here because only PUN342 developed disease with detected level of engraftment. Therefore the data was limited for Treg derived TCR.

Treg derived TCR would generate Tregs in retrogenic mice, whereas there was not Treg cells in retrogenic mice expressing Tconv derived TCR<sup>123</sup>. Overlaid on this, retrogenic mice with PUN342, which was identified from a Treg clonotype, still developed severe spontaneous EAE with early T cell engraftment. Phenotypic analysis were routinely performed on the retrogenic mice during their peak disease, a proportion of Tregs was present in PUN342 retrogenic mice (Spleen:  $7.7 \pm 7.7\%$ ; CNS:  $4.7 \pm 4.2\%$ ) and the absolute Treg cell number was Spleen:  $4.1 \pm 5.3 \times 10^4$  CNS:  $1.3 \pm 1.2 \times 10^4$ . However, the disease seems not to be protected in the presence of this small fraction of Tregs.

There was also a low frequency of Tregs in the PUN308 retrogenic mice, but the actual number was very limited. This might result from the background noise for flow cytometry in retrogenic mice if the mice were poorly engrafted. There were very limited Treg cells in the spleen of retrogenic mice expressing Tconv derived TCRs, which was consistent with prior reports<sup>123,139</sup>. However, in some cases, a small number of Foxp3<sup>+</sup> CD4<sup>+</sup> T cells were observed in CNS. Those CNS Foxp3<sup>+</sup> T cells might be expanded nTreg or induced Treg responding to abundant antigenic stimulation (**Figure 4-5**).

Since the retrogenic mice develop spontaneous EAE with very early T cell engraftment at ~4 wk, characterization of the mechanism undergoing during that time point maybe suggestive. What antigens are those cells recognizing? Whether they are autoantigens or foreign antigens? Why those activated T cells can migrate into CNS? The commensal bacteria is associated with CNS disease<sup>140,141</sup>, so our first intuition was that TCR cross-reactivity to the commensal microbial antigens stimulated the T cells. Then



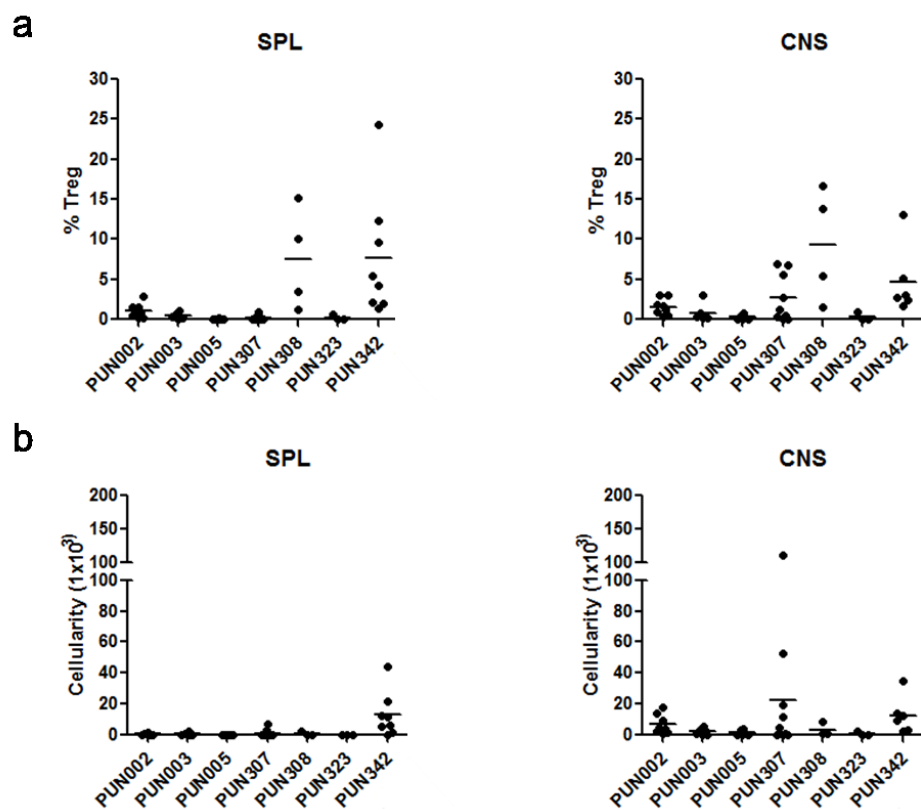


**Figure 4-5. Treg analysis of retrogenic T cells.**

Flow cytometric analysis of surface-stained splenocytes from the indicated type of retrogenic mouse is shown. Mice were sacrificed and analyzed during their peak disease (disease score >3) (a) Frequency of Tregs either in spleen or CNS CD4 T lymphocyte population. (b) Cellularity of Tregs either in spleen or CNS.

we tried to test the responsiveness of four MOG<sub>35-55</sub> specific TCR to MOG<sub>35-55</sub> mimicry peptides. They are PUN002 (Tconv, high MOG<sub>35-55</sub> reactivity), PUN003 (Tconv, moderate MOG<sub>35-55</sub> reactivity), PUN003 (Tconv, low MOG<sub>35-55</sub> reactivity) and PUN342 (Treg, high MOG<sub>35-55</sub> reactivity). Though different TCR demonstrated variability, the common patterns of reactivity when tested with alanine-substituted MOG<sub>35-55</sub> peptides were quite similar (**Figure 4-6**). Similar to prior studies characterizing the R41, F44, R46, and V47 are critical MOG<sub>35-55</sub> residues for specific TCR interacting<sup>142</sup>, stimulation with common patterns of reactivity when tested with alanine-substituted MOG<sub>35-55</sub> peptides alanine-substituted peptides such as F44A, R46A, V47A and V48A greatly blunt the reactivity compared to original MOG<sub>35-55</sub> peptide (**Figure 4-6**). These residues are determinants for epitope specificity at least for these four TCR clonotypes, however, the tolerance of TCR specificity to other alanine-substituted MOG<sub>35-55</sub> peptides suggests the potential cross reactivity of the MOG<sub>35-55</sub> reactive T cells responding to the MOG<sub>35-55</sub> peptide mimicry. Since the experimental mice were conducted under specific germ free condition, the mimicry peptides may be introduced from the commensal bacteria, and lead to activation of the early engrafted MOG<sub>35-55</sub> reactive T cells.

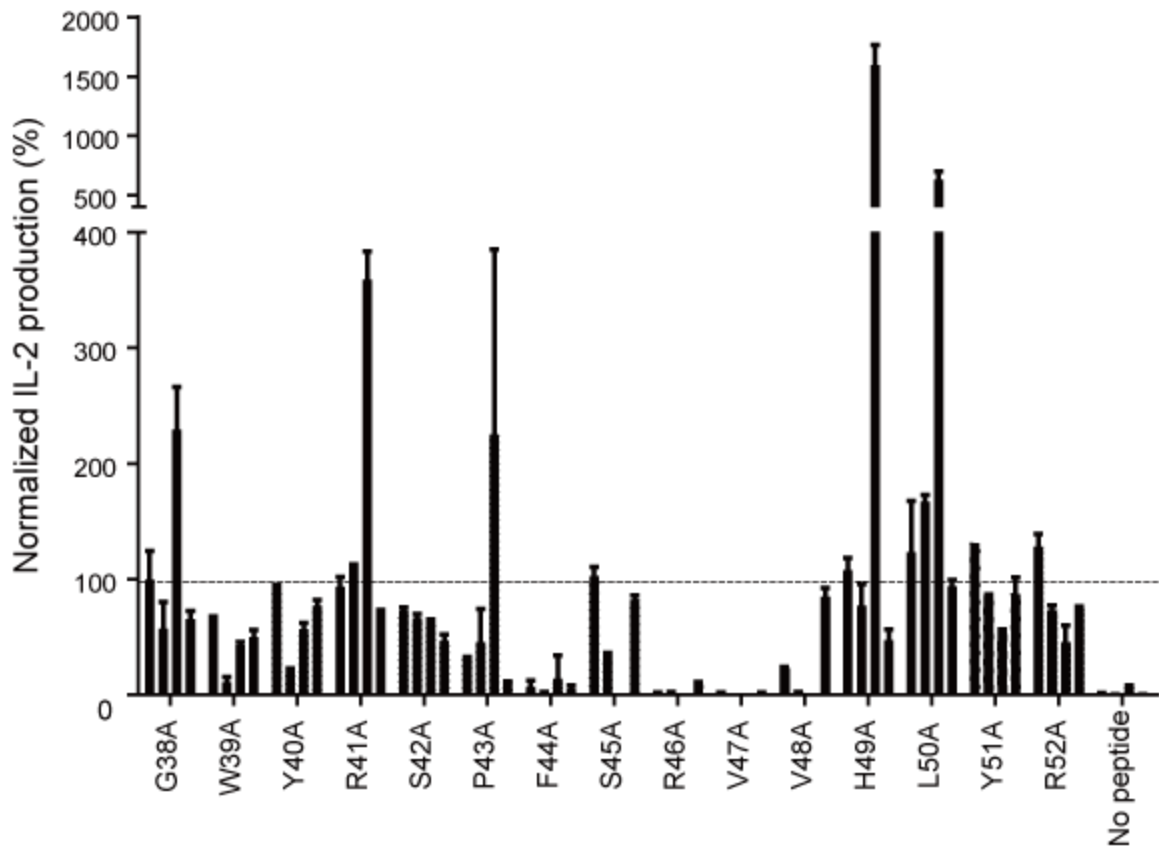


**Figure 4-6. Cross reactivity to MOG<sub>35-55</sub> mimicry.**

Four different 4G4 CD4 cell lines transduced with TCR $\alpha\beta$  were tested for their responsiveness to 100 $\mu$ g/ml MOG<sub>35-55</sub> or MOG<sub>35-55</sub> mimicry peptides by ELISA. The IL-2 production was normalized to MOG<sub>35-55</sub> group. Bars indicate from left to right IL-2 production by clonotype PUN002, PUN003, PUN005 and PUN342. Dashed line was an indicator for MOG<sub>35-55</sub>. Mean  $\pm$ SD is plotted.



## CHAPTER 5. DISCUSSION

### Public TCR in Skewing Repertoire Response and Autoimmune Susceptibility

In previous chapters, we talked about by linking saturation sequencing of disease-associated and unassociated repertoires during EAE with the transgenic expression and in vivo functional analysis of 15 public and private TCR $\beta$ , we identify a selective and prominent role of public TCR in the autoimmune response. Public TCR were preferentially incorporated into the CNS-infiltrating repertoire. The frequency of unique and total public TCR $\beta$  was markedly elevated when compared with TCR $\beta$  unengaged in autoimmunity both from mice with EAE and from pre-immune mice. Three public but no private TCR $\beta$  were able to confer unprimed T cells expressing endogenously rearranged TCR $\alpha$  with overt MOG-reactivity. Enforced expression of two of six CNS-shared TCR $\beta$  provoked spontaneous autoimmunity in a mouse strain that does not otherwise develop spontaneous autoreactivity. Our findings indicate that public TCR $\beta$  distort repertoire response characteristics and foster reactivity to specific autoantigens.

Recombinatorial biases in preselection thymocytes serve as the primary source for the generation of the broad public repertoire<sup>42,143-145</sup>. Predispositions in VDJ usage and activity levels of TdT and nucleases modifying junctional sequences increase the probability these sequences will form<sup>146</sup>. We implicate similar pre-selection biases in also generating the public autoimmune repertoire, and identify substantial ongoing oligoclonal production of public autoimmune-associated TCR within the thymus. As previously documented by Dyson and colleagues with the larger public repertoire<sup>147</sup>, analyses of the frequency of individual receptors in pre- and post-selection thymocytes and splenic T cells further failed to indicate that, once formed, disease associated public TCR are preferentially selected (data not shown).

Our results do not imply that public TCR possess unique structural properties that distinguish them from private TCR. Indeed, despite comprising a small fraction of the total repertoire, public sequences remain diverse. It would therefore seem unlikely that their preferential recruitment into the autoimmune response when compared with private sequences is due to a distinct biochemistry. Rather, because public TCR are pervasive across a population, specificity distortions they introduce within the repertoire will be introduced into all individuals bearing relevant MHC alleles. Thus, MOG<sub>35-55</sub> may serve as the dominant autoantigen in C57BL/6 EAE precisely because the public repertoire in conjunction with the restricting MHC, IA<sup>b</sup>, augments repertoire reactivity toward this autoantigen. Other neuroantigens preferentially engaged by private TCR would only be capable of mediating autoimmunity in the small number of individuals that stochastically possess adequate numbers and subsets of antigen-specific private T cells.

An alternative hypothesis for the preferential incorporation of public sequences in the autoimmune repertoire is that these sequences do predispose TCR $\alpha\beta$  toward self-reactivity. Other repertoire studies, though more limited in scope and definition compared with these, have also identified public sequences among autoreactive T cells<sup>123,125,148</sup>.

That public TCR may more generically confer responsiveness to self-antigens is also suggested by our finding that transgenic expression of the public, EAE-associated TCR $\beta$ 3 chain led to the development of spontaneous alopecia areata and not EAE. Therefore, a single TCR $\beta$  may promote reactivity to disease-associated autoantigens from different tissues. In this regards, it is noteworthy that a previously isolated though distinct TRBV13-2<sup>+</sup> TCR $\beta$  from a MOG<sub>35-55</sub>-specific hybridoma, 1MOG244.2, was identified as possessing two TCR $\alpha$  chains. Transgenic expression of one TCR $\alpha\beta$  led to MOG<sub>35-55</sub> reactive T cells. The second provoked spontaneous alopecia areata, suggesting a broader association between CNS and skin reactivities<sup>149</sup>.

Public TCR use is not only identifiable in the context of autoimmunity, but has also been found in the responses to several pathogens and other antigens<sup>42,127</sup>. One possible explanation is that the recombinatorial activities involved in forming the public repertoire also creates a public sequence space that more broadly supports TCR associations with MHC-antigen complexes. The majority of the TCR interface with antigen-MHC binds the MHC rather than antigenic peptide, and MHC-specific associations are critical to stabilizing this interaction<sup>6,150</sup>. If the public repertoire incorporates TCR better suited to support MHC engagement, these receptors may preferentially enter immune responses. Such a model would suggest a co-evolution of the public TCR repertoire with restricting MHC, presumably by modulating recombination frequencies so as to optimize this component of the response. An element of enhanced self-reactivity would be expected to accompany such increased TCR fitness. Indeed, TCR mutations that enhance TCR-MHC association also promote self-reactivity and can endow TCR with new autoreactivities<sup>151,152</sup>.

We found that 2 of the 6 group 1 (CNS-shared and public) TCR $\beta$  and altogether 3 shared TCR $\beta$  broadly imposed MOG specificity on TCR $\alpha\beta$ . MOG-responsiveness was particularly prominent in mice expressing TCR $\beta$ 1, where nearly 1/3 the number of CD4<sup>+</sup> T cells from disease-free animals responding to  $\alpha$ CD3 proliferated to MOG<sub>35-55</sub>. Unlike antibody-antigen interactions, which may rely on a single Ig chain, the TCR-MHC interface extensively involves both the TCR $\alpha$  and  $\beta$  surfaces. Implicitly, TCR $\beta$ 1 dominates interactions defining specificity during MOG<sub>35-55</sub>-IA<sup>b</sup> recognition, and this is accompanied by more generic interactions with TCR $\alpha$  that are simply non-disruptive and provide requisite supplemental association energy for effective T cell stimulation. However, in the absence of structural definition, it cannot be excluded that TCR $\beta$ 1 and other public TCR $\beta$  chains bind autoantigens in non-conventional manners that minimize reliance on the TCR $\alpha$ <sup>74</sup>.

The capacity to interrogate the repertoire continues to increase with improving sequencing technologies<sup>26</sup>. Data sets are being collected in several disease models and these may be linked to functional analyses of individual TCR, similar to those we describe here, to identify the relevance of specific sequences. Indeed, the identification of preferential TRBV and TRAV usage in several diseases may imply that public TCR $\alpha$  or TCR $\beta$  sequences bearing pre-defined V, J, and CDR3 sequences will strongly skew response characteristics. If so, specific public sequences may prove useful for the

longitudinal monitoring of immune responses during autoimmune diseases. Likewise if public TCR ultimately prove not only to be over-represented and risk factors for the autoimmune response as indicated here, but drivers of it as originally hypothesized by Sercarz and colleagues<sup>153</sup>, it may be possible to broadly modulate the autoimmune response by specifically guiding the selection or activity of T cells bearing public TCR sequences.

### **Functional Characterization of TCR $\alpha$ Repertoire in TCR $\beta$ 1 Retrogenic Mice Model**

Meanwhile, we performed preliminary experiments to characterize the TCR $\alpha$  repertoire by using the TCR $\beta$ 1 mice model, which generated narrowed repertoire diversity with fixed TCR $\beta$ 1 paring with endogenous TCR $\alpha$ . We favor this mice model for the following consideration. First, it is the most commonly shared TCR $\beta$  in immunized mice and pre-immune mice. Second, it is presented on both Treg and Tconv population, narrowing our TCR fine specificity analysis on the paring TCR $\alpha$  repertoire. Third, TCR $\beta$ 1 mice develop spontaneous EAE by imposing a high frequency of MOG-reactive TCR repertoire, implying the close association between TCR $\beta$ 1 derived repertoire with MOG-EAE. Investigation on the composition of TCR $\alpha$  chain repertoire will potentially yield valuable information for the TCR structural features, specificity, responsiveness, and lineage commitment of Treg and Tconv in the context of autoimmune disease.

We were able to identify 52 unique clonotypes from CNS of 3 TCR $\beta$ 1 retrogenic mice. Though only a small number, these clonotypes were heterogeneous and did not overlap between mice, indicating that TCR $\beta$ 1 can associate with diverse TCR $\alpha$ . TCR were reconstituted and transduced into 4G4 CD4 hybridoma cells for MOG<sub>35-55</sub> reactivity test *in vitro*. Fourteen unique TCR showed low to high responses to MOG<sub>35-55</sub> stimulation. In order to investigate their potential pathogenesis against autoantigen in retrogenic mice, we made retrogenic mice which express single TCR $\alpha\beta$ . All the Tconv derived TCR were able to promote early spontaneous EAE, which seemed irrelevant to MOG specificity. However, PUN342, a Treg derived TCR with high MOG<sub>35-55</sub> reactivity, promoted early spontaneous EAE even in the presence of Treg cells. While PUN355 and PUN376, Treg derived TCR with low MOG<sub>35-55</sub> reactivity, failed to promote any disease. This result implicated that the presence of Treg cells were not able to protect the EAE induced by the high MOG<sub>35-55</sub> reactive T cells. Meanwhile, some retrogenic mice expressing PUN308 and several Treg derived TCRs (Br11, Br17, Br25, Br41, Br47) were noticed with poor engraftment. A possible explanation would be that these TCR clonotypes under the surveillance of central tolerance might hardly leak into the periphery. In C57BL/6 mice, Delarasse *et al.* have shown that MOG transcripts are expressed in thymus<sup>154</sup>. Nevertheless, the expression of MOG protein in human and mouse thymus has never been reported so far. Therefore, the MOG specificity of clonotypes may not simply correlated with the pathogenesis. Interestingly, we noticed that CDR3 $\alpha$  sequences of two clonotypes are similar except one additional “S” residue on the 3<sup>rd</sup> position of Treg derived TCR. They are belonging to distinct T cell type, but sharing similar MOG specificity and pathogenesis. This “S” residue can be tolerated due to the degeneracy of

TCR specificity against MOG<sub>35-55</sub>-MHC ligand, but it seems critical for T cell lineage commitment in the thymus. Due to the limited number and poor engraftment capability of some TCR clonotypes, it is too early to come to any final conclusion that how fine specificity of TCR is relevant to T cell commitment or pathogenesis.

### Cross Reactivity, Gut and CNS

Since the retrogenic mice develop spontaneous EAE with very early T cell engraftment, we are curious about what stimuli are recognized by those cells *in vivo*. We examined the responsiveness of four MOG reactive TCR to MOG<sub>35-55</sub> mimicry peptides. Different TCR demonstrated variability, but common patterns of reactivity when tested with alanine-substituted MOG<sub>35-55</sub> peptides was evident. MOG<sub>35-55</sub> mimicry peptides such as F44A, R46A, V47A and V48A greatly blunted the reactivity compared to MOG<sub>35-55</sub> stimulation, suggesting that these residues are critical to sustain the specificity of the MOG<sub>35-55</sub> peptide. Alternatively speaking, it may allow MOG<sub>35-55</sub>-specific T cells to cross-react to various MOG<sub>35-55</sub> mimicry peptides with these four critical residues unchanged. Here we propose these MOG<sub>35-55</sub> mimicry peptide may come from the antigens of commensal bacteria.

Due to the large number of clonotypically unique TCRs that can be generated by V(D)J somatic recombination, it was initially believed that the immune system might be capable of generating a TCR repertoire for virtually every antigenic peptide. However, subsequent estimates of the size of the peptide pool recognized by TCRs revealed that potentially immunogenic peptides in the environment of an individual greatly outnumber the amount of T cells. Each T-cell is estimated to react with  $>10^6$  different MHC-associated peptide epitopes<sup>155</sup>, for which the concept of TCR cross-reactivity has been evoked as an essential mechanism to expand the effective size of the TCR repertoire<sup>156,157</sup>. However, the degeneracy of TCR specificity will increase the pathogenic potential T cells as it augments the likelihood of self-pMHC recognition. Indeed, several studies have reported that TCR cross-reactivity and molecular mimicry is associated with autoimmune disease, whereby the viral or bacterial peptides mimic autoantigens and provoke the autoimmunity<sup>158,159</sup>. Moreover, structural studies provided substantial evidence to reveal the recognition features of several autoreactive TCR-pMHC complexes<sup>151,160-164</sup>. These features were summarized as altered TCR docking topologies, paucity of hydrogen bonds between the TCR and self-peptide, peptide recognition by the CDR3 loops alone, limited interactions between the TCR and MHC, suboptimal fit of the self-peptide in the MHC binding groove and partial occupancy of the groove by the self-peptide<sup>141</sup>. What these cross-reactive TCR actually recognize *in vivo* is unknown. Since the mammalian gastrointestinal track can harbor a highly heterogeneous microbial population comprising over  $1 \times 10^{13}$ - $10^{14}$  resident bacteria, commensal bacteria may provide the most abundant foreign antigens that may mimic autoantigens *in vivo*. Evidence has demonstrated the relationship between CNS demyelinating diseases and commensal bacteria. For instance, in EAE mice model, alteration of the bacterial populations of the gut has been demonstrated to alter the clinical outcome<sup>165</sup>. Oral administration of antibiotics protected against EAE<sup>166</sup>.

Based on this hypothesis, we proposed that microbial antigens may take advantage of the similar molecular mimicries and activate the early engrafted retrogenic T cells in the periphery. To test that in our pilot experiments, we were able to continually treat our retrogenic mice with combined antibiotics. Those mice were either enforced expressing fixed TCR $\beta$  chain (TCR $\beta$ 1, TCR $\beta$ 3) or enforced expressing single TCR $\alpha\beta$  (PUN342). The autoimmune disease was completely prevented (Nguyen, unpublished data). Retrogenic mice of control group were treated with syrup only, they still developed spontaneous autoimmune disease and a substantial number of highly activated CD4 T cells could be isolated from gut tissue and the mesenteric lymph nodes (Nguyen, unpublished data).

In order to further clarify the mechanism, future experiments are necessary to screen out the bacteria and the bacterial antigen if possible. Admittedly, the variation in intestinal microbiota communities of the laboratory mice is dependent on the environmental factors at each institutional facility. To circumvent this problem, germ-free mice line is necessary to identify the association among the gut-microbiota antigen and the CNS demyelinating diseases.

### **Retrogenic Mice Models versus Transgenic Mice Models**

TCR transgenic mice are widely used and have had a large in current immunological research. Several studies focusing on TCR repertoire analyses also successfully utilized transgenic mice enforced the TCR $\beta$  chain with or without a TCR $\alpha$  chain minilocus<sup>97,100</sup>. This approach is much stable and natural since the T cell first develop in the neonatal condition, but it is time consuming and costly, needs careful pre-experiment design. Due to the time and cost inconvenience, this approach doesn't fit a comprehensive functional assessment of multiple public TCR $\beta$ s.

To circumvent these problems, we utilized another commonly used mice model, retrogenic mice, in which specific TCRs were retrovirally transduced into hematopoietic stem cells<sup>136</sup>. This approach is substantially faster than making transgenic mice, (6 weeks versus 6 months), making a comprehensive functional assessment of multiple public TCR $\beta$ s possible. Compared with transgenic mice, there still exists some disadvantage, such as less T lymphocytes, laborious effort to generate each mouse, unnatural phenotype of peripheral T cells with an increased memory-like phenotype in a lymphopenic host condition. In addition, we sublethally irradiated recipient mice to facilitate stem cell engraftment, and how sublethal irradiation itself may affect the mice is hard to judge. Furthermore, bone marrow transfer is required for making retrogenic mice model, the more steps for manipulation, the more risk to expose to environmental antigens, meaning studies about the spontaneous disease imposed by public TCR $\beta$  chains in germ free condition is difficult.

Admittedly, although we have not seen any deleterious consequences per se, these effects can potentially influence experimental results and should be considered in interpreting data from the system.

### **Summary**

In summary, in this project, we were able to couple the high-throughput sequencing of the TCR $\beta$  repertoire in EAE mice model, with functional studies demonstrating the role of public TCR $\beta$  chains in disease susceptibility in retrogenic mice. Analyses of >18 million TCR $\beta$  from Foxp3<sup>+</sup> regulatory and Foxp3<sup>-</sup> conventional T cells from different organs and time points, we identified a high prevalence of public TCR $\beta$  within the autoimmune response. The public TCR $\beta$  are more likely to be formed in pre-selection thymocytes, which also reside in the pre immune repertoire and is preferentially employed in autoimmune responses, suggesting the hidden “foes” may impose disease risk once if the immune system is out of control. We also performed some pilot experiments by treating the retrogenic mice with antibiotics, thus the autoimmune diseases were totally protected, and suggesting the cross-reactivity towards the commensal microbial antigens might activate the retrogenic CD4 T cells in periphery. This experiment provides insights for the relationship between commensal bacteria and the CNS demyelinating diseases. Though the underlying mechanism and the particular antigens are not well understood, this study still provides a potential therapeutic insight. Coupling high-throughput immunosequencing, specific public sequences may prove useful for the longitudinal monitoring of immune responses during autoimmune diseases.

## LIST OF REFERENCES

1. Davis, M.M. & Bjorkman, P.J. T-cell antigen receptor genes and T-cell recognition. *Nature* **334**, 395-402 (1988).
2. Starr, T.K., Jameson, S.C. & Hogquist, K.A. Positive and negative selection of T cells. *Annual review of immunology* **21**, 139-176 (2003).
3. Singer, A., Adoro, S. & Park, J.H. Lineage fate and intense debate: myths, models and mechanisms of CD4- versus CD8-lineage choice. *Nature reviews. Immunology* **8**, 788-801 (2008).
4. Collins, A., Littman, D.R. & Taniuchi, I. RUNX proteins in transcription factor networks that regulate T-cell lineage choice. *Nature reviews. Immunology* **9**, 106-115 (2009).
5. Josefowicz, S.Z. & Rudensky, A. Control of regulatory T cell lineage commitment and maintenance. *Immunity* **30**, 616-625 (2009).
6. Rudolph, M.G., Stanfield, R.L. & Wilson, I.A. How TCRs bind MHCs, peptides, and coreceptors. *Annual review of immunology* **24**, 419-466 (2006).
7. Demant, P. & Graff, R.J. Transplantation Analysis of H-2 System. *Transplant P* **5**, 267-270 (1973).
8. Gorer, P.A., Lyman, S. & Snell, G.D. Studies on the Genetic and Antigenic Basis of Tumour Transplantation - Linkage between a Histocompatibility Gene and Fused in Mice. *Proc R Soc Ser B-Bio* **135**, 499-505 (1948).
9. Snell, G.D. & Higgins, G.F. Alleles at the histocompatibility-2 locus in the mouse as determined by tumor transplantation. *Genetics* **36**, 306-310 (1951).
10. Jerne, N.K. The somatic generation of immune recognition (Reprinted from Eur. J. Immunol. vol 1, pg 1-9, 1971). *European journal of immunology* **34**, 1234-1242 (2004).
11. Rudensky, A.Y., Mazel, S.M. & Yurin, V.L. Presentation of endogenous immunoglobulin determinant to immunoglobulin-recognizing T cell clones by the thymic cells. *European journal of immunology* **20**, 2235-2239 (1990).
12. Falk, K., Rotzschke, O., Stevanovic, S., Jung, G. & Rammensee, H.G. Allele-specific motifs revealed by sequencing of self-peptides eluted from MHC molecules. *Nature* **351**, 290-296 (1991).
13. van Bleek, G.M. & Nathenson, S.G. The structure of the antigen-binding groove of major histocompatibility complex class I molecules determines specific selection of self-peptides. *Proceedings of the National Academy of Sciences of the United States of America* **88**, 11032-11036 (1991).
14. Fremont, D.H., Matsumura, M., Stura, E.A., Peterson, P.A. & Wilson, I.A. Crystal structures of two viral peptides in complex with murine MHC class I H-2Kb. *Science* **257**, 919-927 (1992).
15. Madden, D.R., Garboczi, D.N. & Wiley, D.C. The antigenic identity of peptide-MHC complexes: a comparison of the conformations of five viral peptides presented by HLA-A2. *Cell* **75**, 693-708 (1993).
16. Shiina, T., Inoko, H. & Kulski, J.K. An update of the HLA genomic region, locus information and disease associations: 2004. *Tissue antigens* **64**, 631-649 (2004).

17. Nepom, G.T. & Erlich, H. MHC class-II molecules and autoimmunity. *Annual review of immunology* **9**, 493-525 (1991).
18. Thomson, G. HLA disease associations: models for the study of complex human genetic disorders. *Critical reviews in clinical laboratory sciences* **32**, 183-219 (1995).
19. Genome-wide association study of 14,000 cases of seven common diseases and 3,000 shared controls. *Nature* **447**, 661-678 (2007).
20. Gough, S.C. & Simmonds, M.J. The HLA Region and Autoimmune Disease: Associations and Mechanisms of Action. *Current genomics* **8**, 453-465 (2007).
21. Wordsworth, B.P. *et al.* HLA-DR4 subtype frequencies in rheumatoid arthritis indicate that DRB1 is the major susceptibility locus within the HLA class II region. *Proceedings of the National Academy of Sciences of the United States of America* **86**, 10049-10053 (1989).
22. Redondo, M.J. & Eisenbarth, G.S. Genetic control of autoimmunity in Type I diabetes and associated disorders. *Diabetologia* **45**, 605-622 (2002).
23. Hermann, R. *et al.* Genetic screening for individuals at high risk for type 1 diabetes in the general population using HLA Class II alleles as disease markers. A comparison between three European populations with variable rates of disease incidence. *Diabetes/metabolism research and reviews* **20**, 322-329 (2004).
24. Hoppenbrouwers, I.A. & Hintzen, R.Q. Genetics of multiple sclerosis. *Biochimica et biophysica acta* **1812**, 194-201 (2011).
25. Tsai, S. & Santamaria, P. MHC Class II Polymorphisms, Autoreactive T-Cells, and Autoimmunity. *Frontiers in immunology* **4**, 321 (2013).
26. Sawcer, S. *et al.* Genetic risk and a primary role for cell-mediated immune mechanisms in multiple sclerosis. *Nature* **476**, 214-219 (2011).
27. Hsieh, C.S., Lee, H.M. & Lio, C.W. Selection of regulatory T cells in the thymus. *Nature reviews. Immunology* **12**, 157-167 (2012).
28. Stritesky, G.L., Jameson, S.C. & Hogquist, K.A. Selection of self-reactive T cells in the thymus. *Annual review of immunology* **30**, 95-114 (2012).
29. Bevan, M.J. & Fink, P.J. The influence of thymus H-2 antigens on the specificity of maturing killer and helper cells. *Immunological reviews* **42**, 3-19 (1978).
30. Kappler, J.W., Roehm, N. & Marrack, P. T cell tolerance by clonal elimination in the thymus. *Cell* **49**, 273-280 (1987).
31. Van Laethem, F. *et al.* Deletion of CD4 and CD8 coreceptors permits generation of alphabeta T cells that recognize antigens independently of the MHC. *Immunity* **27**, 735-750 (2007).
32. Dai, S. *et al.* Crossreactive T Cells spotlight the germline rules for alphabeta T cell-receptor interactions with MHC molecules. *Immunity* **28**, 324-334 (2008).
33. Lefranc, M.P. *et al.* IMGT, the international ImMunoGeneTics database. *Nucleic acids research* **27**, 209-212 (1999).
34. Nikolich-Zugich, J., Slifka, M.K. & Messaoudi, I. The many important facets of T-cell repertoire diversity. *Nature reviews. Immunology* **4**, 123-132 (2004).
35. Arstila, T.P. *et al.* A direct estimate of the human alphabeta T cell receptor diversity. *Science* **286**, 958-961 (1999).
36. Shortman, K., Egerton, M., Spangrude, G.J. & Scollay, R. The generation and fate of thymocytes. *Seminars in immunology* **2**, 3-12 (1990).



37. Casrouge, A. *et al.* Size estimate of the alpha beta TCR repertoire of naive mouse splenocytes. *Journal of immunology* **164**, 5782-5787 (2000).
38. Simone, E. *et al.* T cell receptor restriction of diabetogenic autoimmune NOD T cells. *Proceedings of the National Academy of Sciences of the United States of America* **94**, 2518-2521 (1997).
39. Cibotti, R. *et al.* Public and private V beta T cell receptor repertoires against hen egg white lysozyme (HEL) in nontransgenic versus HEL transgenic mice. *The Journal of experimental medicine* **180**, 861-872 (1994).
40. Mendel Kerlero de Rosbo, N. & Ben-Nun, A. Delineation of the minimal encephalitogenic epitope within the immunodominant region of myelin oligodendrocyte glycoprotein: diverse V beta gene usage by T cells recognizing the core epitope encephalitogenic for T cell receptor V beta b and T cell receptor V beta a H-2b mice. *European journal of immunology* **26**, 2470-2479 (1996).
41. Osman, G.E., Toda, M., Kanagawa, O. & Hood, L.E. Characterization of the T cell receptor repertoire causing collagen arthritis in mice. *The Journal of experimental medicine* **177**, 387-395 (1993).
42. Li, H., Ye, C., Ji, G. & Han, J. Determinants of public T cell responses. *Cell research* **22**, 33-42 (2012).
43. Robins, H.S. *et al.* Overlap and effective size of the human CD8+ T cell receptor repertoire. *Science translational medicine* **2**, 47ra64 (2010).
44. Venturi, V., Price, D.A., Douek, D.C. & Davenport, M.P. The molecular basis for public T-cell responses? *Nature reviews. Immunology* **8**, 231-238 (2008).
45. Pantaleo, G. *et al.* Major expansion of CD8+ T cells with a predominant V beta usage during the primary immune response to HIV. *Nature* **370**, 463-467 (1994).
46. Wilson, J.D. *et al.* Oligoclonal expansions of CD8(+) T cells in chronic HIV infection are antigen specific. *The Journal of experimental medicine* **188**, 785-790 (1998).
47. Argaet, V.P. *et al.* Dominant selection of an invariant T cell antigen receptor in response to persistent infection by Epstein-Barr virus. *The Journal of experimental medicine* **180**, 2335-2340 (1994).
48. Callan, M.F. *et al.* Large clonal expansions of CD8+ T cells in acute infectious mononucleosis. *Nature medicine* **2**, 906-911 (1996).
49. Price, D.A. *et al.* Avidity for antigen shapes clonal dominance in CD8+ T cell populations specific for persistent DNA viruses. *The Journal of experimental medicine* **202**, 1349-1361 (2005).
50. Wills, M.R. *et al.* The human cytotoxic T-lymphocyte (CTL) response to cytomegalovirus is dominated by structural protein pp65: frequency, specificity, and T-cell receptor usage of pp65-specific CTL. *Journal of virology* **70**, 7569-7579 (1996).
51. Trautmann, L. *et al.* Selection of T cell clones expressing high-affinity public TCRs within Human cytomegalovirus-specific CD8 T cell responses. *Journal of immunology* **175**, 6123-6132 (2005).
52. Aebischer, T., Oehen, S. & Hengartner, H. Preferential usage of V alpha 4 and V beta 10 T cell receptor genes by lymphocytic choriomeningitis virus glycoprotein-specific H-2Db-restricted cytotoxic T cells. *European journal of immunology* **20**, 523-531 (1990).

53. Kedzierska, K., Turner, S.J. & Doherty, P.C. Conserved T cell receptor usage in primary and recall responses to an immunodominant influenza virus nucleoprotein epitope. *Proceedings of the National Academy of Sciences of the United States of America* **101**, 4942-4947 (2004).
54. Moss, P.A. *et al.* Extensive conservation of alpha and beta chains of the human T-cell antigen receptor recognizing HLA-A2 and influenza A matrix peptide. *Proceedings of the National Academy of Sciences of the United States of America* **88**, 8987-8990 (1991).
55. Lehner, P.J. *et al.* Human HLA-A0201-restricted cytotoxic T lymphocyte recognition of influenza A is dominated by T cells bearing the V beta 17 gene segment. *The Journal of experimental medicine* **181**, 79-91 (1995).
56. Acha-Orbea, H. *et al.* Limited heterogeneity of T cell receptors from lymphocytes mediating autoimmune encephalomyelitis allows specific immune intervention. *Cell* **54**, 263-273 (1988).
57. Godthelp, B.C., van Tol, M.J., Vossen, J.M. & van den Elsen, P.J. Longitudinal analysis of T cells responding to tetanus toxoid in healthy subjects as well as in pediatric patients after bone marrow transplantation: the identification of identical TCR-CDR3 regions in time suggests long-term stability of at least part of the antigen-specific TCR repertoire. *International immunology* **13**, 507-518 (2001).
58. Kelly, J.M. *et al.* Identification of conserved T cell receptor CDR3 residues contacting known exposed peptide side chains from a major histocompatibility complex class I-bound determinant. *European journal of immunology* **23**, 3318-3326 (1993).
59. McHeyzer-Williams, M.G. & Davis, M.M. Antigen-specific development of primary and memory T cells in vivo. *Science* **268**, 106-111 (1995).
60. Babbe, H. *et al.* Clonal expansions of CD8(+) T cells dominate the T cell infiltrate in active multiple sclerosis lesions as shown by micromanipulation and single cell polymerase chain reaction. *The Journal of experimental medicine* **192**, 393-404 (2000).
61. Oksenberg, J.R. *et al.* Selection for T-cell receptor V beta-D beta-J beta gene rearrangements with specificity for a myelin basic protein peptide in brain lesions of multiple sclerosis. *Nature* **362**, 68-70 (1993).
62. Baker, F.J., Lee, M., Chien, Y.H. & Davis, M.M. Restricted islet-cell reactive T cell repertoire of early pancreatic islet infiltrates in NOD mice. *Proceedings of the National Academy of Sciences of the United States of America* **99**, 9374-9379 (2002).
63. Torres-Nagel, N., Deutschlander, A., Herrmann, T., Arden, B. & Hunig, T. Control of TCR V alpha-mediated positive repertoire selection and alloreactivity by differential J alpha usage and CDR3 alpha composition. *International immunology* **9**, 1441-1452 (1997).
64. Sim, B.C., Zerva, L., Greene, M.I. & Gascoigne, N.R. Control of MHC restriction by TCR Valpha CDR1 and CDR2. *Science* **273**, 963-966 (1996).
65. Sim, B.C., Lo, D. & Gascoigne, N.R. Preferential expression of TCR V alpha regions in CD4/CD8 subsets: class discrimination or co-receptor recognition? *Immunology today* **19**, 276-282 (1998).

66. Hogquist, K.A., Baldwin, T.A. & Jameson, S.C. Central tolerance: learning self-control in the thymus. *Nature reviews. Immunology* **5**, 772-782 (2005).
67. Miller, J.F. & Heath, W.R. Self-ignorance in the peripheral T-cell pool. *Immunological reviews* **133**, 131-150 (1993).
68. Schwartz, R.H. A cell culture model for T lymphocyte clonal anergy. *Science* **248**, 1349-1356 (1990).
69. Curotto de Lafaille, M.A. & Lafaille, J.J. Natural and adaptive foxp3<sup>+</sup> regulatory T cells: more of the same or a division of labor? *Immunity* **30**, 626-635 (2009).
70. Gershon, R.K. & Kondo, K. Cell interactions in the induction of tolerance: the role of thymic lymphocytes. *Immunology* **18**, 723-737 (1970).
71. Nishizuka, Y. & Sakakura, T. Thymus and reproduction: sex-linked dysgenesis of the gonad after neonatal thymectomy in mice. *Science* **166**, 753-755 (1969).
72. Asano, M., Toda, M., Sakaguchi, N. & Sakaguchi, S. Autoimmune disease as a consequence of developmental abnormality of a T cell subpopulation. *The Journal of experimental medicine* **184**, 387-396 (1996).
73. Sakaguchi, S., Sakaguchi, N., Asano, M., Itoh, M. & Toda, M. Immunologic self-tolerance maintained by activated T cells expressing IL-2 receptor alpha-chains (CD25). Breakdown of a single mechanism of self-tolerance causes various autoimmune diseases. *Journal of immunology* **155**, 1151-1164 (1995).
74. Fontenot, J.D. *et al.* Regulatory T cell lineage specification by the forkhead transcription factor foxp3. *Immunity* **22**, 329-341 (2005).
75. Wildin, R.S. & Freitas, A. IPEX and FOXP3: clinical and research perspectives. *Journal of autoimmunity* **25 Suppl**, 56-62 (2005).
76. Brunkow, M.E. *et al.* Disruption of a new forkhead/winged-helix protein, scurf, results in the fatal lymphoproliferative disorder of the scurfy mouse. *Nature genetics* **27**, 68-73 (2001).
77. Khattry, R., Cox, T., Yasayko, S.A. & Ramsdell, F. An essential role for Scurfin in CD4<sup>+</sup>CD25<sup>+</sup> T regulatory cells. *Nature immunology* **4**, 337-342 (2003).
78. Hori, S., Nomura, T. & Sakaguchi, S. Control of regulatory T cell development by the transcription factor Foxp3. *Science* **299**, 1057-1061 (2003).
79. Wan, Y.Y. & Flavell, R.A. Regulatory T-cell functions are subverted and converted owing to attenuated Foxp3 expression. *Nature* **445**, 766-770 (2007).
80. Fontenot, J.D., Gavin, M.A. & Rudensky, A.Y. Foxp3 programs the development and function of CD4<sup>+</sup>CD25<sup>+</sup> regulatory T cells. *Nature immunology* **4**, 330-336 (2003).
81. Fontenot, J.D. & Rudensky, A.Y. A well adapted regulatory contrivance: regulatory T cell development and the forkhead family transcription factor Foxp3. *Nature immunology* **6**, 331-337 (2005).
82. D'Cruz, L.M. & Klein, L. Development and function of agonist-induced CD25<sup>+</sup>Foxp3<sup>+</sup> regulatory T cells in the absence of interleukin 2 signaling. *Nature immunology* **6**, 1152-1159 (2005).
83. Jordan, M.S. *et al.* Thymic selection of CD4<sup>+</sup>CD25<sup>+</sup> regulatory T cells induced by an agonist self-peptide. *Nature immunology* **2**, 301-306 (2001).

84. Kawahata, K. *et al.* Generation of CD4(+)CD25(+) regulatory T cells from autoreactive T cells simultaneously with their negative selection in the thymus and from nonautoreactive T cells by endogenous TCR expression. *Journal of immunology* **168**, 4399-4405 (2002).
85. Lee, H.M., Bautista, J.L., Scott-Browne, J., Mohan, J.F. & Hsieh, C.S. A broad range of self-reactivity drives thymic regulatory T cell selection to limit responses to self. *Immunity* **37**, 475-486 (2012).
86. van Santen, H.M., Benoist, C. & Mathis, D. Number of T reg cells that differentiate does not increase upon encounter of agonist ligand on thymic epithelial cells. *The Journal of experimental medicine* **200**, 1221-1230 (2004).
87. Apostolou, I. & von Boehmer, H. In vivo instruction of suppressor commitment in naive T cells. *The Journal of experimental medicine* **199**, 1401-1408 (2004).
88. Apostolou, I., Sarukhan, A., Klein, L. & von Boehmer, H. Origin of regulatory T cells with known specificity for antigen. *Nature immunology* **3**, 756-763 (2002).
89. Fantini, M.C. *et al.* Cutting edge: TGF-beta induces a regulatory phenotype in CD4+CD25- T cells through Foxp3 induction and down-regulation of Smad7. *Journal of immunology* **172**, 5149-5153 (2004).
90. Benson, M.J., Pino-Lagos, K., Roseblatt, M. & Noelle, R.J. All-trans retinoic acid mediates enhanced T reg cell growth, differentiation, and gut homing in the face of high levels of co-stimulation. *The Journal of experimental medicine* **204**, 1765-1774 (2007).
91. Mucida, D. *et al.* Reciprocal TH17 and regulatory T cell differentiation mediated by retinoic acid. *Science* **317**, 256-260 (2007).
92. Kretschmer, K. *et al.* Inducing and expanding regulatory T cell populations by foreign antigen. *Nature immunology* **6**, 1219-1227 (2005).
93. Sun, C.M. *et al.* Small intestine lamina propria dendritic cells promote de novo generation of Foxp3 T reg cells via retinoic acid. *The Journal of experimental medicine* **204**, 1775-1785 (2007).
94. Coombes, J.L. *et al.* A functionally specialized population of mucosal CD103+ DCs induces Foxp3+ regulatory T cells via a TGF-beta and retinoic acid-dependent mechanism. *The Journal of experimental medicine* **204**, 1757-1764 (2007).
95. Hsieh, C.S., Zheng, Y., Liang, Y., Fontenot, J.D. & Rudensky, A.Y. An intersection between the self-reactive regulatory and nonregulatory T cell receptor repertoires. *Nature immunology* **7**, 401-410 (2006).
96. Caton, A.J. *et al.* CD4(+) CD25(+) regulatory T cell selection. *Annals of the New York Academy of Sciences* **1029**, 101-114 (2004).
97. Hsieh, C.S. *et al.* Recognition of the peripheral self by naturally arising CD25+ CD4+ T cell receptors. *Immunity* **21**, 267-277 (2004).
98. Pacholczyk, R., Ignatowicz, H., Kraj, P. & Ignatowicz, L. Origin and T cell receptor diversity of Foxp3+CD4+CD25+ T cells. *Immunity* **25**, 249-259 (2006).
99. Lathrop, S.K., Santacruz, N.A., Pham, D., Luo, J. & Hsieh, C.S. Antigen-specific peripheral shaping of the natural regulatory T cell population. *The Journal of experimental medicine* **205**, 3105-3117 (2008).
100. Wong, J. *et al.* Adaptation of TCR repertoires to self-peptides in regulatory and nonregulatory CD4+ T cells. *Journal of immunology* **178**, 7032-7041 (2007).

101. Liu, X. *et al.* T cell receptor CDR3 sequence but not recognition characteristics distinguish autoreactive effector and Foxp3(+) regulatory T cells. *Immunity* **31**, 909-920 (2009).
102. Nguyen, P. *et al.* Discrete TCR repertoires and CDR3 features distinguish effector and Foxp3+ regulatory T lymphocytes in myelin oligodendrocyte glycoprotein-induced experimental allergic encephalomyelitis. *Journal of immunology* **185**, 3895-3904 (2010).
103. Rosati, G. The prevalence of multiple sclerosis in the world: an update. *Neurological sciences : official journal of the Italian Neurological Society and of the Italian Society of Clinical Neurophysiology* **22**, 117-139 (2001).
104. Gold, R., Linington, C. & Lassmann, H. Understanding pathogenesis and therapy of multiple sclerosis via animal models: 70 years of merits and culprits in experimental autoimmune encephalomyelitis research. *Brain : a journal of neurology* **129**, 1953-1971 (2006).
105. Lassmann, H. Models of multiple sclerosis: new insights into pathophysiology and repair. *Current opinion in neurology* **21**, 242-247 (2008).
106. Zamvil, S.S. *et al.* T-cell epitope of the autoantigen myelin basic protein that induces encephalomyelitis. *Nature* **324**, 258-260 (1986).
107. Tuohy, V.K., Lu, Z., Sobel, R.A., Laursen, R.A. & Lees, M.B. Identification of an encephalitogenic determinant of myelin proteolipid protein for SJL mice. *Journal of immunology* **142**, 1523-1527 (1989).
108. Kerlero de Rosbo, N., Mendel, I. & Ben-Nun, A. Chronic relapsing experimental autoimmune encephalomyelitis with a delayed onset and an atypical clinical course, induced in PL/J mice by myelin oligodendrocyte glycoprotein (MOG)-derived peptide: preliminary analysis of MOG T cell epitopes. *European journal of immunology* **25**, 985-993 (1995).
109. McGeachy, M.J., Stephens, L.A. & Anderton, S.M. Natural recovery and protection from autoimmune encephalomyelitis: contribution of CD4+CD25+ regulatory cells within the central nervous system. *Journal of immunology* **175**, 3025-3032 (2005).
110. Reddy, J. *et al.* Myelin proteolipid protein-specific CD4+CD25+ regulatory cells mediate genetic resistance to experimental autoimmune encephalomyelitis. *Proceedings of the National Academy of Sciences of the United States of America* **101**, 15434-15439 (2004).
111. Stephens, L.A., Gray, D. & Anderton, S.M. CD4+CD25+ regulatory T cells limit the risk of autoimmune disease arising from T cell receptor crossreactivity. *Proceedings of the National Academy of Sciences of the United States of America* **102**, 17418-17423 (2005).
112. Moon, J.J. *et al.* Naïve CD4(+) T cell frequency varies for different epitopes and predicts repertoire diversity and response magnitude. *Immunity* **27**, 203-213 (2007).
113. Wynn, K.K. *et al.* Narrowing of T-cell receptor beta variable repertoire during symptomatic herpesvirus infection in transplant patients. *Immunology and cell biology* **88**, 125-135 (2010).
114. Pacholczyk, R. & Kern, J. The T-cell receptor repertoire of regulatory T cells. *Immunology* **125**, 450-458 (2008).

115. Boudinot, P. *et al.* New perspectives for large-scale repertoire analysis of immune receptors. *Molecular immunology* **45**, 2437-2445 (2008).
116. Kedzierska, K., La Gruta, N.L., Stambas, J., Turner, S.J. & Doherty, P.C. Tracking phenotypically and functionally distinct T cell subsets via T cell repertoire diversity. *Molecular immunology* **45**, 607-618 (2008).
117. Freeman, J.D., Warren, R.L., Webb, J.R., Nelson, B.H. & Holt, R.A. Profiling the T-cell receptor beta-chain repertoire by massively parallel sequencing. *Genome research* **19**, 1817-1824 (2009).
118. Wu, Y.C. *et al.* High-throughput immunoglobulin repertoire analysis distinguishes between human IgM memory and switched memory B-cell populations. *Blood* **116**, 1070-1078 (2010).
119. Porter, D.L., Levine, B.L., Kalos, M., Bagg, A. & June, C.H. Chimeric antigen receptor-modified T cells in chronic lymphoid leukemia. *The New England journal of medicine* **365**, 725-733 (2011).
120. Maecker, H.T. *et al.* New tools for classification and monitoring of autoimmune diseases. *Nature reviews. Rheumatology* **8**, 317-328 (2012).
121. Venturi, V. *et al.* TCR beta-chain sharing in human CD8+ T cell responses to cytomegalovirus and EBV. *Journal of immunology* **181**, 7853-7862 (2008).
122. Persons, D.A. *et al.* Retroviral-mediated transfer of the green fluorescent protein gene into murine hematopoietic cells facilitates scoring and selection of transduced progenitors in vitro and identification of genetically modified cells in vivo. *Blood* **90**, 1777-1786 (1997).
123. Alli, R., Nguyen, P. & Geiger, T.L. Retrogenic modeling of experimental allergic encephalomyelitis associates T cell frequency but not TCR functional affinity with pathogenicity. *Journal of immunology* **181**, 136-145 (2008).
124. Ishizuka, J. *et al.* The structural dynamics and energetics of an immunodominant T cell receptor are programmed by its Vbeta domain. *Immunity* **28**, 171-182 (2008).
125. Menezes, J.S. *et al.* A public T cell clonotype within a heterogeneous autoreactive repertoire is dominant in driving EAE. *The Journal of clinical investigation* **117**, 2176-2185 (2007).
126. Fazilleau, N. *et al.* Persistence of autoreactive myelin oligodendrocyte glycoprotein (MOG)-specific T cell repertoires in MOG-expressing mice. *European journal of immunology* **36**, 533-543 (2006).
127. Venturi, V. *et al.* Sharing of T cell receptors in antigen-specific responses is driven by convergent recombination. *Proceedings of the National Academy of Sciences of the United States of America* **103**, 18691-18696 (2006).
128. Mendel, I., Kerlero de Rosbo, N. & Ben-Nun, A. A myelin oligodendrocyte glycoprotein peptide induces typical chronic experimental autoimmune encephalomyelitis in H-2b mice: fine specificity and T cell receptor V beta expression of encephalitogenic T cells. *European journal of immunology* **25**, 1951-1959 (1995).
129. Nguyen, P. *et al.* Identification of errors introduced during high throughput sequencing of the T cell receptor repertoire. *BMC genomics* **12**, 106 (2011).
130. Robins, H. Immunosequencing: applications of immune repertoire deep sequencing. *Current opinion in immunology* **25**, 646-652 (2013).

131. Jenkins, M.K. & Moon, J.J. The role of naive T cell precursor frequency and recruitment in dictating immune response magnitude. *Journal of immunology* **188**, 4135-4140 (2012).
132. Huseby, E.S. *et al.* How the T cell repertoire becomes peptide and MHC specific. *Cell* **122**, 247-260 (2005).
133. Jenkins, M.K., Chu, H.H., McLachlan, J.B. & Moon, J.J. On the composition of the preimmune repertoire of T cells specific for Peptide-major histocompatibility complex ligands. *Annual review of immunology* **28**, 275-294 (2010).
134. Taniguchi, R.T. *et al.* Detection of an autoreactive T-cell population within the polyclonal repertoire that undergoes distinct autoimmune regulator (Aire)-mediated selection. *Proceedings of the National Academy of Sciences of the United States of America* **109**, 7847-7852 (2012).
135. Elong Ngono, A. *et al.* Frequency of circulating autoreactive T cells committed to myelin determinants in relapsing-remitting multiple sclerosis patients. *Clinical immunology* **144**, 117-126 (2012).
136. Holst, J. *et al.* Generation of T-cell receptor retrogenic mice. *Nature protocols* **1**, 406-417 (2006).
137. Sabatino, J.J., Jr., Huang, J., Zhu, C. & Evavold, B.D. High prevalence of low affinity peptide-MHC II tetramer-negative effectors during polyclonal CD4+ T cell responses. *The Journal of experimental medicine* **208**, 81-90 (2011).
138. Krishnamoorthy, G. *et al.* Myelin-specific T cells also recognize neuronal autoantigen in a transgenic mouse model of multiple sclerosis. *Nature medicine* **15**, 626-632 (2009).
139. Picca, C.C. *et al.* Role of TCR specificity in CD4+ CD25+ regulatory T-cell selection. *Immunological reviews* **212**, 74-85 (2006).
140. Ochoa-Reparaz, J., Mielcarz, D.W., Begum-Haque, S. & Kasper, L.H. Gut, bugs, and brain: role of commensal bacteria in the control of central nervous system disease. *Annals of neurology* **69**, 240-247 (2011).
141. Yin, Y., Li, Y. & Mariuzza, R.A. Structural basis for self-recognition by autoimmune T-cell receptors. *Immunological reviews* **250**, 32-48 (2012).
142. Petersen, T.R. *et al.* Characterization of MHC- and TCR-binding residues of the myelin oligodendrocyte glycoprotein 38-51 peptide. *European journal of immunology* **34**, 165-173 (2004).
143. Nishana, M. & Raghavan, S.C. Role of recombination activating genes in the generation of antigen receptor diversity and beyond. *Immunology* **137**, 271-281 (2012).
144. Furmanski, A.L. *et al.* Public T cell receptor beta-chains are not advantaged during positive selection. *Journal of immunology* **180**, 1029-1039 (2008).
145. Madi, A. *et al.* T-cell receptor repertoires share a restricted set of public and abundant CDR3 sequences that are associated with self-related immunity. *Genome research* (2014).
146. Fazilleau, N. *et al.* T cell repertoire diversity is required for relapses in myelin oligodendrocyte glycoprotein-induced experimental autoimmune encephalomyelitis. *Journal of immunology* **178**, 4865-4875 (2007).

147. Madakamutil, L.T., Maricic, I., Sercarz, E.E. & Kumar, V. Immunodominance in the TCR repertoire of a [corrected] TCR peptide-specific CD4+ Treg population that controls experimental autoimmune encephalomyelitis. *Journal of immunology* **180**, 4577-4585 (2008).
148. Marrack, P., Scott-Browne, J.P., Dai, S., Gapin, L. & Kappler, J.W. Evolutionarily conserved amino acids that control TCR-MHC interaction. *Annual review of immunology* **26**, 171-203 (2008).
149. Udyavar, A., Alli, R., Nguyen, P., Baker, L. & Geiger, T.L. Subtle affinity-enhancing mutations in a myelin oligodendrocyte glycoprotein-specific TCR alter specificity and generate new self-reactivity. *Journal of immunology* **182**, 4439-4447 (2009).
150. Holler, P.D., Chlewicki, L.K. & Kranz, D.M. TCRs with high affinity for foreign pMHC show self-reactivity. *Nature immunology* **4**, 55-62 (2003).
151. Hahn, M., Nicholson, M.J., Pyrdol, J. & Wucherpfennig, K.W. Unconventional topology of self peptide-major histocompatibility complex binding by a human autoimmune T cell receptor. *Nature immunology* **6**, 490-496 (2005).
152. Wilson, S.S. *et al.* Residual public repertoires to self. *Journal of neuroimmunology* **107**, 233-239 (2000).
153. Sercarz, E.E. *et al.* Dominance and crypticity of T cell antigenic determinants. *Annual review of immunology* **11**, 729-766 (1993).
154. Delarasse, C. *et al.* Myelin/oligodendrocyte glycoprotein-deficient (MOG-deficient) mice reveal lack of immune tolerance to MOG in wild-type mice. *The Journal of clinical investigation* **112**, 544-553 (2003).
155. Mason, D. A very high level of crossreactivity is an essential feature of the T-cell receptor. *Immunology today* **19**, 395-404 (1998).
156. Holler, P.D. & Kranz, D.M. T cell receptors: affinities, cross-reactivities, and a conformer model. *Molecular immunology* **40**, 1027-1031 (2004).
157. Wucherpfennig, K.W. T cell receptor crossreactivity as a general property of T cell recognition. *Molecular immunology* **40**, 1009-1017 (2004).
158. Wucherpfennig, K.W. & Strominger, J.L. Molecular mimicry in T cell-mediated autoimmunity: viral peptides activate human T cell clones specific for myelin basic protein. *Cell* **80**, 695-705 (1995).
159. Harkiolaki, M. *et al.* T cell-mediated autoimmune disease due to low-affinity crossreactivity to common microbial peptides. *Immunity* **30**, 348-357 (2009).
160. Li, Y. *et al.* Structure of a human autoimmune TCR bound to a myelin basic protein self-peptide and a multiple sclerosis-associated MHC class II molecule. *The EMBO journal* **24**, 2968-2979 (2005).
161. Maynard, J. *et al.* Structure of an autoimmune T cell receptor complexed with class II peptide-MHC: insights into MHC bias and antigen specificity. *Immunity* **22**, 81-92 (2005).
162. Yin, Y., Li, Y., Kerzic, M.C., Martin, R. & Mariuzza, R.A. Structure of a TCR with high affinity for self-antigen reveals basis for escape from negative selection. *The EMBO journal* **30**, 1137-1148 (2011).
163. Sethi, D.K. *et al.* A highly tilted binding mode by a self-reactive T cell receptor results in altered engagement of peptide and MHC. *The Journal of experimental medicine* **208**, 91-102 (2011).



164. Bulek, A.M. *et al.* Structural basis for the killing of human beta cells by CD8(+) T cells in type 1 diabetes. *Nature immunology* **13**, 283-289 (2012).
165. Ochoa-Reparaz, J. *et al.* Role of gut commensal microflora in the development of experimental autoimmune encephalomyelitis. *Journal of immunology* **183**, 6041-6050 (2009).
166. Yokote, H. *et al.* NKT cell-dependent amelioration of a mouse model of multiple sclerosis by altering gut flora. *The American journal of pathology* **173**, 1714-1723 (2008).

# APPENDIX A. SUPPLEMENTAL TABLES

**Table A-1. Annealing oligo sequences for CDR3 $\beta$ .**

TCR	Oligo	5' to 3' nucleotide sequence
TCR $\beta$ 1	sense	TCGAGTTGGCTACCCCCTCTCAGACATCAGTGTACTTCT GTGCCAGCGGTGAGACTGGGGGAAACTATGCTGAGCAG TTCTTCGGACCAGGGACACGACTCACCGTCCTAGAA
	anti-sense	GATCTTCTAGGACGGTGAGTCGTGTCCCTGGTCCGAAGA ACTGCTCAGCATAGTTTCCCCCAGTCTCACCGCTGGCAC AGAAGTACACTGATGTCTGAGAGGGGGTAGCCAAC
TCR $\beta$ 2	sense	TCGAGTTGGCTACCCCCTCTCAGACATCAGTGTACTTCT GTGCCAGCGGTGACAGGTATGAACAGTACTTCGGTCCC GGCACCAGGCTCACGGTTTTAGAA
	anti-sense	GATCTTCTAAAACCGTGAGCCTGGTGCCGGGACCGAAG TACTGTTTCATACCTGTCACCGCTGGCACAGAAGTACACT GATGTCTGAGAGGGGGTAGCCAACCTCGAG
TCR $\beta$ 3	sense	TCGAGTTGGCTACCCCCTCTCAGACATCAGTGTACTTCT GTGCCAGCGGCTATGAACAGTACTTCGGTCCCGGCACCA GGCTCACGGTTTTAGAAAGATCT
	anti-sense	GATCTTCTAAAACCGTGAGCCTGGTGCCGGGACCGAAG TACTGTTTCATAGCCGCTGGCACAGAAGTACACTGATGTC TGAGAGGGGGTAGCCAACCTCGAG
TCR $\beta$ 4	sense	TCGAGTTGGCTACCCCCTCTCAGACATCAGTGTACTTCT GTGCCAGCGGTGAAACAGCAAACCTCCGACTACACCTTC GGCTCAGGGACCAGGCTTTTGGTAATAGAAGATCT
	anti-sense	GATCTTCTATTACCAAAGCCTGGTCCCTGAGCCGAAGG TGAGTCGGAGTTTGCTGTTTCACCGCTGGCACAGAAGT ACACTGATGTCTGAGAGGGGGTAGCCAACCTCGAG
TCR $\beta$ 5	sense	TCGAGTTGGCTACCCCCTCTCAGACATCAGTGTACTTCT GTGCCAGCGGTGATGCTGGGGGGTCTATGAACAGTAC TTCGGTCCCGGCACCAGGCTCACGGTTTTAGAAAGATCT
	anti-sense	GATCTTCTAAAACCGTGAGCCTGGTGCCGGGACCGAAG TACTGTTTCATAGGACCCCCCAGCATCACCGCTGGCACAG AAGTACACTGATGTCTGAGAGGGGGTAGCCAACCTCGAG
TCR $\beta$ 6	sense	TCGAGTTGGCTACCCCCTCTCAGACATCAGTGTACTTCT GTGCCAGCGGTGATGGTGAACAGTACTTCGGTCCCGGC ACCAGGCTCACGGTTTTAGAAAGATCT
	anti-sense	GATCTTCTAAAACCGTGAGCCTGGTGCCGGGACCGAAG TACTGTTTCACCATCACCGCTGGCACAGAAGTACACTGAT GTCTGAGAGGGGGTAGCCAACCTCGAG
TCR $\beta$ 7	sense	TCGAGTTGGCTACCCCCTCTCAGACATCAGTGTACTTCT GTGCCAGCGGTGAGCAACAGGGGACTGAGCAGTTCTTC GGACCAGGGACACGACTCACCGTCCTAGAAGATCT

**Table A-1. (Continued).**

<b>TCR</b>	<b>Oligo</b>	<b>5' to 3' nucleotide sequence</b>
<b>TCR<math>\beta</math>8</b>	anti-sense	GATCTTCTAGGACGGTGAGTCGTGTCCCTGGTCCGAAGA ACTGCTCAGTCCCCTGTTGCTCACCGCTGGCACAGAAGT ACACTGATGTCTGAGAGGGGGTAGCCAACCTCGAG
	sense	TCGAGTTGGCTACCCCCCTCTCAGACATCAGTGTACTTCT GTGCCAGCGGTGATGGACTGGGGGGCTCCTATGAGCAG TACTTCGGTCCCGGCACCAGGCTCACGGTTTTAGAAGAT CT
<b>TCR<math>\beta</math>9</b>	anti-sense	GATCTTCTAAAACCGTGAGCCTGGTGCCGGGACCGAAG TACTGCTCATAGGAGCCCCCAGTCCATCACCGCTGGCA CAGAAGTAACTGATGTCTGAGAGGGGGTAGCCAACCTC GAG
	sense	TCGAGTTGGCTACCCCCCTCTCAGACATCAGTGTACTTCT GTGCCAGCGGTGATGTCCGGGGCTATAATTCGCCCCCTCT ACTTTGCGGCAGGCACCCGGCTCACTGTGACAGAAGAT CT
<b>TCR<math>\beta</math>10</b>	anti-sense	GATCTTCTGTACAGTGAGCCGGGTGCCTGCCGCAAAGT AGAGGGGCGAATTATAGCCCCGGACATCACCGCTGGCA CAGAAGTAACTGATGTCTGAGAGGGGGTAGCCAACCTC GAG
	sense	TCGAGTTGGCTACCCCCCTCTCAGACATCAGTGTACTTCT GTGCCAGCGGTGATGGAACATCAAACCTCCGACTACACC TTTGGGCCAGGCACTCGGCTCCTCGTGTTAGAAGATCT
<b>TCR<math>\beta</math>11</b>	anti-sense	GATCTTCTAACACGAGGAGCCGAGTGCCTGGCCCCAAAG GTGTAGTCGGAGTTTGATGTTCCATCACCGCTGGCACAG AAGTAACTGATGTCTGAGAGGGGGTAGCCAACCTCGAG
	sense	TCGAGTTGGCTACCCCCCTCTCAGACATCAGTGTACTTCT GTGCCAGCGGGATAGGGGACACCCAGTACTTTGGGCCA GGCACTCGGCTCCTCGTGTTAGAAGATCT
<b>TCR<math>\beta</math>12</b>	anti-sense	GATCTTCTAACACGAGGAGCCGAGTGCCTGGCCCCAAAG TACTGGGTGTCCCCTATCCCGCTGGCACAGAAGTAACT GATGTCTGAGAGGGGGTAGCCAACCTCGAG
	sense	TCGAGTTGGCTACCCCCCTCTCAGACATCAGTGTACTTCT GTGCCAGCGGTGACGCCGGGACAGGGTATGAACAGTAC TTCGGTCCCGGCACCAGGCTCACGGTTTTAGAAGATCT
<b>TCR<math>\beta</math>13</b>	anti-sense	GATCTTCTAAAACCGTGAGCCTGGTGCCGGGACCGAAG TACTGTTATACCTGTCCCGGCGTCACCGCTGGCACAG AAGTAACTGATGTCTGAGAGGGGGTAGCCAACCTCGAG
	sense	TCGAGTTGGCTACCCCCCTCTCAGACATCAGTGTACTTCT GTGCCAGCGGGGACTGGGGGGGCGAAGACACCTTGAC TTTGGTGCGGGCACCCGACTATCGGTGCTAGAAGATCT
	anti-sense	GATCTTCTAGCACCGATAGTCGGGTGCCCCGACCAAAGT ACAAGGTGTCTTCGCCCCCCCCAGTCCCCGCTGGCACAGA AGTAACTGATGTCTGAGAGGGGGTAGCCAACCTCGAG

**Table A-1. (Continued).**

<b>TCR</b>	<b>Oligo</b>	<b>5' to 3' nucleotide sequence</b>
<b>TCR<math>\beta</math>14</b>	sense	TCGAGTTGGCTACCCCCTCTCAGACATCAGTGTACTTCT GTGCCAGCGGTGATGAGACTGGGGGGGCCTATGAACAG TACTTCGGTCCCGGCACCAGGCTCACGGTTTTAGAAGAT CT
	anti- sense	GATCTTCTAAAACCGTGAGCCTGGTGCCGGGACCGAAG TACTGTTCATAGGCCCCCCCAGTCTCATCACCGCTGGCA CAGAAGTAACTGATGTCTGAGAGGGGGTAGCCAACTC GAG
<b>TCR<math>\beta</math>15</b>	sense	TCGAGTTGGCTACCCCCTCTCAGACATCAGTGTACTTCT GTGCCAGCGGTGGGGGACTGGGGGGTACTAGTGCAGAA ACGCTGTATTTTGGCTCAGGAACCAGACTGACTGTTCTC GAAGATCT
	anti- sense	GATCTTCGAGAACAGTCAGTCTGGTTCCTGAGCCAAAAT ACAGCGTTTCTGCACTAGTACCCCCCAGTCCCCCACC GC TGGCACAGAAGTAACTGATGTCTGAGAGGGGGTAGCC AACTCGAG

Nucleotide sequences of sense and anti-sense oligos for 15 CDR3 $\beta$  are listed.

## APPENDIX B. SUPPLEMENTAL FIGURES

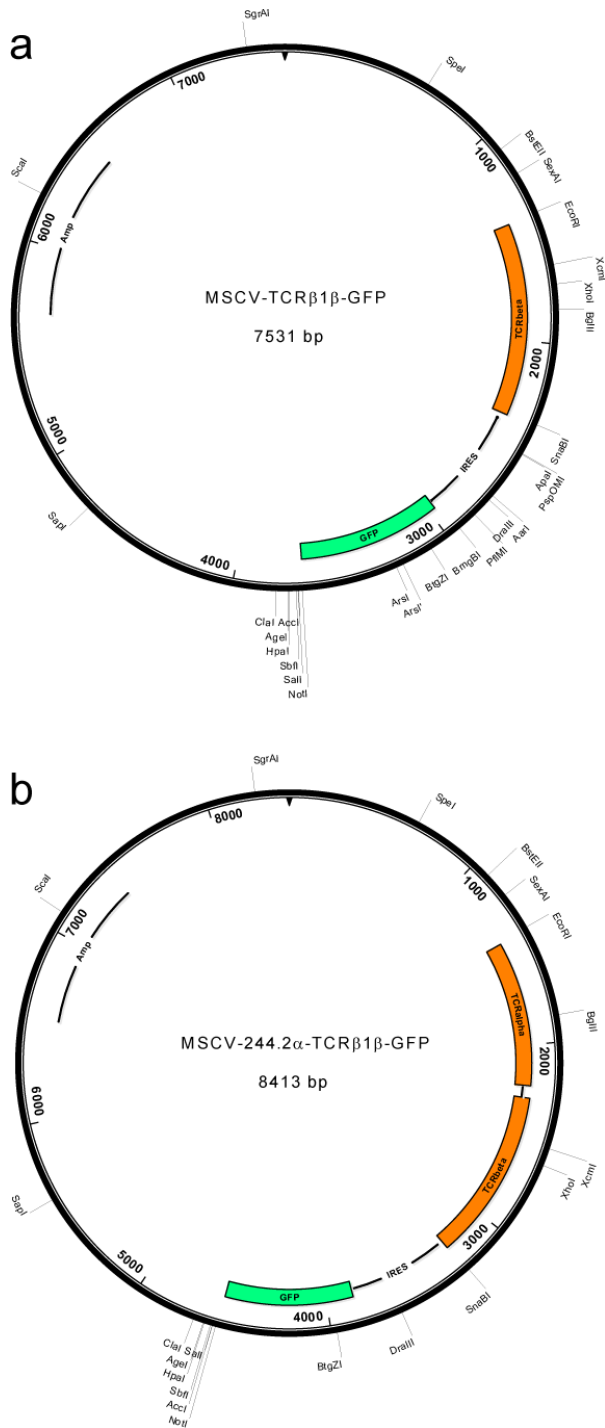


**Figure B-1. Diagram of two main plasmids.**  
(a). MSCV-TCR $\beta$ 1 $\beta$ -GFP. (b). MSCV-244.2 $\alpha$ -TCR $\beta$ 1 $\beta$ -GFP

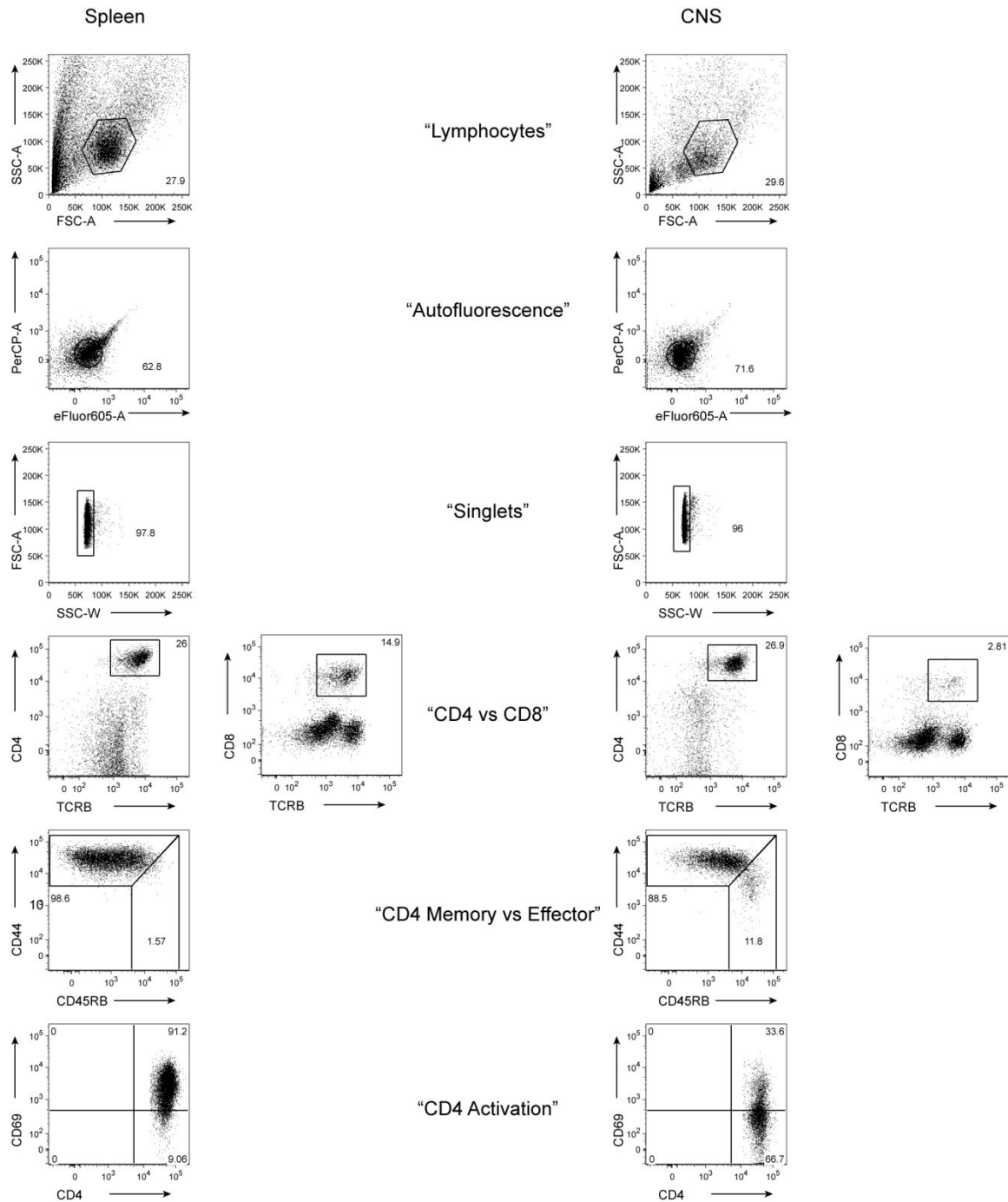


**Figure B-2. Gating strategy for surface staining on TCRβ1 retrogenic mice.** Cells were isolated from spleen and CNS and stained with specific antibodies. Flow cytometric analysis was performed on an LSRFortessa and analyzed by using FlowJo software. The cells were first gated on lymphocytes, gated out autofluorescent cells, doublets, and gated on CD4<sup>+</sup>TCR<sup>+</sup> or CD8<sup>+</sup>TCR<sup>+</sup> lymphocytes. CD4<sup>+</sup>TCR<sup>+</sup> lymphocytes were further analyzed based on their CD44 (memory/effector), CD45Rb (naïve), and CD69 (activation) markers.

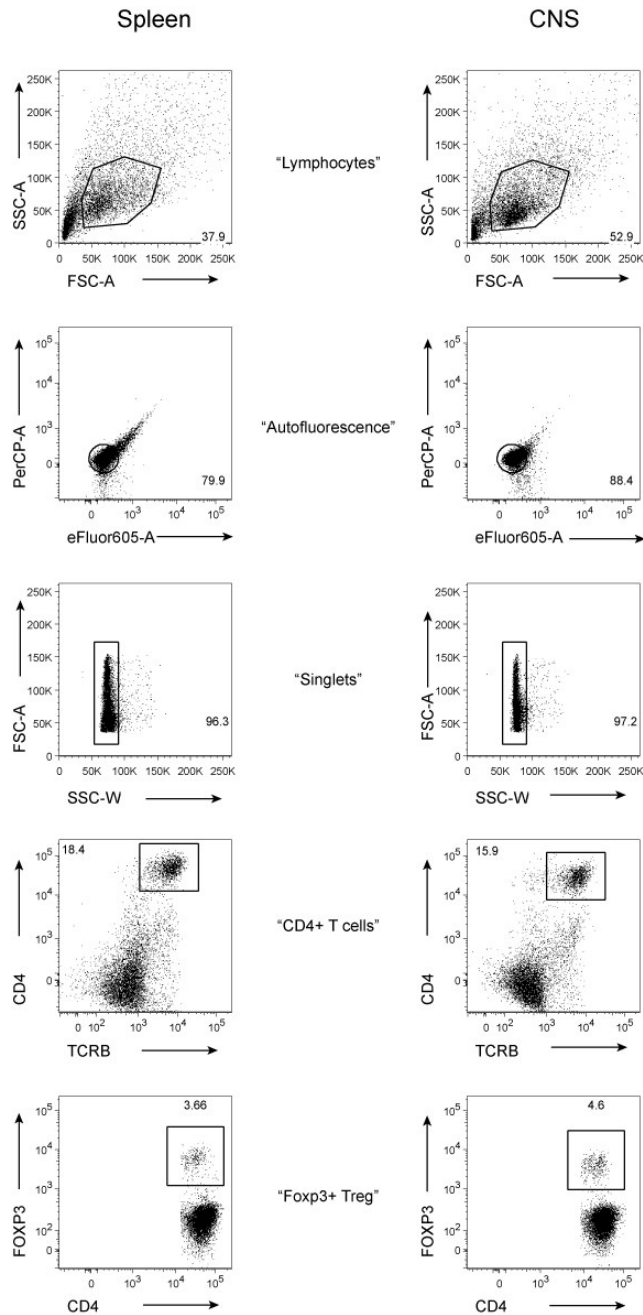


**Figure B-3. Gating strategy for Foxp3 intracellular staining on TCRβ1 retrogenic mice.**

Cells were isolated from spleen and CNS and stained with specific antibodies. Cells were first stained with surface markers, fixed, permeabilized and stained for intracellular Foxp3 with the Foxp3 Staining Buffer Set. The cells were first gated on lymphocytes, gated out autofluorescent cells, doublets, and gated on CD4<sup>+</sup>TCR<sup>+</sup> lymphocytes. CD4<sup>+</sup>TCR<sup>+</sup> lymphocytes were further analyzed based on their Foxp3 marker.

## VITA

Yunqian Zhao was born in Shanghai, China in 1982. In 2000, he was enrolled in Fudan University and majored in life sciences. After achieving his Bachelor of Science degree in 2004, he worked in Chinese Human Genome Center at Shanghai in the research on targets for drug discovery. In August 2009, he was enrolled in the Integrated Program in Biomedical Sciences at the University of Tennessee Health Science Center pursuing a Ph.D. degree. In 2010, he selected to join Dr. Terrence L. Geiger's laboratory at St. Jude Children's Research Hospital and carried out research on autoimmune encephalomyelitis-associated public TCR $\beta$  repertoire and its correlated pathogenesis. He will graduate with Doctor of Philosophy degree.